TRIPOWER UP: Mechanical Design

Floating structure in a wave energy converter

Diogo Telo de Castro Rodrigues

Master Dissertation

Supervisors at FEUP: Prof. Augusto Barata da Rocha
Inv. Carlos Moreira da Silva
Prof. José António dos Santos Almacinha
Prof. António Torres Marques

U. PORTO
FEUP FACULDADE DE ENGENHARIA
UNIVERSIDADE DO PORTO

Dissertation submitted in partial fulfilment of the requirements
for the degree of
Master of Science in Mechanical Engineering

June 23, 2017

"Cada coisa a seu tempo, assim de repente é impossível"

Abstract

FEUP has several contributions shaping the renewable energy technology. It is FEUP's interests to be in the vanguard of innovation through the development of disruptive concepts.

TRIPOWER UP, developed by former colleague, is a new concept and patented idea of a hybrid device that can absorb energy from waves, wind, and currents. The wave energy converter mechanism was developed in this work. As it is modular, the wind and current converters should be added in the future.

The development of the mechanical design was made in collaboration with Miguel Godinho, a colleague in the master course of Mechanical Engineering. The wave energy converter was divided into two main areas; The kinematic system was Godinho's responsibility, while the structural part was developed by myself. Both parts are described throughout this project.

This machine should be in a final design phase after several concept's problems were solved. It is now possible to create all the technical drawings for the TRIPOWER prototype.

Firstly, on this dissertation, ocean wave's behaviors and characteristics were studied.

Secondly, a comparison between floating and submerged point absorber was done as TRIPOWER UP is considered to be a point absorber, which is a type of wave energy converter.

Thirdly, after the floating point absorber presented some advantages, a more profound description of its design steps was described.

For the mechanical design of the TRIPOWER UP, the initial conditions of FEUP's wave tank were established.

During the structural mechanical design, there were several constraints not only due to Macieira's concept adaptation but also due to the Godinho's mechanism inclusion.

In conclusion, stability analysis, as well as environment simulation, was done for the new TRIPOWER UP.

During this dissertation, a new concept was created and patented, called SPIDER UP. It is a new type of wave energy converter that will create future projects.

Resumo

O contributo da FEUP para o desenvolvimento da tecnologia das energias renováveis tem sido notável, é do interesse da instituição estar na vanguarda da inovação e do desenvolvimento dos mais variados produtos.

O TRIPOWER UP, concebido por Miguel Macieira, é um novo conceito de dispositivo híbrido que permite o aproveitamento da energia dos ventos, ondas e correntes. Apenas o mecanismo de aproveitamento da energia das ondas foi desenvolvido durante este trabalho. Uma vez que a sua constituição é modular, os conversores de correntes e ventos deverão ser adicionados em projetos futuros.

O desenvolvimento do design mecânico foi feito em colaboração com o Miguel Godinho, atual colega no Mestrado Integrado de Engenharia Mecânica. Por sua vez, o dispositivo de conversão da energia das ondas foi subdividido em duas grandes áreas: A cadeia cinemática, da responsabilidade do Miguel Godinho, e a parte estrutural, desenvolvida pelo autor; ambas descritas ao longo deste trabalho.

Após vários problemas de conceito terem sido solucionados, conseguiu-se assim obter o atual design mecânico.

Esta dissertação comporta várias etapas. Inicialmente o estudo do comportamento das ondas bem como as suas características foi elaborado. Seguidamente, visto que o TRIPOWER UP se enquadra no conceito de absorsor pontual, aprofundou-se este conceito de conversor de energia das ondas, através da comparação entre absorsores pontuais flutuantes e submersos. Por último, como os absorsores pontuais flutuantes apresentam várias vantagens, foi feita uma descrição dos vários pontos a ter em consideração aquando do seu design.

O design mecânico do TRIPOWER UP elaborou-se tendo como base as características do tanque de ondas existentes na FEUP.

Na elaboração da vertente estrutural foram tidos em conta os conceitos apresentados pelo Miguel Macieira e a cadeia cinemática desenvolvida por Miguel Godinho.

Na fase final do projeto, foi elaborada a análise da estabilidade do sistema bem como a simulação de condições ambientais adversas ao sistema.

Ou longo deste trabalho foi criado e submetida a patente de um novo conceito denominado SPIDER UP. Este novo dispositivo de aproveitamento da energia das ondas irá criar projetos futuros.

Acknowledgements

Gostaria de começar por agradecer ao Prof. Augusto Barata da Rocha pela oportunidade de trabalhar neste projeto tão desafiador. Agradeço também pela orientação e entusiasmo demonstrados durante a realização deste trabalho e pela sua personalidade humana sempre presente.

Gostaria também de agradecer ao Inv. Carlos Moreira da Silva pela genialidade das discussões que em muito contribuíram para este trabalho. Agradeço também pela frontalidade ao longo de todo o projeto.

Ao Prof. José Antonio Almacinha pelo seu rigor, preocupação e àvontade transmitidos durante todo o trabalho.

Ao Prof. Torres Marques pela discussão dos possíveis rumos desta tese bem como os tópicos inovadores que sempre trás para uma discussão.

Ao Miguel Godinho pelo companheirismo e apoio, não só no trabalho, mas também na vida académica.

Aos meus pais, Benigno Rodrigues e Irene Castro, pelo apoio em todas as frentes e pela alegria e confiança transmitida desde o inicio de vida.

À minha namorada, Susana Sousa, pelo apoio e presença ao longo dos momentos da minha vida.

À minha família, pois todos contribuíram para este percurso.

A todos aqueles que posso chamar de amigos, desde os que fiz na Faculdade até aos de Viseu.

To all the ERASMUS friends that made me look at life from a different perspective.

A todos aqueles que tiveram o cuidado de rever este documento tendo em vista o aperfeiçoamento do mesmo.

A todos os professores que me marcaram durante esta vida académica.

Por último, gostaria de agradecer à vida pela sorte que tenho e pelos bons momentos que me dá e irá continuar a dar.

O meu muito obrigado por fazerem de mim Engenheiro.

Diogo Telo de Castro Rodrigues

Contents

Acronyms and Symbols

d_1	1st cylinder diameter
h_1	1st cylinder height
d_2	2nd cylinder diameter
h_2	2nd cylinder height
d_3	3th cylinder diameter
h_3	3th cylinder height
d_4	4th cylinder diameter
h_4	4th cylinder height
C_a	Added coefficient
C_a	Added coefficient
m_w	Added mass
ω	Angular frequency
I_O	Area moment in the water level
a	Buoy radius
Imp	Buoyancy
Imp	Buoyancy Force
Imp_2	Buoyancy force of the second cylinder
Imp_3	Buoyancy force of the third cylinder
C	Celerity
C_I	Center of buoyancy
C_I	center of buoyancy
C_F	Center of fluctuation
C_G	Center of gravity
C_G	center of gravity
S	Cross section
S	Cross section area
V	Cylinder's volume
V	Cylinder's volume per unit height
b	Damping coefficient
d_s	Distance between the center of mass and the water surface
h_w	Distance between water surface and the 3rd cylinder
C_d	Drag coefficient

C_d	Drag coefficient
F_D	Drag force of the inverted parachute
dA	Element of added submerged area
J	Energy flux
EU	European Union
Fg	Gravitational force
g	Gravity
m_d	Mass of the device
Ms	mass of the structure
$Mext$	Mass of the WEC's structure
M	Metacenter
$\overline{C_G M}$	Metacentric height
M	Moment
L_{zz}	Moment of area in the SolidWork
Fm	Mooring forces
F_H	Mooring horizontal forces
F_V	Mooring vertical forces
ω_0	Natural frequency
T	Period
PA	Point Absorber
r	positional vector
P_c	Power created by WEC when the waves are spread in a radial direction.
PTO	Power take off
$\overline{GZ}$	Righting lever arm
l	Rope length
FP7	Seventh Framework Programme
cmn	Spring coefficient
c	Spring coefficient
Fgs	structural gravitation force
¥	Submerged volume
¥	Submerged volume
Imp	Sum of all buoyancy forces
e	Thickness
α	Tilting angle
amn	Total mass
a	Virtual mass

ρ_w	Water Density
d	Water depth
A	Wave amplitude
WEC	Wave energy converter
H	Wave height
k	Wave number
θ	Wave phase
P_w	Wave Power
λ	wavelength
F_{gWEC}	WEC gravitational force
d_5	WEC's Structure exterior diameter
w	Weight of the chain

List of Figures

List of Tables

1 Introduction

In the first chapter, the problem statement and motivation are presented. It describes the global investment in wave energy converters, and it shows why this device has some competitive advantages when compared to its rivals.

Then the dissertation context section shows the starting point of this project as well as the changes and challenges that came with it.

In the end, it gives the project objectives and the dissertation structure.

1.1 Problem statement and Motivation

Due to the petrol crisis in the 70s, governments and institutions started to see renewable energy as a possibility. Stephen Salter, the father of wave energy, started to explore the wave power with his invention, "*Salters duck*". From that moment on, the development of wave energy converters begun to grow, but not as fast as it was expected due to the revival of the petrol economy.

Nowadays, global warming and the conflicts in the Middle East make petrol not reliable, causing negative effects on the global economy. This global issue makes governments and institutions investing more in renewable energy, such as wave energy.

The European Commission is investing in wave energy development. This support is done through financing initiatives with the several EU funding such as *FP7* and *Horizon 2020*. Other funding, such as *NER300*, are an essential tool for the development of this technology. It is not only Portugal or the European Union that is betting on wave energy technology, but also the world, as it can be seen in Figure 1.

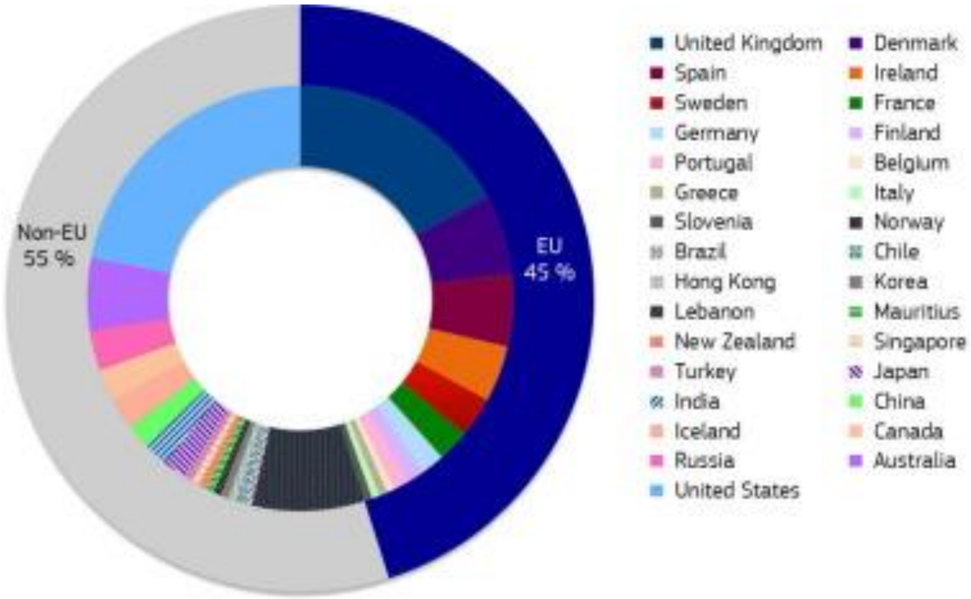

Figure 1- Relative distribution of companies that invest in wave energy technology around the world. (Magagna and Uihlein 2015)

Nowadays, it is believed that this is the right moment to invest in ideas that can transform the energy production system.

As the key to success is all about timing, *TRIPOWER UP* can be seen as one possible investment and solution for hybrid systems. A hybrid converter can absorb three types of energy, such as wind, currents or waves. Furthermore, one of the reasons why humanity still depends on fossil fuel is because wind, waves and currents do not present continue and stable forces.

TRIPOWER UP also presents some other innovative factors: The power take off (*PTO*) system is purely mechanical, creating a differentiation from the common wave energy converters (WECs). Most of them use a hydraulic pump or a turbine to produce energy. The WEC of TRIPOWER UP is considered a floating point absorber because it has a floating structure instead of being fixed to the seabed. Since it is not attached to the floor, it can easily be maintained.

This innovative and disruptive project is what motivates the author during this project, always expecting a better future.

1.2 Dissertation Context

The current dissertation continues Miguel Macieira's dissertation (Macieira 2017). Macieira is a former student of the masters in mechanical engineering.

Macieira developed the idea of *TRIPOWER UP*, but only the main concept was created and patented. Now the objective of this document is to detail and solve the design and the constraints resulting from the main idea. Even though TRIPOWER UP converts the three types of energy, only the WEC was designed due to time constrains.

As it is an ambitious project, the mechanical design of *TRIPOWER UP* was developed by two mechanical engineering students, Miguel Godinho and the author. Miguel Godinho´s dissertation is referred in this document.

The WEC has the transmission and structure subgroups, Miguel Godinho's job was to create WEC´s transmission and the job of the author was to develop the WEC's structure.

In WEC´s transmission, there was a part of the device that was made by both authors, so, in that case, it will be mentioned in the text. When nothing is said regarding this matter, it can be assumed that the work was done by the author of this dissertation.

During this project, another idea of a WEC was created and patented, called *SPIDER UP*. Instead of investing in this new project, it was decided to continue the design of *TRIPOWER UP* as it was on a more developed stage.

Even though only the mechanical design is introduced in this dissertation, the final objective was to create a prototype. To get capital to build the *TRIPOWER UP* prototype, this team applied for Portuguese governmental program called "*StartUP Voucher*" created by IAPMEI (Instituto de Apoio a Pequenas e Médias Empresas e à Inovação) and ended up being selected.

This investment created some changes in the route of this project. One of the main components, the freewheel system, that was developed by the team, due to the high cost in the market, was no longer used. It was decided to select it from the market as it was faster than producing it. Although it is not used it is presented in this dissertation.

This project was conducted having an innovative and straightforward approach to create a functional mechanical design.

1.3 Project objectives

The purpose of the current dissertation is to present a mechanical design for a wave energy converter system created by a former colleague Miguel Macieira, *TRIPOWER UP (Macieira 2017).*

At the same time, this project has to follow the constraints created by the WEC´s transmission done by Miguel Godinho (Macieira 2017).

Due to the lack of time, the goal of the current project was only to focus in the wave energy converter, set aside the wind and current energy converters. However, the two other converters can be the aim of further development because a modular solution is presented.

This dissertation is more focused on the structural part of the wave energy converter, while Godinho's one is more about the kinematic chain. There were two types of structures that were designed: the support structure that supports all the device and the wave energy converter structure, which oscillates with the wave excitation forces.

There are also other requirements that the WEC must have:

- Be floating and low weight;
- Have good hydrodynamic profile;
- Resist to the wave impact and water corrosion;
- Be anchored in deep, intermediate or shallow water;

There were more specific requirements according to the *TRIPOWER UP* idea:

- Both structures needed to have significant different acceleration, to create a displacement between the two structures;
- The support structure had to be almost static;
- The WEC's structure had to absorb horizontal wave forces and to transmit vertical wave forces to WEC´s transmission;
- The TRIPOWER UP had to be stable when placed in water;

During the design, other constraints were created to maximize the structure chances of surviving to extreme environment conditions.

The key component of the kinematic chain (WEC´s transmission), the freewheel, was developed to follow the financial restriction that is no longer a constraint. After getting the investment, it was decided to get it from the market.

1.4 Dissertation structure

This dissertation is organized by chapters that address different topics considered fundamental for TRIPOWER UP mechanical design.

Chapter 2 introduces ocean waves, describing their characteristics according to different approaches.

Chapter 3 not only compares two different types of PA, reaching the best solution, but also presents the design steps and requirements for designing a floating point absorber.

Chapter 4 describes the *TRIPOWER UP* starting point. It reviews the hybrid mechanism that was done in a previous dissertation. It is the starting point of this work.

Chapter 5 not only reveals the wave initial conditions that were used in the mechanical design, but also presents the overall design of the new *TRIPOWER UP*.

Chapter 6 studies the dimensions needed for the buoy to be stable, and simulates the environment conditions that the TRIPOWER UP is submitted.

Chapter 7 empathize the SPIDER UP patent, that was developed, and its key features.

Chapter 8 concludes this dissertation and presents the future works that can be developed.

2 Ocean waves

The ocean wave energy is created by several interactions of different forces. These forces are created by the wind, the gravity of the earth and celestial bodies (moon and sun), Coriolis forces (due to the rotation of the earth) and ocean's superficial tension.

The wind is the main way to create waves. The wave formation starts with a pressure difference between air and the ocean surface. This gap, is due to wind turbulence that acts in the surface.

The fast variation of shear stress as well as pressure difference, creates small waves. These waves increase their sizes due to the resonance with the turbulent wind.

Energy is transferred from wind to waves throughout these processes. The quantity of energy transferred deepens on the wind speed, the wind blows duration, and the distance of water over which the wind is blowing, call the *"fetch". (Thorpe 1999)*

2.1 Regular waves

2.1.1 Linear wave theory

The linear wave theory explains the behavior of regular wave energies.

In deep waters, according to Southgate, 1981, waves can be described as sinusoidal. The basic parameters are:

- Wavelength, λ, is the distance between two consecutives crests or troughs. It is the distance between two point separated by 360°;
- Period, T, is the time between two consecutive crests or troughs. It is the time that it takes to do one wavelength;
- Celerity, c, is the rate at which the phase propagates in space. This is the velocity that any wave phase travels. It varies according to deepness; (phase velocity)
- Crest is the highest point in a wave;
- Trough is the lowest point in a wave;
- Amplitude, A, is the vertical distance between crest or trough and the medium water level;
- Wave height, H, is the vertical distance between a consecutive crest and trough;
- Wave number, k, is equal to $2\pi/\lambda$;
- Angular frequency, ω, is equal to $2\pi/$T;
- Wave phase, θ, equals to $kx - \omega t$
- xx- horizontal position; yy- vertical position; t-time; d-water depth

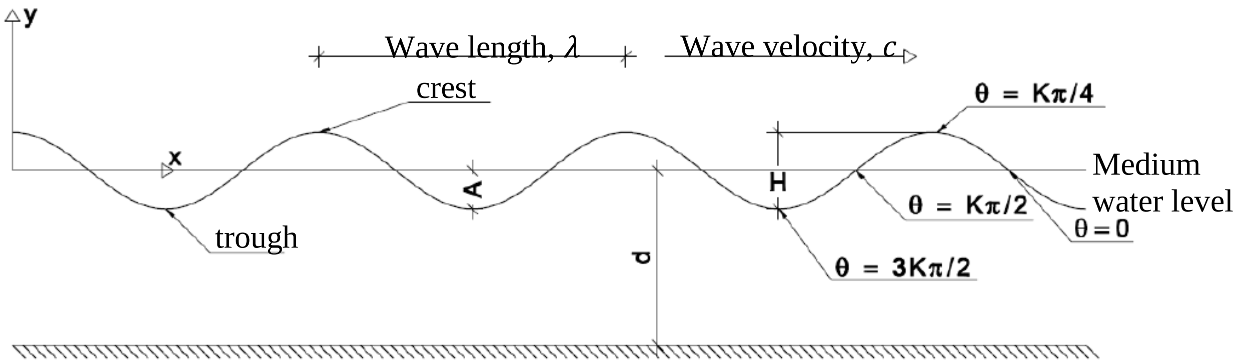

Figure 2- Regular wave's parameters. (Paredes 2008)

2.1.2 Celerity

The celerity, also known as wave or phase velocity, is the velocity at which the wave phase travels. For example, Figure 2, it is the velocity between a through phase, $\theta = \frac{3K\pi}{2}$ and a crest phase, $\theta = \frac{K\pi}{4}$. It changes with wavelengths and water depth. Equation 2.1 gives the general expression of celerity, which is valid for all the wavelength and the water depth: (Paredes 2008)

$$C = \sqrt{\frac{g\lambda}{2\pi} tanh(\frac{2\pi d}{\lambda})} \tag{2.1}$$

There are some conclusions that can be drawn from equation 2.1:

- For a certain water depth, if the wavelength increases the celerity also increases;
- For a given wavelength, deeper water has a larger celerity than shallower water;

As it was presented earlier, the celerity can be written like in equation 2.2:

$$C = \frac{\lambda}{T} \tag{2.2}$$

Combining equation 2.1 with equation 2.2, it can be said that:

$$C = \frac{gT}{2\pi} tanh(\frac{2\pi d}{\lambda}) \tag{2.3}$$

Combining equation 2.3 and equation 2.2, equation 2.4 can be obtained:

$$\lambda = \frac{gT^2}{2\pi} tanh(\frac{2\pi d}{\lambda}) \quad (2.4)$$

Equation 2.1, 2.3 and 2.4 can be applied to every wavelength and every depth. Equation 2.4 has to be solved iteratively because the wavelength is presented on both sides of the equation.

For shallow waters, it can be considered that $\frac{d}{\lambda} < \frac{1}{25}$. Taking in consideration that $\frac{d}{\lambda} = z$, equation 2.1 can be rewritten:

$$C = \sqrt{\frac{gd}{2\pi z} \tanh(2\pi z)} \quad (2.5)$$

The constant of equation 2.5 can be approximated by equation 2.6 (for $z < \frac{1}{25}$):

$$\frac{\tanh(2\pi z)}{2\pi z} \sim 1 \quad (2.6)$$

The equation 2.7 represents celerity for shallow waters:

$$C = \sqrt{gd} \quad (2.7)$$

If the depth is much larger than the wavelength, $d \gg \lambda$, the argument of equation 2.1:

$$tanh(\frac{2\pi d}{\lambda}) \sim 1 \quad (2.8)$$

Rewriting equation 2.1, assuming equation 2.8, equation 2.9 is created. It shows the celerity for deeper water:

$$C = \sqrt{\frac{g\lambda}{2\pi}} \quad (2.9)$$

Combining equation 2.9 and equation 2.2, the deeper water wavelength is presented in equation 2.10:

$$\lambda = \frac{gT^2}{2\pi} \tag{2.10}$$

More equations for wave parameters can be seen in Appendix A.

Figure 3 shows two graphs where a comparison between phase velocity, wave period, and wavelength was done. Different water depth is presented. (*Adapted from Van Dorn, 1974*)

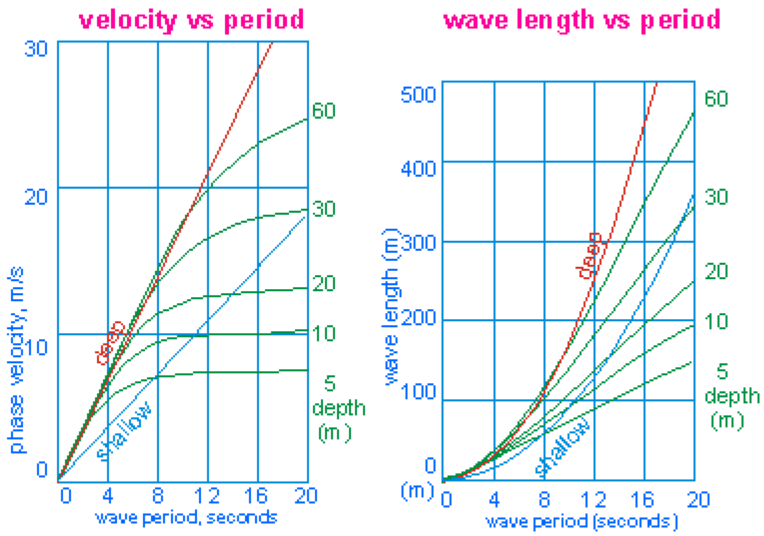

Figure 3- Relationships between phase velocity and period for various depths (left), wavelength (right) and period, for periodic and progressive surface waves (Anthoni 2000)

2.2 Irregular waves

The regular wave profile cannot be observed when the waves are under the environment influence. The wind creates irregularities in wavelength, period and wave height that cannot be predicted. (Morais 2009) Figure 4 shows the wave height captured by a measure buoy placed in deeper water (Leixões, Portugal):

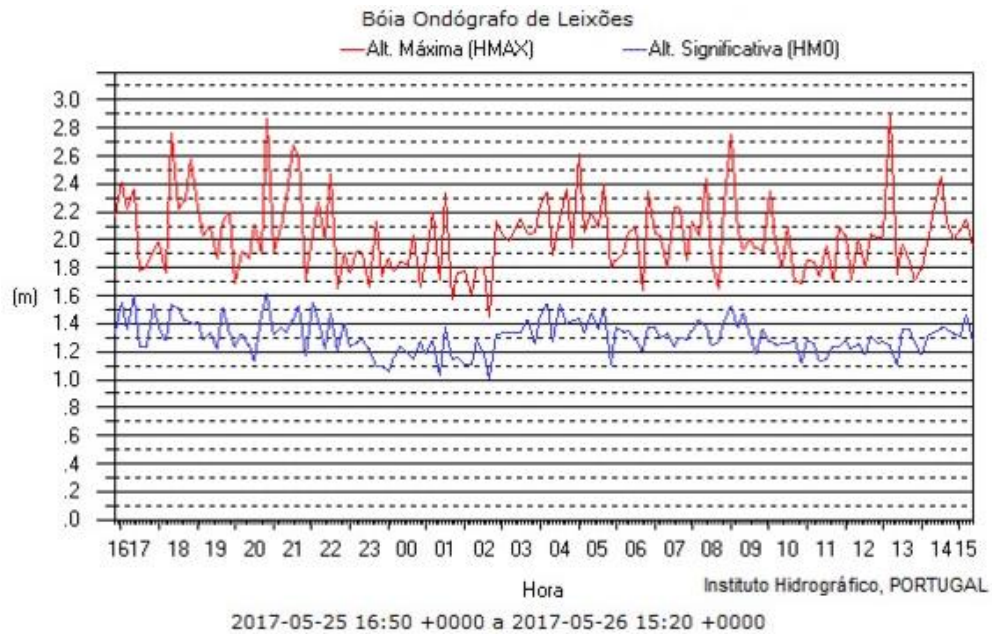

Figure 4- 24h report of wave height. Capture by a measure buoy placed in Leixões on 26 of May 2017 (Marinha 2017)

It can be seen in Figure 4, that real waves do not present a regular behavior. The red line shows the maximum wave height, and the blue line shows the significant height (an average of $\frac{1}{3}$ of the highest waves during a given period).

The regular framework is used in a mathematical approach. For instance, if the objective is to design or to understand the overlap effects, the regular approach is used.

The sea waves do not present a regular behavior, so, a statistic method is used to calculate their parameter. It can be done in the time or frequency domain.

The wave energy is an intermittent power source. Although it might be possible to predict the wave power at a particular location, it can only be a few days ahead. (Morais 2009)

2.3 How sea depth influences waves

The ocean waves exhibit a clear sense of motion and direction. It seems that the wave's water is transported towards shore. However, in reality, it is only energy that is being transported, while the water moves in circles with only a slight transportation of mass taking place. For instance, this phenomenon can be seen if a piece of wood is placed in water, it moves towards the shore at a much lower speed then waves.(Waters 2008)

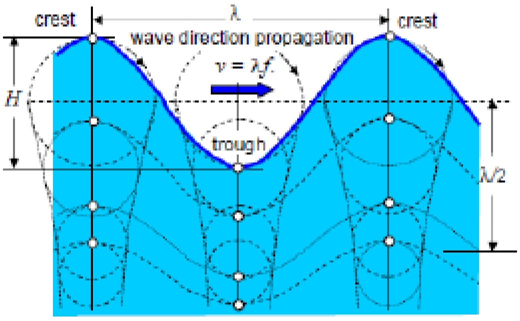

Figure 5-Water mass transportation in sea waves (Morais 2009)

As it can be seen in Figure 5, at the wave crest the wave moves forward. At the troughs it moves backwards.

As Figure 6 shows, that waves in shallow water are affected by the seabed, which forces the circles to become elliptical paths and energy is dissipated through friction against the seabed. If the water depth decreases, the wave period also decreases and the waves become steeper.

In deeper water, the circles are almost perfect, and the water mass transportation is tiny as it is not affected by the sea bed. Importantly, the lack of friction make it possible to transmit energy along the ocean with very few losses. (Waters 2008)

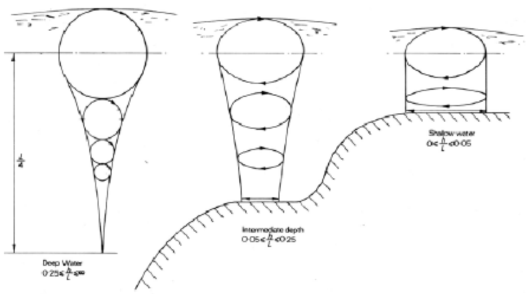

Figure 6- Circular trajectories done by water particles according to different water depth (Morais 2009)

2.4 Wave energy flux

Since sea water is about 850 times heavier than air, water carries more energy than air. If energy is transferred across the ocean, the amount of energy lost due to internal friction, or viscosity, is very small. For instance, when McNamara surfed Nazaré's biggest wave, it was created by a storm in the East Cost of United States. The Earth's rotation drove the wave towards Portugal, and its size increased due to strong winds. (Rodrigues 2014)

The wave energy flux waves is usually presented as an average power per meter of a wave crest length, (*W/m*). So, for one wave, it is the average energy per second that a meter of wave crest has. In deeper water, the wave power density is expressed by equation 2.11, (Boyle 2004)

$$J = \frac{\rho_w g^2 T H^2}{32\pi} \tag{2.11}$$

Where ρ_w is the seawater density and g is the acceleration due to gravity. The wave energy flux changes according to the location, the day, and the weather conditions.

The worldwide power distribution is presented in Figure 7. The highest energy flux is concentrated on the western coast in 40-60° latitude range north and south, where Portugal is located.

In Portugal, the wave energy flux varies between *30* and *40 kW/m*. The energetic peak is located in the northern coast. Viana do Castelo, Figueira da Foz, Peniche and Cabo da Roca are the areas with the highest potential for exploration. (C. Guedes Soares 2008)

Figure 7- World wave energy resource. The numbers represent average energy flux [kW/m] (Waters 2008)

2.5 Water Density

In the ocean, the water density changes with temperature and salinity. The studies of water density influenced the buoyancy force. Water density variation can affect the buoyancy of a body since they are related by equation 2.12. If density increases, buoyancy also increases.

$$Imp = \rho \; g \; \not{V} \tag{2.12}$$

Where, $\not{V}$ is the body submerged volume.

2.5.1Temperature

Due to solar activity, the water surface temperature can change. Heating, cooling, evaporation, and precipitation contribute in some way to change the water density. Water is denser at 4 °C. Above and below that temperature, the density decreases until it reaches its boiling and freezing points. Figure 8 shows the relationship between water density and temperature. (Strömgren 2005)

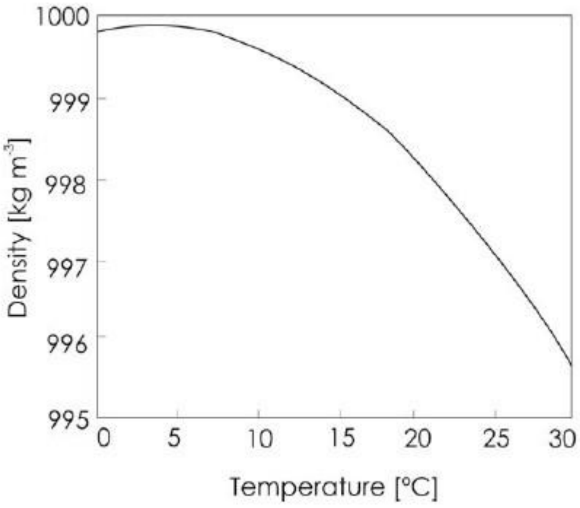

Figure 8-Water density variation according to different temperatures. Maximum density is reached at 4°C (Strömgren 2005)

Even though it is not clear in Figure 8, at 4 °C the density is 1000 kg/m^3. The average density can change according to the place where it is installed, it can go from 110 mm to 250 mm under the surface.

2.5.2Salinity

There is a linear relation between water density and salinity to the density of the sea water (see Figure 9). For the same temperature, the higher the salinity, the higher the density. (Strömgren 2005)

The Atlantic Ocean has a salinity of 3.5%.

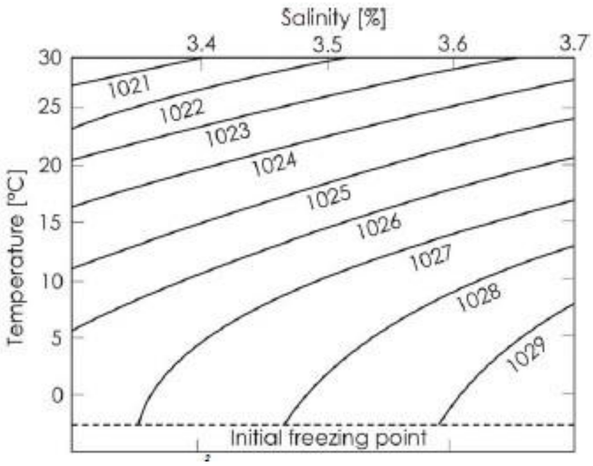

Figure 9-Variation of water density according to temperature and salinity (Strömgren 2005)

The salinity plays a huge role if the prototype is tested in the open sea. The buoyancy of the device is affected.

3 Point Absorbers

Point absorbers (*PA*) are based on the relative movement between a floating buoy and a fixed structure that is moored on the seabed through a large foundation mass. (V. Piscopo 2017)

PAs can be designed to operate on or just below the water surface, extracting wave power from the heaving motion, as it can be seen in Figure 10. (N.Y. Sergiienko 2017)

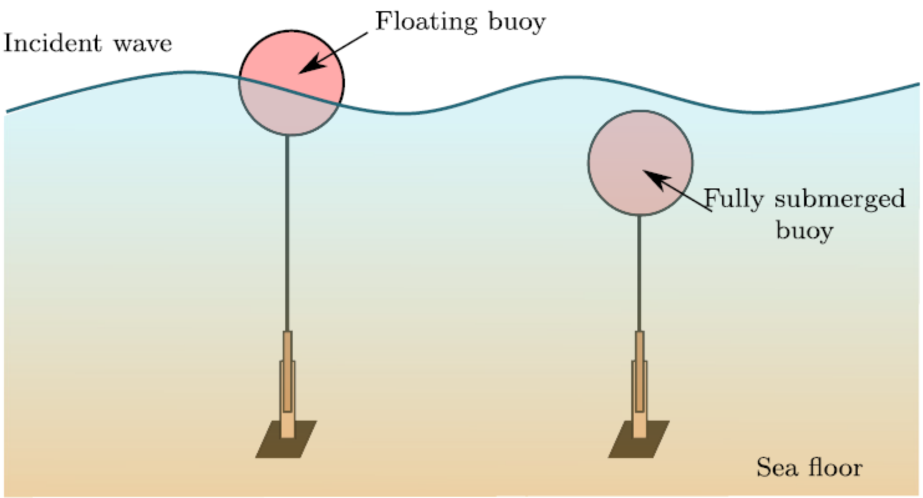

Figure 10- Schematic draw representing the floating and fully submerged WECs (N.Y. Sergiienko 2017)

PA is a type of wave energy converters (WECs) which dimension are smaller than the wavelength, usually axisymmetric about a vertical axis. (Thomas 2008)

A comparison between a PA and another types of WEC can be seen in Figure 11.

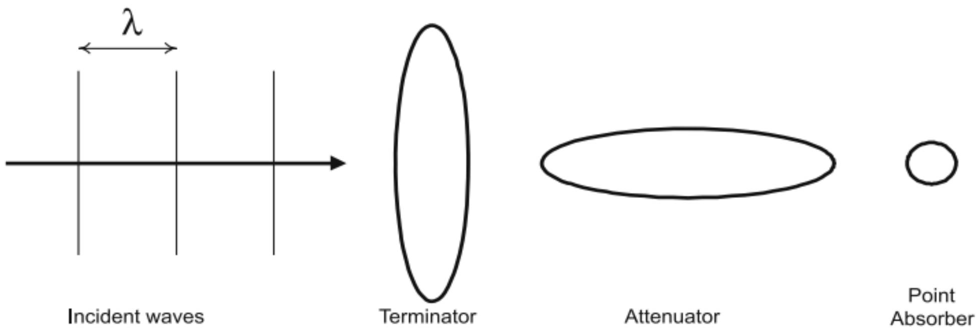

Figure 11- Schematic draw showing the scale and orientation of a Terminator, Attenuator, and Point Absorber (Thomas 2008)

3.1 Floating Vs fully submerged point absorber

During this section, a comparison between floating and submerged point absorbers is made based on N.Y. Sergiienko's research. Both types of PA were compared according to power limits for regular waves, power output in irregular waves, and resonance bandwidth. (N.Y. Sergiienko 2017)

Importantly, Floating converters have the advantage of requiring less maintenance, easy access to the buoy and easy installation constraints. However, fully submerge WECs have the benefit of increase the survivability of the system during a storm, and less visual impact.

3.1.1Power limit for regular waves

A body placed in water, only captures energy when it moves in an oscillatory manner and radiates waves to counteract the incident wave front. Equation 3.1 shows the maximum power absorbed, *W*, by an axisymmetric body in the monochromatic wave. (N.Y. Sergiienko, 2017)

$$Pmax = \varsigma \frac{J}{k} \tag{3.1}$$

Where ς is a coefficient that depends on the motion oscillation mode (ς =1 for heave, ς =2 for surge or pitch, and ς =3 when the body oscillates in heave, surge and pitch simultaneously), k is the wave number, J is the energy flux, *W/m*, shown in equation 3.2,

$$J = \frac{\rho_w g D^2(kh) A^2}{4\omega} \tag{3.2}$$

Where *A* is the wave amplitude, ρ_w is water density, ω is the wave frequency and *D(kh)* is the depth function which is equal to 1 in deeper water.

The power absorption of a floating and a submerged buoy has one upper boundary and two lower boundaries. The upper boundary does not change with the type of PA. However, the lower boundary is influenced not only by the type but also by the shape. Cylindrical and spherical shapes were studied. (N.Y. Sergiienko, 2017) Appendix D shows the upper and lower boundaries that were assumed for the power absorption.

Figure 12 shows the power absorption for the spherical shape. The power limits are represented by the dashed lines. The extracted power tends to both boundaries. d_s represents the distance between the center of mass and the water surface.

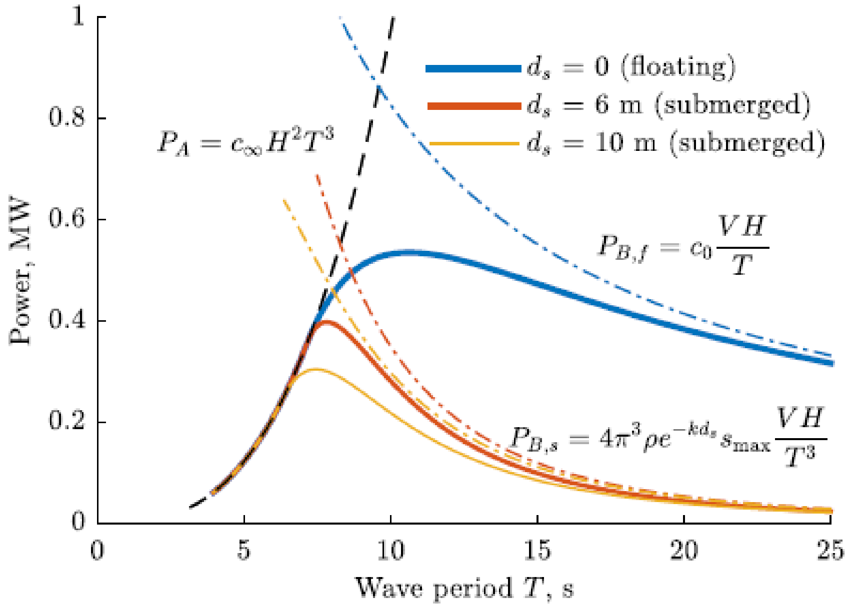

Figure 12-Power absorbed by the floating and submerged spheres in regular waves vs. wave period. Sphere radius is a = 5 m, displacement in heave is constrained to 0.6a, wave height is H = 2 m. The dashed curve corresponds to upper and lower boundaries (N.Y. Sergiienko 2017)

In the next graph, for the cylindrical shape, it is shown that power extraction for different wavelengths according to the d_s, distance between the mass center and the water surface.

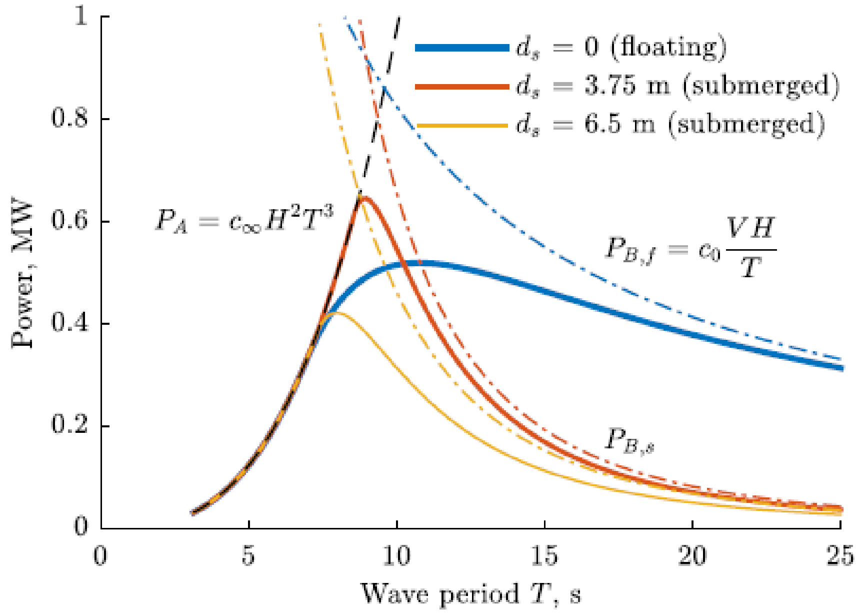

Figure 13- Power absorbed by the floating and submerged truncated vertical cylinders in regular waves vs. wave period. Cylinder radius and height are hc =a = 5.5 m, heave displacement is constrained to 0,5hc, wave height is H = 2 m. The dashed curve corresponds to upper and lower boundary (N.Y. Sergiienko 2017)

The conclusions drawn from the previous graphs should be considered in the mechanical design phase: (N.Y. Sergiienko 2017)

- For a spherical shape, Figure 12, the floating PA can extract more power for wavelengths bigger than 6 s. It can also be seen that the closer the surface is, the more power can be extracted from the wave.
- For a cylindrical shape, Figure 13, shows that the submerge PAs can extract more power from wave period between 6 s and 11 s than the floating PA. After this period, the floating PA can extract more power. Moreover, after 11 s, it can also be concluded that if the buoy is closer to the surface, it can extract more power.

3.1.2Power output in irregular waves

After showing the results considering regular waves, the comparison between submerged and floating buoy was made under irregular waves, representing the real sea state.

In Figure 14, the power absorption is presented in terms of the relative capture width (a ratio between the absorbed power and the wave power).

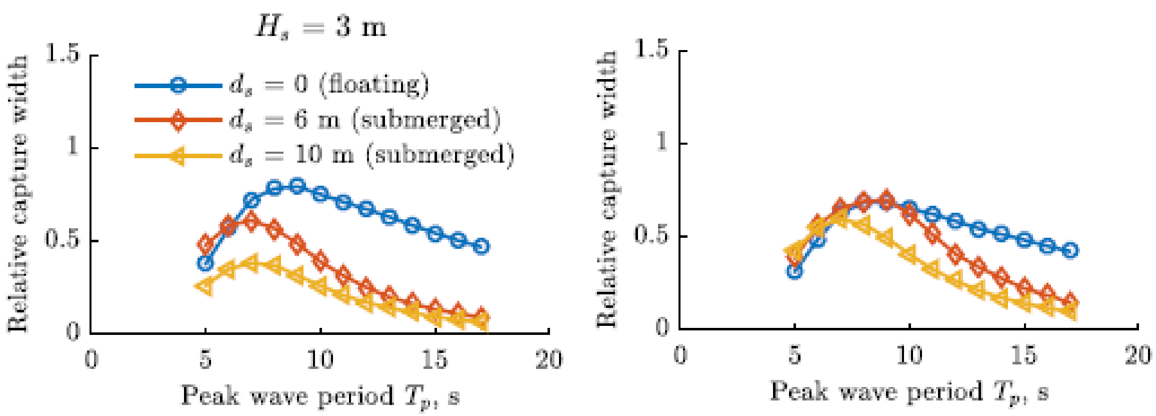

Figure 14- Relative capture width of floating and submerged WECs in irregular waves. Different shapes: 1st spherical; 2nd Cylindrical. Wave height Hs=3m (N.Y. Sergiienko 2017)

The conclusions drawn from the previous graphs should be considered in the mechanical design phase.

- If compared with submerged buoys, the floating PA demonstrate better relative capture width after 6 s (spherical shape) and 9 s (cylindrical shape),
- The previous finding regarding cylindrical devices that generate more power between T=6 s and 11 s cannot be confirmed in irregular wave analyses.
- Another observation is that the device with the d_s=10 m shows the worst performance across both shapes.

3.1.3 Resonance bandwidth

The resonance zone, where the wave frequency is very close to the natural frequency, a PA can maximize the wave power absorption.

Resonance bandwidth of a PA corresponds to the frequency range which the absorbed power stays within 50% of its maximum value. Figure 15 compares the resonance bandwidth between a floating and a submerged PA. (for spherical shape)

It was assumed that the same would happen to the cylindrical shape. The natural frequency, ω_0, was determined assuming that the device was tuned with one wave energy converter.

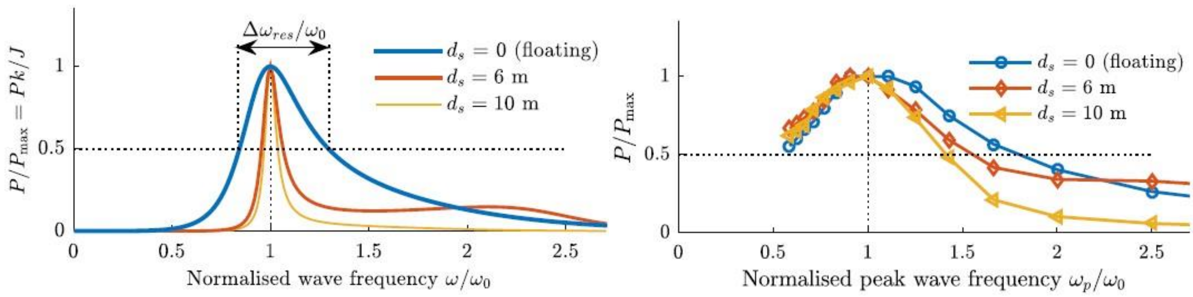

Figure 15- Resonance bandwidth of the spherical PAs 1st in regular waves and 2nd in irregular waves. Non-dimensional absorbed power according to the normalized peak wave frequency (N.Y. Sergiienko 2017)

To conclude, in both cases, the floating device has a larger bandwidth then the submerged ones.

3.2 Floating Point Absorber

After comparing the floating and submerged point absorber, it was concluded that the floating wave energy converter has several advantages. As it was seen in the previous chapter, a floating point absorber absorbs more wave power then a submerged one. It also has a bigger bandwidth maximizing the absorbed power. Due to these advantages, floating point absorber studies were conducted.

In this chapter, the topics that are discussed are:

- The different types power take-off systems;
- The wave-structure interactions;
- The stability of a floating device;
- The natural frequency of a device;
- The different types of WECs mooring systems and their forces;
- The shapes' influence in power absorption;
- The distribution of several WECs along the sea;
- The scale model considerations to create a WEC's prototype;

Figure 16, summarizes the several steps that are necessary to be taken into consideration to come up with a prototype. They are analyzed in this chapter. The wave characteristics were already studied in chapter 2. Due to the lack of time, the natural frequency topic was not fully analyzed, only the main equations are presented. It can be a topic for future discussion.

In this chapter, all the other topics that are outlined in Figure 16 are presented in a theoretical perspective. In Chapter 5 and 6 the topics are applied to the TRIPOWER UP mechanical design.

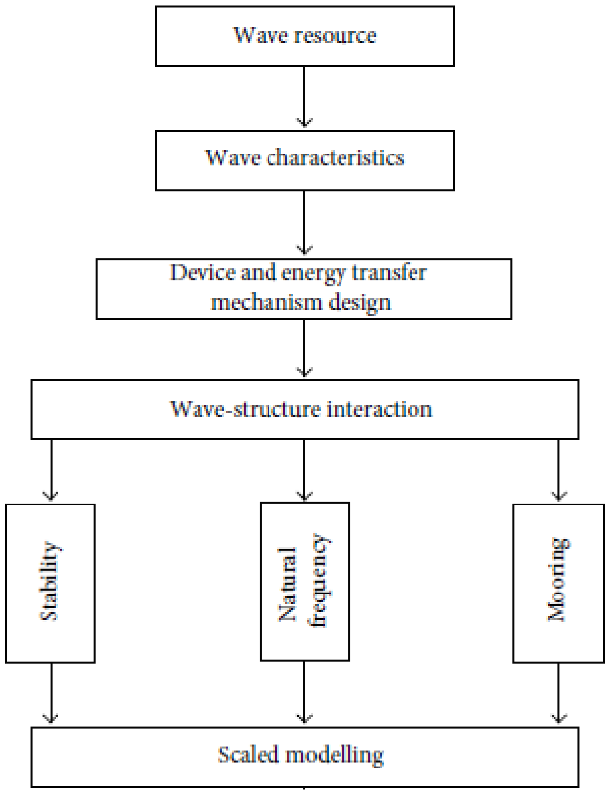

Figure 16- Summary of the topics that should be considered when planning a floating point absorber WEC (Faizal, Ahmed, and Lee 2014)

3.2.1 Power take-off systems

The power take-off (PTO) systems are mechanisms used to transfer energy from waves to the generator. It converts mechanical energy into electrical energy. The energy that is produced by a WEC is not continuous. In order to connect the device to the main grid, electricity has to be converted from irregular mechanical energy to electrical energy, with a constant frequency and amplitude. There are two types off PTO systems: (Faizal, Ahmed, and Lee 2014)

- Direct drive system- The moving part of the WEC is connected to the moving part of the electrical generator, eliminating the intermediate converting devices, such as hydraulic systems and air turbines;

- Buffered system- The oscillating energy is captured and stored in a buffered system, such as hydraulic storage or elastic component. After this process, it is transferred to the generator;

On one hand, the rack and pinion system is considered to be a direct drive system. That said, a multiplication factor does not influence this classification. On the other hand, a hydraulic pumps system is described as a buffered system.

The conversion between the electrical power and the mechanical power is more complex when the mechanical power is not constant. One solution could be applying a flywheel to maintain a continuous rotation at the design speed. (Faizal, Ahmed, and Lee 2014)

3.2.2 Wave-Structure Interaction

If a WEC absorbs wave energy, it will remove energy from the wave. The WEC captures energy from an incident wave and a circular radiating wave is generated, as it can be seen in Figure 17. If a WEC does not absorb energy from an incident wave, it will remain static, destroying the incoming waves.

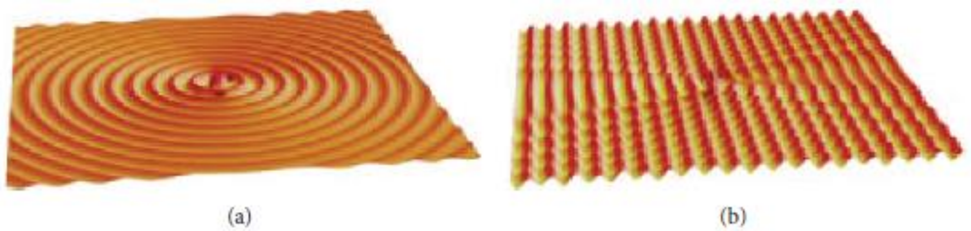

Figure 17- Wave radiation by a buoy in heave (a) in a clam water (b) for incident wave interacting with the device (Faizal, Ahmed, and Lee 2014)

In a generic way, equation 4.1 shows how the absorbed power, P_{abs}, can be calculated.

$$P_{abs} = P_w - P_c \tag{4.1}$$

Where P_w is the wave power and P_c is the power created by WEC when the waves are spread in a radial direction.

Figure 18 is used to make a comparison between the dimension of the point absorber and waves. In a point absorber, the dimensions should be smaller than *x/2*.

If the wave gets steeper, a floating WEC with a length greater than *x* will submerge.

Even if there is no structural damage, the power output will not be maximized. (Faizal, Ahmed, and Lee 2014)

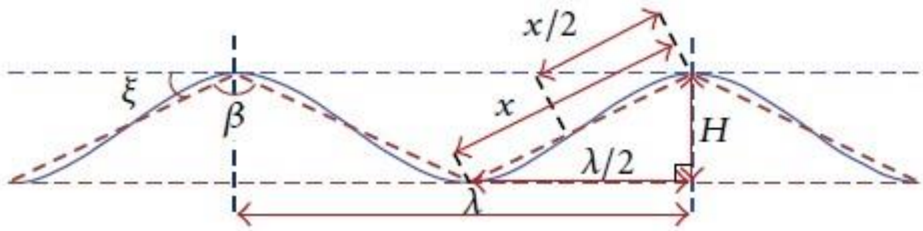

Figure 18- Schematic diagram of wave characteristics (Faizal, Ahmed, and Lee 2014)

In Figure 18,   is pitch angle (greater than 30∘ in a breaking wave), β is the internal crest angle (less than 120∘ in a breaking wave), and x is the linear distance the trough to crest.

There are several loads that affect the PA structure:

- The radiation forces are formed when the body pushes the fluid out of the way, creating radiating waves; (OpenCourseWare 2009)
- The wind drag forces created by the deflection of the fluid from its course;
- The dynamic pressure load integrated over the body surface, assuming that the presence of the body does not affect the flows; (OpenCourseWare 2009)
- The inertia and drag forces are created when a surface wave runs into the structure. The drag forces are due to the current and wave movement. The inertia forces are due to the device response to the wave excitation. Both forces are described by Morison's Equation. (Haym Benaroya 2009)

Morison's equation is only used for small structures, which the diameter of the device is less than 20% of the wavelength. For larger structures, the drag forces become irrelevant.(Faizal, Ahmed, and Lee 2014)

Even though the Morison equation was not used during this project, it is presented for future developments. It was not studied because the device was not determined. Also, there are coefficients that need an empirical approach to be determined.

In Morison's equation, there are two equations according to the device's characteristics, floating or fixed. They can be used to calculate the wave forces acting on a cylindrical shape. For floating bodies, equation 4.2 should be used. (Sato 2009)

$$F = \rho V\dot{u} + \rho C_a V(\dot{u} - \dot{v}) + \frac{1}{2}\rho_w C_d S(u - v)|u - v| \tag{4.2}$$

Where, v is the horizontal velocity of the floating body, u, is the horizontal velocity of the water at the radial direction, V is cylinder's volume per unit height, S is the cross section area, and ρ_w is the water density.

Morison's equation has two empirical hydrodynamic coefficients, a drag coefficient, C_d,and an added coefficient, $C_{a,}$ which are obtained by experimental data.

The first term is created by the unsteady pressure field generated by the undisturbed waves (Froude-Krylov force), the second represents the inertial force, and the third is due to the drag force.

3.2.2.1 Added mass

In a hydrodynamic study, when the wave-structure is made, the body is considered to be heavier than it actually is. The body has an extra mass called added or virtual mass.

When a body moves through a liquid, it pushes the fluid out of the way. If the body wants to accelerate, the surrounding fluid will also be accelerated.

Importantly, when the natural frequency is studied, the buoyancy effect and the added mass term should be considered.(White 1999)

Although the hydrodynamic analysis was not performed, it could be taken into account for future projects.

3.2.3 Stability

Bearing in mind the floating body presented in Figure 19, in a steady state analysis, when the body is in equilibrium, it only has two forces: Force of gravity and buoyancy created by the displacement of the fluid around the body.

Assuming a balanced body, the sum of the horizontal and vertical forces are equal to zero, which means that the forces are equal and in opposite direction.

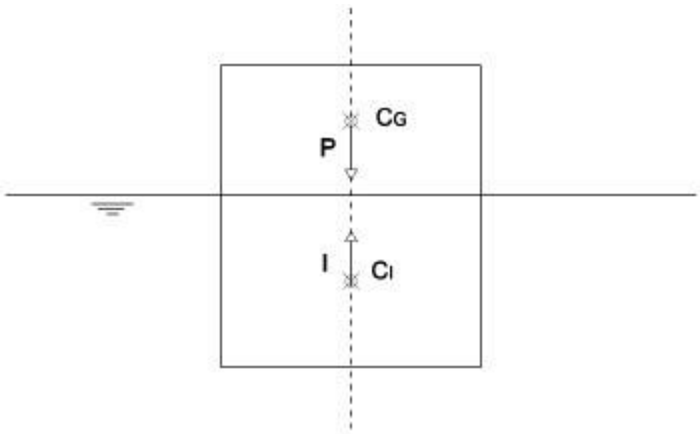

Figure 19- Equilibrium state for a floating body (Paredes, 2008)

Archimedes' theory says that buoyancy is a vertical force exerted by a fluid that opposes the weight of an immersed body. It is proportional to the displaced fluid by the body, ~~V.~~ If floating, like in Figure 19, the body displaces a weight of the fluid equal to his own weight, C_G is the center of gravity and C_I is the center of buoyancy which is the centroid of the displaced volume of fluid:

$$\boldsymbol{C_I = \frac{1}{\forall} \iiint_{\forall} r \, d\forall} \tag{4.3}$$

Where $\forall$ is the submerged volume, r is the positional vector. The center of buoyancy is where the buoyancy force is applied.

Now, let's consider Figure 27 where the body is slightly steep.

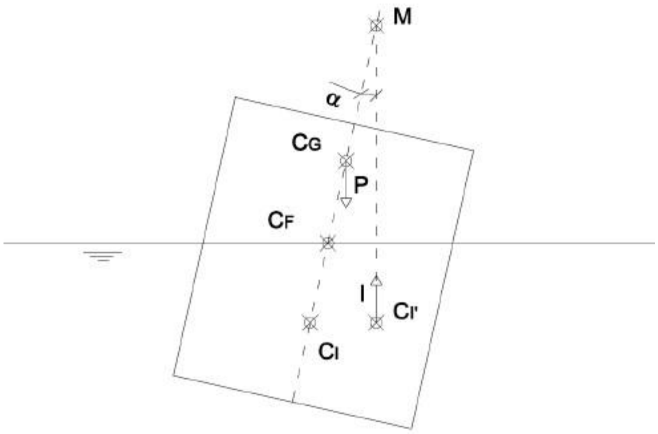

Figure 20- Floating body slightly steep (Paredes, 2008)

Considering the center of fluctuation, C_F, where the slightly rotation moment is applied. It is sown in Figure 20 that although the center of gravity did not change, the center of buoyance slightly changed to the right to C_r due to the change in the submerged volume. With this change the heeling moment is given by equation 4.4:

$$P * \overline{C_G M} * sen(\alpha) = I * \overline{C_G M} * sen(\alpha) = \forall \rho g * \overline{C_G M} * sen(\alpha) \tag{4.4}$$

Where P is the gravitational force, α is the angel between the line that crossed C_G and C_I and another line in the buoyance direction (Figure 20). The interception point of both lines is called metacenter, M. For angles between 10-15° , M and C_F can be consider static.

The segment $\overline{C_G M}$ is called metacentric height. It is considered positive when M is above C_G and negative when is below C_G.

As it can be seen in Figure 21, according to the variation in step there is a change in the metacenter. Let's consider a small rotation, where the metacenter is above C_G. The heeling moment is positive, equation 4.4, creating a reconstructive torque. When the metacenter is below C_G, the torque created by the weight and the righting arm flips over the body. The righting lever arm is the horizontal distance between the buoyancy and gravitational force, also known as $\overline{GZ}$.

$$\overline{GZ} = \overline{C_G M} * sen(\alpha) \quad (4.5)$$

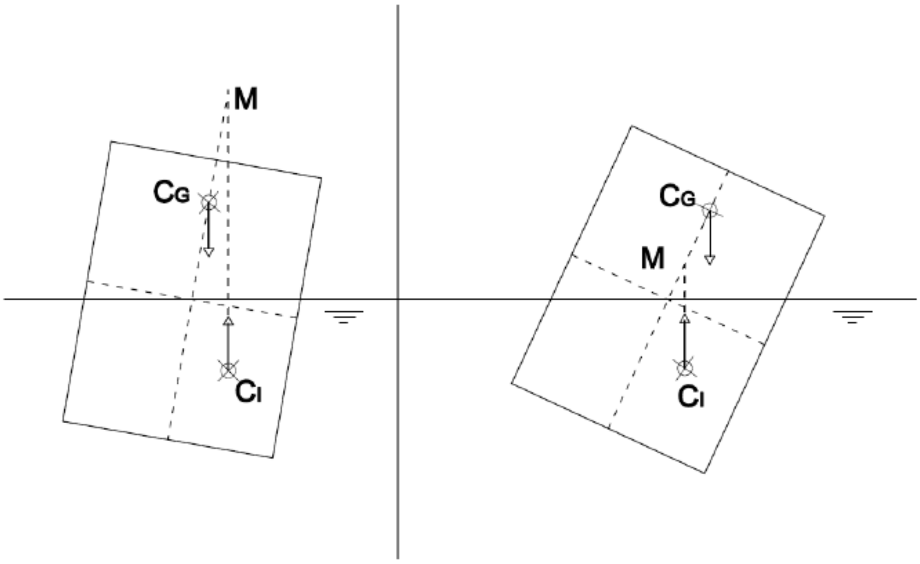

Figure 21- Variation of the metacenter according to the steep (Paredes, 2008)

For a floating or submerged body, during a positive metacentric height the device is stable. If there is a negative height the body will rotate to a more stable position. Two examples of submerged bodies can be seen in Figure 22, left side is unstable and the right side is stable.

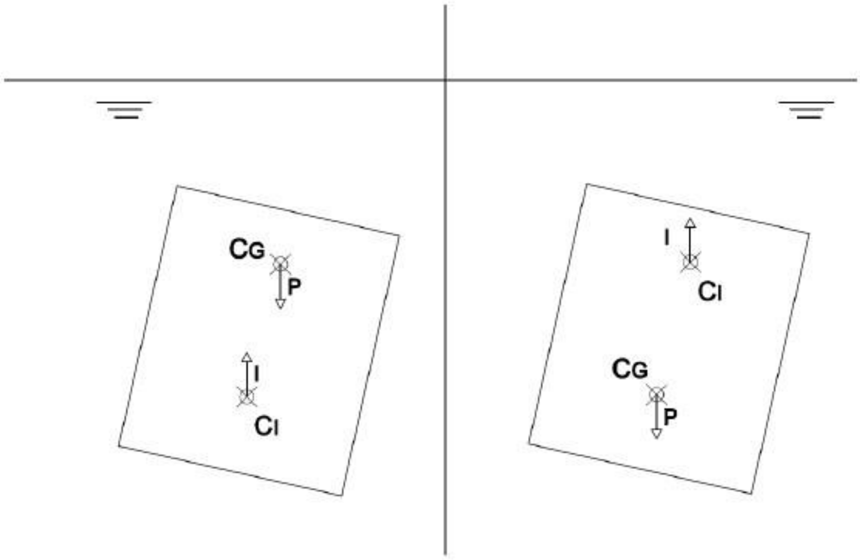

Figure 22-Equilibrium in a submerged body (Paredes, 2008)

In Figure 23 there is a symmetric body regarding the y axis, where de O (center of fluctuation) can be considered steady. The angle between the surface line and the z axis is α. For the next analysis please take into consideration that dA is the element of added submerged area with $ztan(\alpha)$ as its height, and that the axes move with the body.

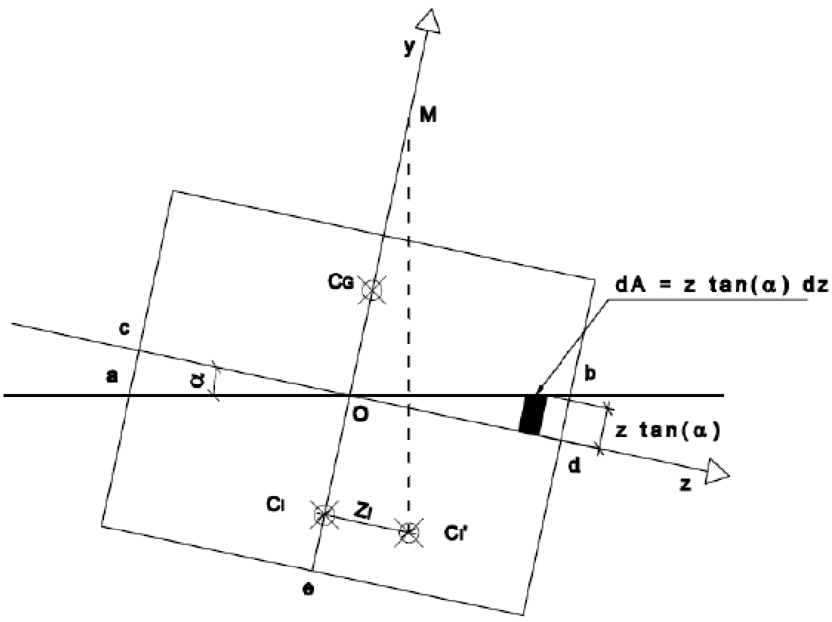

Figure 23- Image for analytic calculation of the metacenter (Paredes, 2008)

Figure 23 is used to understand the formulation to calculate the metacenter analytically.

With the rotation of the body, cOa corresponds to the emerged area and Obd is the submerged area. As the submerged volume is constant cOa is equal to Obd. The new center of impulsion position is calculated by equation 4.6.

$$\boldsymbol{z_l * V_{aObde}} = \int_{cOdea} \boldsymbol{z\, dV} + \int_{Obd} \boldsymbol{z\, dV} - \int_{cOa} \boldsymbol{z\, dV} \tag{4.6}$$

Due to symmetry, the first integral is zero. Saying that $dV = L * dA$, where L is the dimension perpendicular to the figure and dA is the plan area. Considering V_{aObde} as $\not{V}$, submerged volume:

$$\begin{aligned} \boldsymbol{z_l * \not{V}} &= \int_{Obd} \boldsymbol{z\, L\, dA} - \int_{cOa} \boldsymbol{z\, L\, dA} \\ &= \int_{Obd} \boldsymbol{z\, L\, (z\, tan(\alpha))dz} - \int_{cOa} \boldsymbol{z\, L\, (-z \tan(\alpha))\, dz} \\ &= \boldsymbol{\tan(\alpha)} * \left(\int_{Obd} \boldsymbol{z^2\, L\, dz} + \int_{cOa} \boldsymbol{z^2\, L\, dz} \right) \\ &= \boldsymbol{\tan(\alpha)} * \left(\int_{Obd} \boldsymbol{z^2\, dA'} + \int_{cOa} \boldsymbol{z^2\, dA'} \right) \\ &= \boldsymbol{\tan(\alpha)} * \int_{water\ line} \boldsymbol{z^2 dA'} = \boldsymbol{I_O \tan(\alpha)} \end{aligned} \tag{4.7}$$

Where dA' is the element of area for the horizontal section obtained with the water line, I_O is the area moment of inertia form the same horizontal section regarding O (xx axis). From Equation 4.7,

$$Z_l * \not{V} = I_0 \tan(\alpha) \tag{4.8}$$

As

$$\frac{Z_l}{\tan(\alpha)} = \overline{MC_l} \tag{4.9}$$

So

$$\frac{I_o}{V} = \overline{MC_I} = \overline{MC_G} + \overline{C_G C_I} \tag{4.10}$$

$$\overline{MC_G} = \frac{I_o}{V} - \overline{C_G C_I} \tag{4.11}$$

Equation 4.11 allows calculating the metacentric height analytically. (Paredes 2008)

3.2.3.1 Stability curve

For the floating device to be stable, the righting lever arm, $\overline{GZ}$, should be positive. In Figure 24 it is sown a schematic diagram of a stability curve. This curve depends of the applied loads, size and shape of the body that is studied. The area under the curve gives the righting energy, and the larger this area is the greater the capacity of the floating device to be stable.

For a particular angle, the maximum $\overline{GZ}$ will occur. It will give the largest steady heeling moment that a floating device can resist without overturning. When $\overline{GZ}$ is equal to zero that particular angel is call vanishing stability. As was told before when $\overline{GZ}$ is negative the capsize occurs.

When the geometry is too complex, simulation software is used to compute the stability curve.

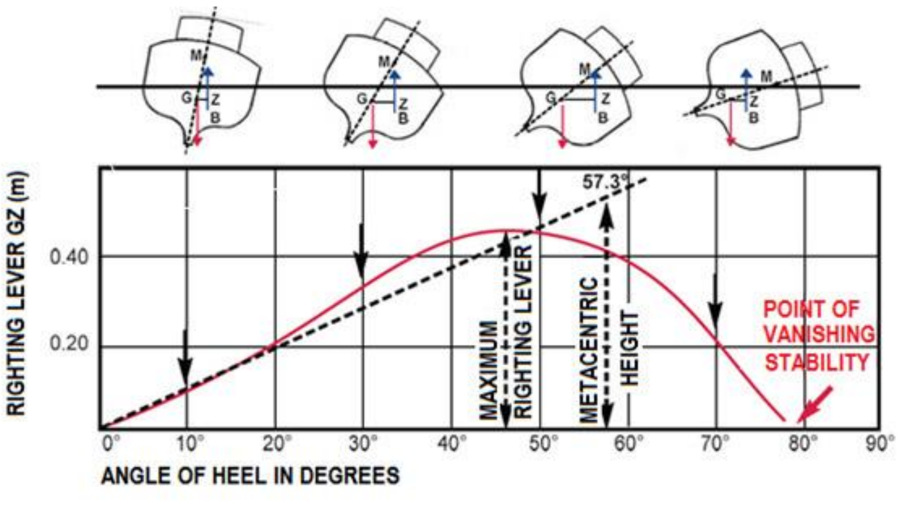

Figure 24- Schematic diagram of a static stability curve (Vefnámskeid)

The mass distribution of the device can change due to effects of liquids with free surfaces, due to freely suspended loads, and due to loads applied from the mooring system. This can lead to a change in $\overline{GZ}$ creating instability.(Faizal, Ahmed, and Lee 2014)

3.2.4 Natural frequency

The structure of a floating device has its own natural frequency which is determined not only by its mass and the elastic characteristics of the structure. The response of a point absorber depends on the frequency of the exciting waves. When the natural frequency of the device is the same as the frequency of the excitation waves, maximum power can be generated.

In the device, it can occur two types of oscillation; free oscillation, there are no external forces acting on the device, and forced oscillation there are external forces acting on the device forcing it to vibrate. The last one continues as long as the excitation force is presented.

Damping is the dissipation of energy by resistance. For small damping, the device will take longer to be in the equilibrium position. For large damping, the device may not oscillate at all before coming back to rest, even when the device is excited externally at its natural frequency. For wave energy converters, damping is introduced due to the buoyant and mooring forces.

Because the wave energy converters usually have multiple degrees of freedom. The differential equation of motion for several degrees of freedom can be seen in equation 4.11. (Faizal, Ahmed, and Lee 2014)

$$a_{mn}\frac{d^2x}{dt^2} + b_{mn}\frac{dx}{dt} + c_{mn}x = d_{mn} \tag{4.11}$$

Where amn is the total mass in m direction due to a motion in n direction, bmn is the damping in $m$direction due to a motion in n direction, cmn is the spring coefficient in m direction due to a motion in n direction, and dmn is a linear reaction force in m direction due to a motion in n direction. a is the virtual mass ($m_d + m_w$), m_d is the mass of the device, m_w is the added mass, b is the damping coefficient, c is the spring coefficient, and d is the excitation force. For a single degree of freedom, $X_a \sin \omega t$.

In multi degree of freedom system, each degree of freedom can be related to each other. It is used Laplace transforms to solve this problem.(Faizal, Ahmed, and Lee 2014)

3.2.5 Mooring System

According to the forces acting on the structure, referenced in section 3.2.2, the floating device needs a mooring system in order to be placed in the open sea. Otherwise, with several forces acting, it will not remain in the desired place.

The depth of water, costs, and complexity of the system can determine which type of mooring show will be used. For example, for shallow waters one of the most regular options is to use a rigid structure. For deep water, when the reduced cost is an objective, or when a certain degree of freedom is necessary, anchors are used.

In a WEC, some requirements should be taken into consideration: (Paredes 2008)

- Displacement limitation should be rigid enough to support constant forces, avoiding significant displacements. Although, a certain degree of freedom is needed in order to respond to the wave excitation;
- Easy to install and positioning;
- Low maintenance;

The associated costs for a mooring system can exceed the other subsystem costs. It is a determining factor in the cost-effectiveness of the total system.(Faizal, Ahmed, and Lee 2014)

The mooring system has three components: the line, the anchor and the structure connection, Figure 25.

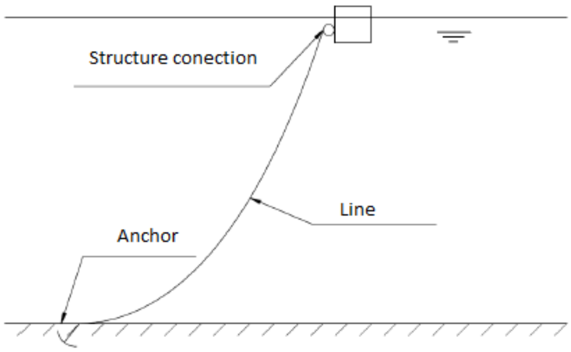

Figure 25- Mooring system components(Paredes 2008)

3.2.5.1 Mooring lines

Two categories of material are mostly used for mooring: metals (wire or chain) or synthetic materials (poliamide nylon cord, polyester). Metal chains are heavier and less elastic, so they create more vertical forces due to their weight. Synthetically ropes are more elastic, lighter, and sometimes even with higher breaking strength.

According to the different configuration of mooring line the rope or chain suffer different forces, so things like material, weight, elasticity, and breaking strength have to be taking into account when selecting the mooring line. The loads that are applied in the structure are transmitted to the mooring system and the other way around it's also true.

There are four types of mooring, Figure 26, catenary, taut line, semi-taut line, and vertical. The catenary presents an arc profile while on the taut line the lines are straight. Vertical mooring presents the lines straight to the floor.

The mooring objective is to confine the structure to a specific area in the surface of the sea.

The rising and falling of the tide and as well as the degrees of freedom are considered when selecting the type of mooring. Taut-line is able to support vertical and horizontal forces while catenary line supports much more vertical than horizontal. Vertical profile support mainly vertical forces. (Dias 2013, Paredes 2008)

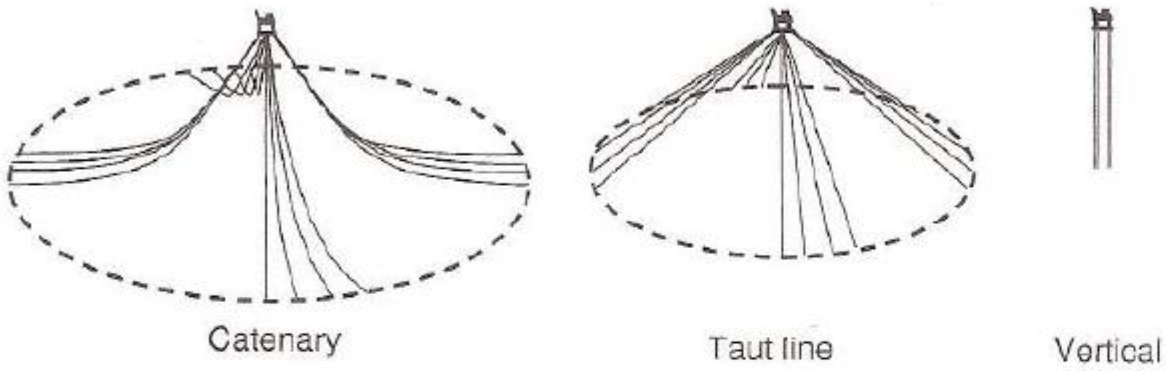

Figure 26- Different configuration of a mooring line (Dias 2013)

3.2.5.2 Catenary

For the purpose of this work, it is only going to be analyzed the catenary system because it is the selected mooring for our WEC.

The catenary profile creates vertical and horizontal forces in the structure. The main formulas to calculate this forces are: (Paredes 2008)

Catenary mooring horizontal forces:

$$F_H = \frac{w\,l}{\cosh(\frac{w\,h}{F_H} + 1)} \quad (4.11)$$

Catenary mooring vertical forces:

$$F_V = w\,s \quad (4.12)$$

Total force on the line in a y position:

$$F_m = F_H + w\,y \quad (4.13)$$

The length of the line in the x position:

$$s = \frac{F_H}{w}\sinh(\frac{w\,x}{F_H}) \quad (4.14)$$

y position according to an x position:

$$y = \frac{F_H}{w}\left(\cosh\left(\frac{w\,x}{F_H}\right) - 1\right) \tag{4.15}$$

Where, *y, s, x,* and *h* can be seen in Figure 27, *w* is the weight of the chain and *l* is the rope's length. To apply the previous equation is fundamental to use the origin and the axis like in Figure 28.

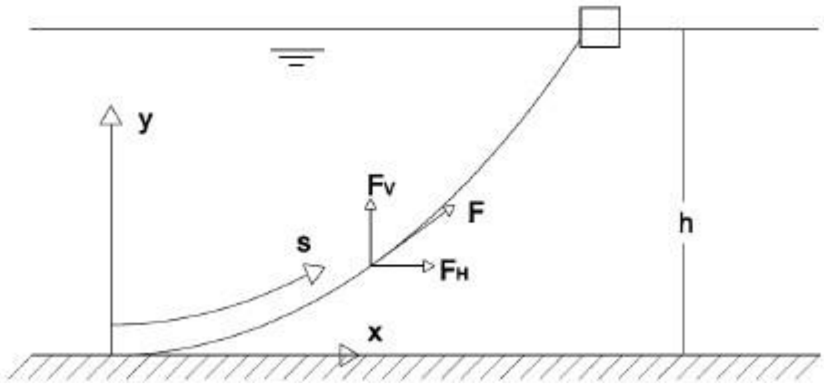

Figure 27- Axis and parameters used for catenary forces analyzed (Paredes 2008)

This expression can only be used if the line is tangent to the seabed and there is no line on the bottom of the ocean. If the line is not tangent, the virtual tangent point has to be calculated and the referential has to start from there. If there is a line on the bottom of the ocean, Figure 28, an iterative process as to be done until the equilibrium point is discovered (several cable lengths should be used). In this case, the expressions are only valid after the last point that is in touch with the seabed.

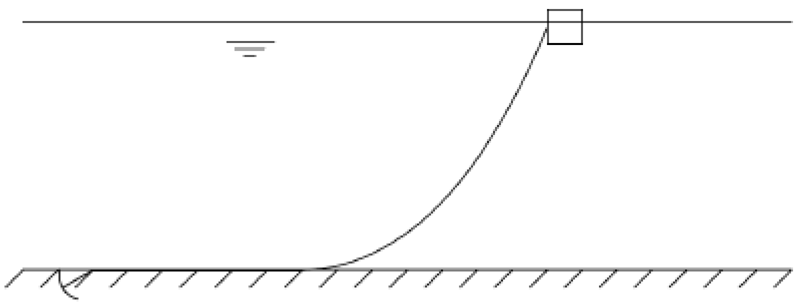

Figure 28- Line partially on the bottom of the ocean. (Paredes 2008)

In equation 4.11, the vertical force F_H has to be done iteratively as it appears in both sides of the equation. For each catenary, it only has to be calculated once, as it does not depend of x position. (Paredes 2008)

3.2.5.3 Mooring configuration

In Table 1, it is presented the three types of mooring systems, single point, spread mooring and dynamic mooring.

Table 1- Possible mooring configurations that can be applicable to floating point absorbers. Adaptation of (Faizal, Ahmed, and Lee 2014)

Single point mooring	
Turret mooring	A turret is a device that is directly built into the floating device and attached to the seabed using catenary anchor lines. A bearing arrangement on the turret allows for weathervaning of the floating point absorber.
Fixed tower mooring	A tower is installed with a turntable to carry the mooring line to allow weathervaning of the point absorber.
Catenary anchor leg mooring	A buoy is a catenary moored to the seabed, and then the point absorber is moored to the buoy.
Single anchor leg mooring	This is the simplest one. A single vertical tensioned/catenary mooring leg is installed in the seabed
Spread mooring	
Spread mooring consists of multiple mooring lines connected to a floating device and extending outwards and anchored to the seabed, providing a restriction to weathervaning. This system can be used in deep waters and in applications where the wave direction concern is not high. However, since weathervaning will be restricted, the wave and current forces on the floating device as well as the mooring system will be really high.	
Dynamic mooring	
A dynamic positioning system automatically maintains the floating device at the desired position through the use of thrusters or propulsion either on the device or mooring line ends.	

3.2.6 WEC's shapes

Four different shapes were considered to perform a power-volume analyses, as can be seen in Figure 29.

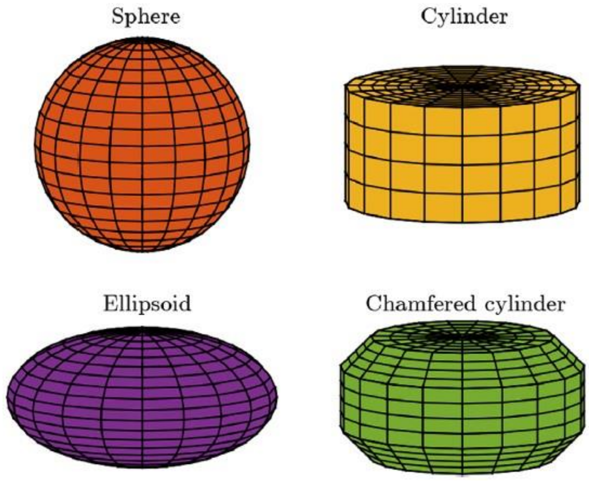

Figure 29- Shapes of WECs utilized in the power-volume analysis (N.Y. Sergiienko, 2017)

The submerged buoys had different forms, so an equivalent spherical radius was created in order to be possible to compare the different geometries, called equivalent spherical radius. For the floating PAs, a cylinder shape was used.

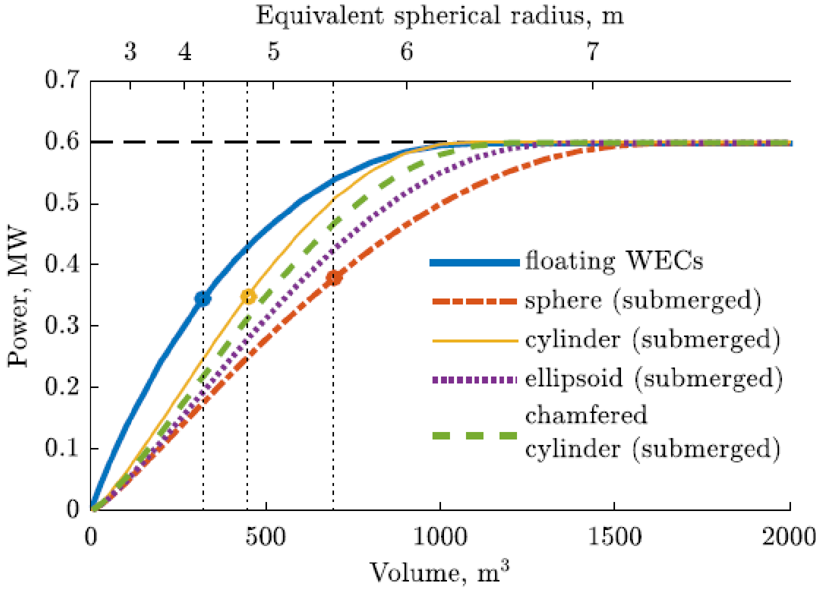

Figure 30- Power-volume analysis of WECs for the regular wave of H = 2 m; T = 8,5 s. The several colors represent the different shapes and the floating vs. submerged buoy.(N.Y. Sergiienko 2017)

Some conclusions can be drawn from Figure 30:

- For submerged shapes, to extract the same power it is needed less volume with the cylindrical floating buoy.
- The floating PA is more efficient then the submerged ones when considering the ratio between power and volume.
- The size of submerged buoys designed for the same site should be 1.4-2.2 larger than the floating one with approximately the same power capacity.
- Among the submerged case, a body with cylindrical shape is the smallest for the same power generated.

The level of the average absorbed power and the relative capture width are shown in Figure 31.

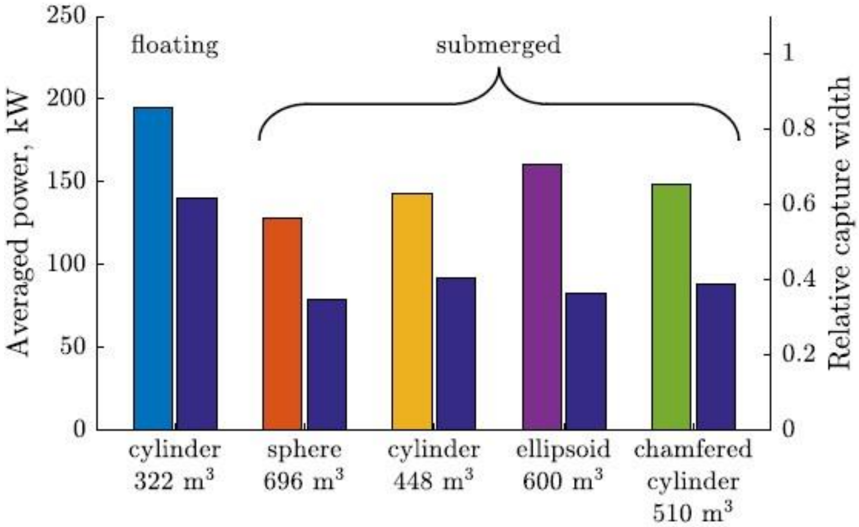

Figure 31-Levels of the average absorbed power (color bars on the left) and relative capture width (dark blue bars on the right) of the floating and submerged converters at the irregular wave time-series of Hs = 2,83 m and Tp = 10 s. (N.Y. Sergiienko 2017)

The floating and the shape cylinder PAs are the ones with more average power and relative capture width. (N.Y. Sergiienko, 2017)

3.2.7 WEC's dimensions

3.2.7.1 Single Buoy

The size can influence the power that is absorbed by a PA.

The first analysis was according to the size variation in a spherical shape. The body size influences the power efficiency of the point absorber. The power absorption curves for floating spherical bodies of six different radius, a, (3-8m) are shown in figure 10.

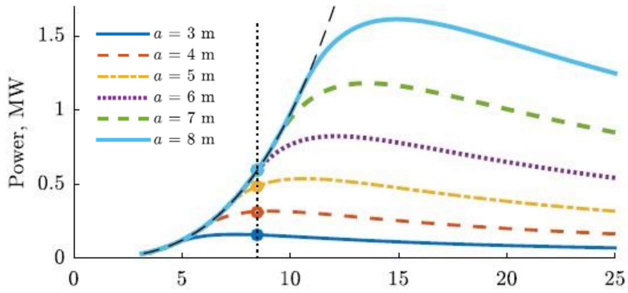

Figure 32- Power absorbed by the floating spherical WECs of different radius according to various wave periods. The dotted vertical line and points on curves correspond to the targeted wave period of T = 8,5 s. (N.Y. Sergiienko, 2017)

In Figure 32, it can be concluded that for the same wave period the bigger the radius more power can de PA produce.

3.2.7.2 Array of small buoys

In this section, for a floating and cylinder buoy, different arrays were studied. The objective was to compare, with the same volume, a large buoy or different size combination of several buoys. In Figure 33 results are described.

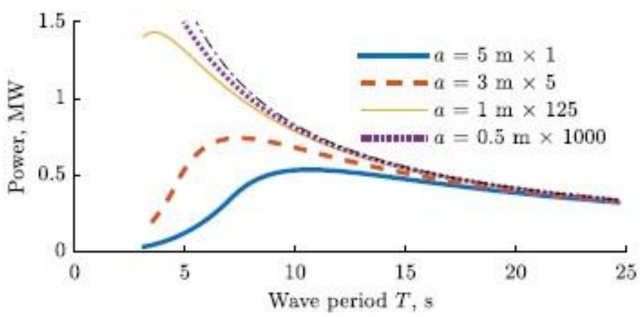

Figure 33- Power absorbed by floating structure, all with the same total volume V=524m^3 in regular waves of 2m of height. The different arrays are represented by different colors. (N.Y. Sergiienko, 2017)

As it can be concluded from the graph, for floating structures, if the number of buoys increases and the size of each one decreases, more power can be extracted in each wave period.

It this case the economy of scale is also an advantage as increase the quantity, the price per unit drops significantly.

3.2.7.3 Design of the arrays

It was previously studied that the arrays can extract more power than a single buoy. So, this study from Guedes Soares, Ashank Sinha, D. Karmakar was conducted. In Figure 34, the different arrays are presented.

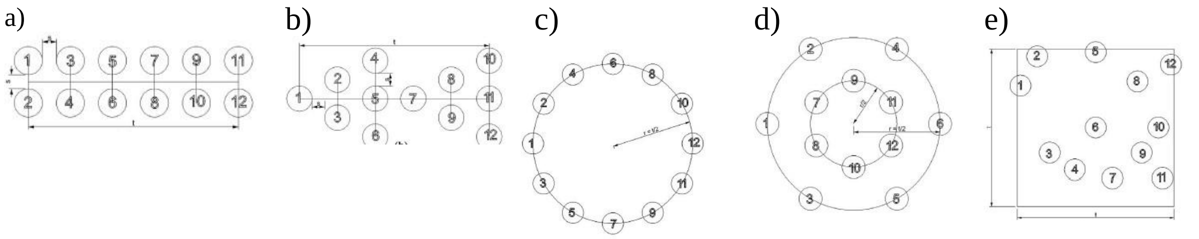

Figure 34- a) Linear arrangement of array of floaters. b) grid arrangement of array of floaters c) circular arrangement of floaters d)Concentric arrangement of array of floaters e) Random arrangement of array of floaters (Ashank Sinha 2016)

This several arrays were analyzed according to the wave heading, as it can be seen in Figure 35. The wave heading is the direction of propagation of the wave according to the beach. For a wave heading of $\theta = 0°$ the incoming waves would propagate from left to right.

An optimization and controlled parameters was done in order to obtain the better spatial organization. The results that were obtained are. (Ashank Sinha 2016)

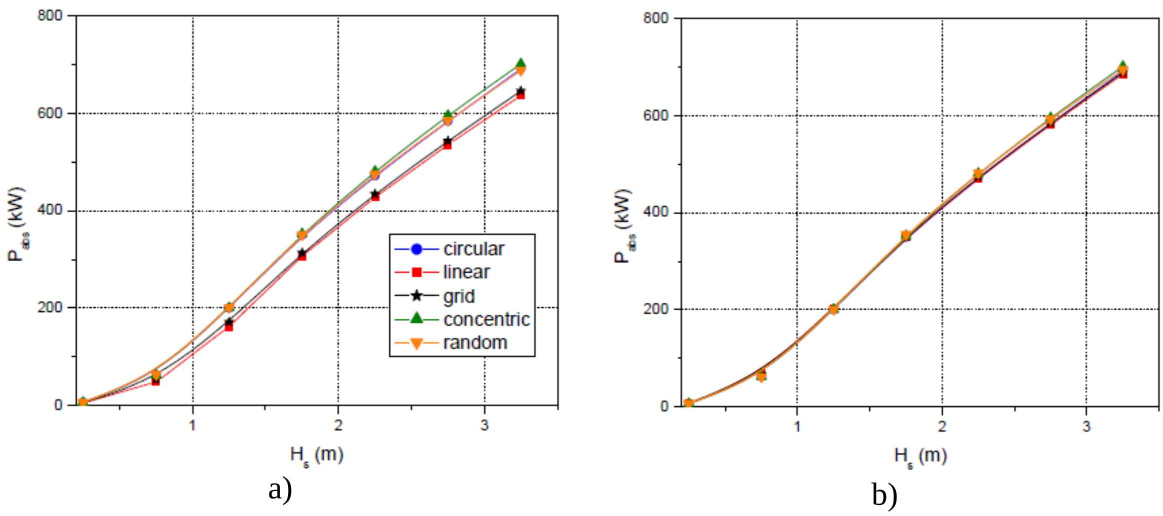

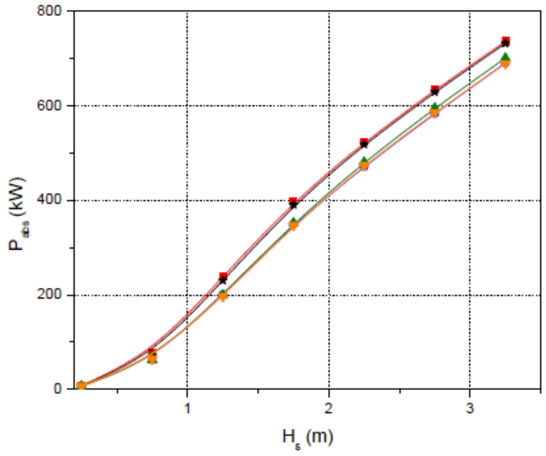

c)

Figure 35- Power absorbed with the converter according to the height of the wave. Different arrays were analyze a) wave heading where $\theta = 0°$ b) wave heading where $\theta = 45°$ c) wave heading where $\theta = 90°$ (Ashank Sinha 2016)

From Figure 35, it can be said that there are two groups that present similar power absorbed according to different wave headings. The first group, are the ones that extract more power when faced with 0° wave heading, corresponding to circular, concentric and random arrays. The second group, corresponded to the ones that extracted more power when faced with 90° wave heading, corresponding to linear and grid arrays. For a 45° wave heading the direction the type of array is not relevant.

To conclude, it has to be analyzed the type of wave heading that the implementation site has in order to select the array.

3.2.8 Scaled modeling

For scaled modeling, first, the real WEC is mechanically designed and measured according the real environment conditions.

Then, a scaled model is created to provide design and concept validation, and empirical coefficients that would be used in simulation and design of the real scale prototype. Normally offshore WEC model test have between 1:80-1:25. A normal wave-structure interaction involves the Reynold number, Froud number and Keulegan-Carpenter number. It is very difficult to satisfy simultaneously all the numbers, so it has to be given priority according the main characteristics that want to be tested. (Faizal, 2014)

Even though it is not common, there are some devices that were planed the other way around. First it was created, model a small prototype. Then it was thought what the problems and constrains were if a real scale prototype wanted to be created.

Creating a prototype or a model varies according to the surrounding conditions that are applied to our system. It is an iterative process that has more than one answer to solve the same problem.

4 TRIPOWER UP: Concept Presentation

In this section, the starting point of the hybrid ocean energy converter, *TRIPOWER UP*, is presented. This device can produce electricity from renewable energy such as waves, wind and/or currents. (Macieira 2017)

Here, Miguel Macieira's dissertation is referred to as it presents the first design of the WEC that is now going to be dimensioned and redesigned.

First, the general device description is introduced, then the previews of the kinematic system is shown. In the end, the two structures are examined, WEC structure and support structure. WEC it is used to produce energy and the support structure is used to support all of the system.

4.1 General device description

The main lines of the project that were developed are presented in Figure 36.

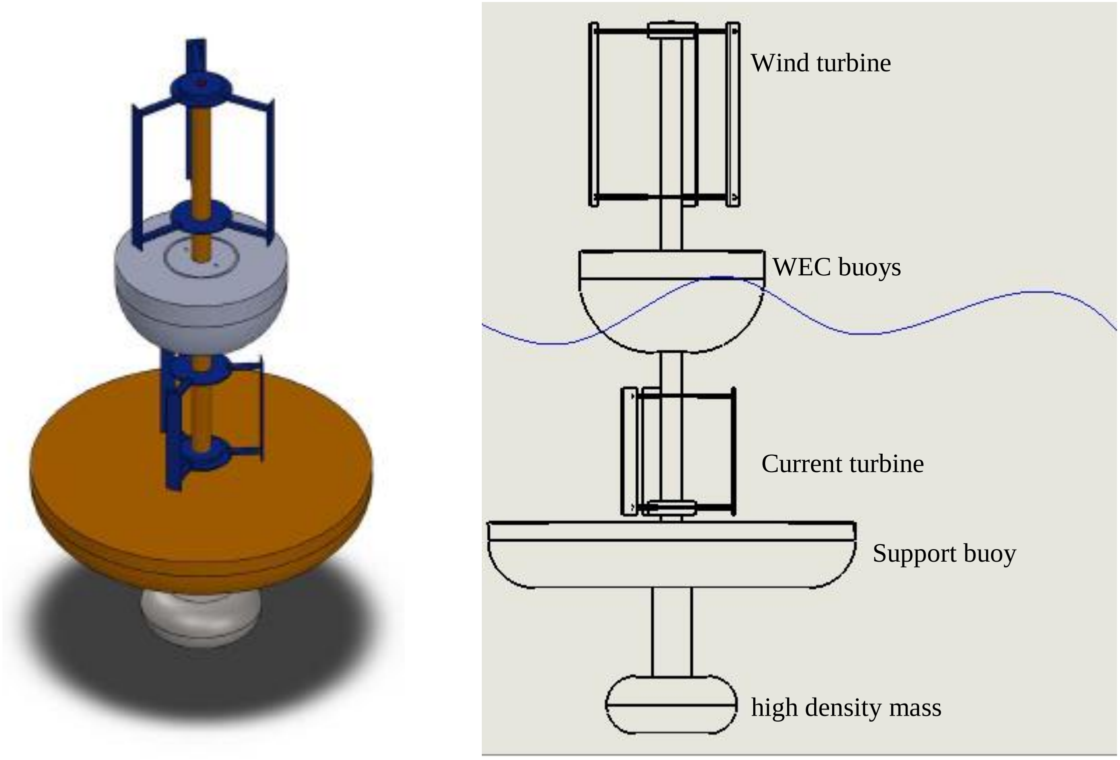

Figure 36- Hybrid ocean energy converter – *TRIPOWER UP* (Macieira 2017)

On the middle height of the device, occurs the conversion of the variation of potential energy of a buoy that oscillates vertically in accordance with the passage of the waves' crests and trough around the buoy.

The energy collected from each of the ocean energy sources is transferred to a single vertical rotor shaft, in a mechanical additive mode. This creates a more uniform production rate as the rotation can be made by one of the three sources (wave, wind, or currents) or any combination of them. The system has only one generator to convert the mechanical energy into electrical energy.

Each device is designed to be installed on-shore, near the shore or off-shore, with all of them in shallow or deep waters. It aims to operate at any levels of low and high tides, wave amplitude, wind speed and current speed. In all cases, the basic kinematics of each individual device is the same.

This ocean energy conversion device is also designed to be disconnected from the mooring system, in order to be towed back to land for maintenance purposes or in extreme weather conditions. This feature leads to lower maintenance costs and assures the survival of the device in the ocean.

A commercial industrial power production plant can be achieved with the combination of several hybrid devices, disposed of in a grid, producing electrical energy. (Macieira 2017)

4.2 WEC's mechanical transmission

The PTO system is purely mechanical. As it can be seen in Figure 37, it has a WEC's mechanical transmission that transmits the movement from the rack until a single shaft. This shaft is connected to the wind and current converter as well as the generator.

The waves' oscillation moves a structure that induces a descendant and ascendant move of the racks. Energy can be extracted in both directions as the shaft rotates in the same direction independent of the direction of the movement. A linear movement in both directions is converted in one rotation direction.

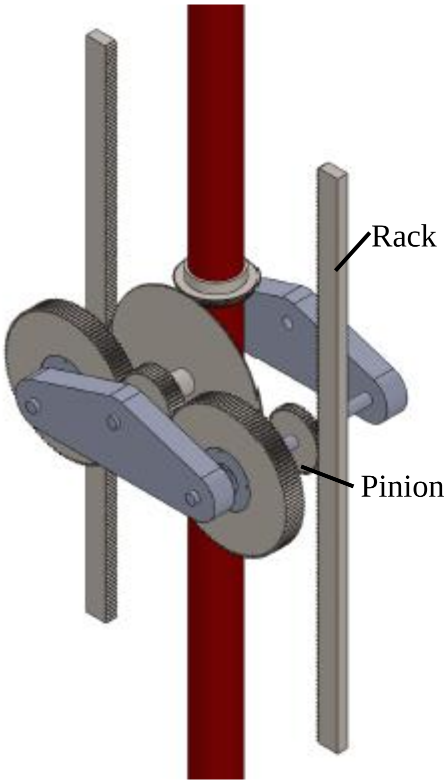

Figure 37-WEC's transmission or kinematic chain. They are located inside the inner buoy of WEC's structure

This transfer of movements is only possible due to a key component, the freewheel in Figure 38. The freewheel is a system that only works if it rotates to one side and it pelts in the other direction.

The freewheel allows the gear, that is connected to the rack, to only transmit the movement to the shaft when it rotates in the direction where freewheel works. Freewheel is described in detail in section 5.3.3.1.

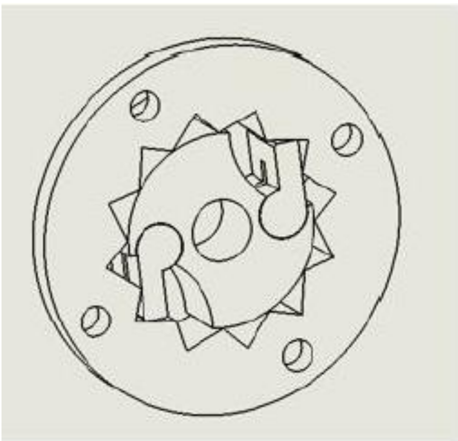

Figure 38- TRIPOWER UP initial freewheel (Macieira 2017)

4.3 WEC's mechanical structure

WEC's mechanical structure is the structure used to extract energy and in this case is mainly composed by the buoys.

The movement of the racks is due to an oscillation of a floating structure that is presented in Figure 39. It can be seen that the structure has three components, named inner buoy and outer buoy that are connected by an elastomer component.

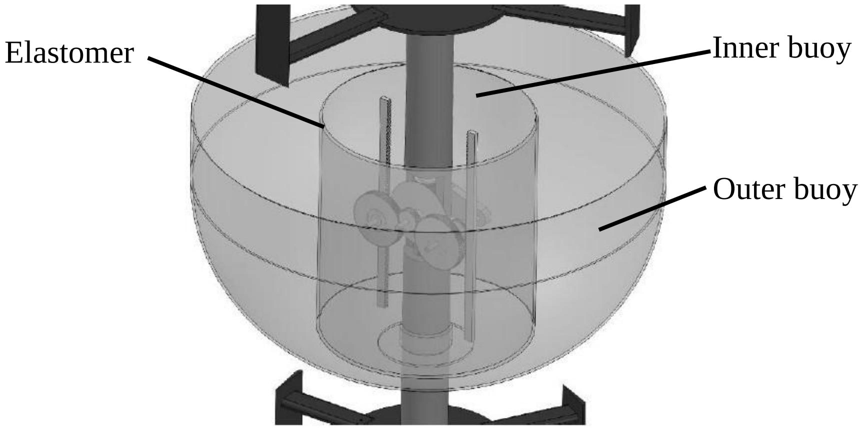

Figure 39-External, inner buoy (transparent) and WEC's transmission

Each element of the structure has different purpose:

- The outer buoy is done to support the impact of the waves. It is a protection from vertical and horizontal wave forces.
- The inner buoy is where the racks are placed. The aim of this buoy is to collect only the vertical force of the waves that will allow the vertical movement of the rack. It is also a protection of the WEC's transmission from the maritime environment.
- The elastomer component is what connects both buoys. Its objective is to transmit only the vertical forces from the external buoy to the internal one. The horizontal forces are not advisable as they can bend the racks and the system will not work properly.

In order for these components to absorb the waves' oscillation, they have to have another structure that is not moving with the same speed as the wave energy converter structure. There has to be a relative movement between this structure and the support structure for the racks to move.

Note that the racks are placed in the inner buoy but the rest of the kinematic has to be placed in a support structure, otherwise, if they move together, the gears will never rotate.

This device will be redesigned and dimensioned in much more detail, in one of the next chapters.

4.4 Support structure

The support structure bears the kinematic chain, not only from the WEC but also from wind and currents converters. It is the structure that braces and connects the three sub-devices.

As it can be seen in Figure 40, this is also a floating structure. The support structure has to have a much bigger inertia than WEC structure in order to create a lag between the floating of both structures. In this way, it is possible to create movement between structures and extract energy.

The Figure 40, shows that it also has a buoy, a high density mass, and a structural colon:

- The buoy has the aim of floating the main structure. Its shape is to increase the drag force that will oppose the movement. This resistance will create a lay between both buoy floating structures, main structure and the inner buoy of the WEC;
- The high density mass on the bottom of the structure has the aim of lowering the center of gravity in order to be under the center of impulsion. In this way, the main structure will be more stable when the environmental forces excite the device;
- The structural column is where all the converters will be attached. Inside this column there is the rotating shaft that is connecting all the kinematic devices, Figure 37.

The mooring system, although not represented, was planned to be in the bottom mass. This structure will be redesigned and dimensioned with much more detail in one of the next chapters.

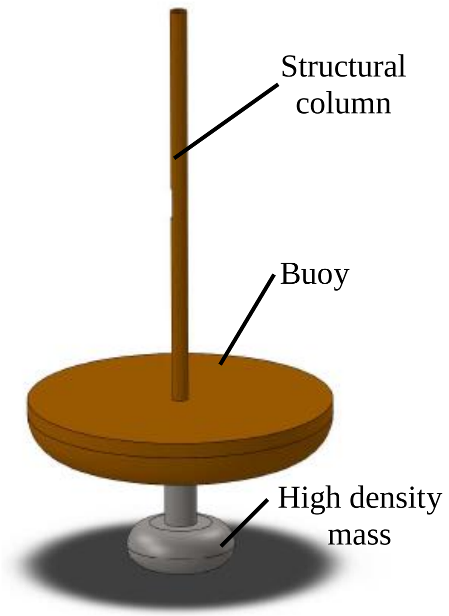

Figure 40-Support structure with support column, buoy, and high density mass. (Macieira 2017)

5 TRIPOWER UP: Mechanical Design

In this chapter is shown the mechanical design of the new *TRIPOWER UP*. After studying the previous *TRIPOWER UP*, there were some changes in the design. All the assumptions and thoughts are evidenced in this section.

5.1 Initial Conditions

5.1.1 Wave tank

Initially, the design was intended to test the prototype in the wave tank of the department of Civil Engineering in FEUP. The wave tank has the following dimensions: 12 m of width, 28 m of length and the maximum depth of 1.2 m. The depth was a huge constrain for the project. In order to fit in the tank, the WEC needed a 1:100 scale. However, there was another constraint to the project that was even more important. It was needed to dimension the prototype according to the parameters that the wave generator was able to generate. So, this constraint was assumed as priority.

Another important aspect is that the wave generator can only operate with the maximum depth of 1 m which, consequently, diminished the possible submerged height of the device.

.

5.1.2 Wave Characteristics

A study to understand the main characteristics of the sea was performed. To obtain the wave and wind characteristics, a data from the year 2016/2017 was used, this data is related to the beach zone was Matosinhos, Porto. Being close to our location and having an area with great energy density (North of Portugal), Matosinhos is one of the places where the actual wave energy absorber can be tested and used, as it is possible to see in section 2.4.

From the Windguru, the maximum, average and minimum sea parameters were calculated as it can be seen in Table 2, Table 3 and Table 4:

Table 2- Statistic of maximum sea conditions in Matosinhos, Portugal, between 01/01/2016 and 31/12/2016

Maximum			
Wind velocity	Wave height	Wave period	Temperature
30 kt => 15.43 m/s	6.10 m	20 s	29°C

Table 3- Statistic of average sea conditions in Matosinhos, Portugal, between 01/01/2016 and 31/12/2016

Average			
Wind velocity	Wave height	Wave period	Temperature
7.66 kt => 3.94 m/s	1.73 m	11.08 s	14.69°C

Table 4- Statistic of minimum sea conditions in Matosinhos, Portugal, between 01/01/2016 and 31/12/2016

Minimum			
Wind velocity	Wave height	Wave period	Temperature
0kt => 0 m/s	0.4 m	5 s	3°C

After observing the actual parameters, it was set initial parameters, considering the tank and the wave generator capability to support and generate waves, as it can be seen in Table 5. These parameters were created to have the same angular speed in the gears of the WEC's transmission, has in the real model.

Table 5- Tank parameters

Tank characteristics			
Wind velocity	Wave height	Wave period	Temperature
1.53 kt => 0.79 m/s	0.35 m	2.22 s	14.69°C

The Reynold's number, the Froude's number, and Keulegan-Carpenter's number are used to modulate a scaled model. For this project, these concepts were not used because it would be a very theoretical and heavy approach, although it could be developed in the future.

The wave parameters were used to examine the forces acting in the device, and also to dimension some structural components. However, the structural resistance for the maximum loads that the WEC could have, will not be analyzed in this project.

The rest of the wave parameters were calculated using the linear wave theory, described in section 2.1.

The wave parameters were calculated assuming that WEC is placed in deeper water. The waves have more energy in this location, as it was mentioned in section 2.3.

The results for the average tank characteristics are presented in Table 6:

Table 6- Tank characteristics

Wavelength (λ)	7.6 m
Period (T)	2.22 s
Celerity (C)	2.32 m/s
Amplitude (A)	0.175 m
Wave height (H)	0.35 m
Wave number (k)	0.83 (m^{-1})
Angular frequency (ω)	2.83 rad/s
Wave phase (θ)	0.83x-2.83t
Power per meter of a wave crest length(J)	260.331 W/m

These are the parameters that were used in the mechanical design.

5.2 Overall design

Due to time constraints, it was only possible to focus the majority of the attention in the WEC. It was done modularly in order to be able to add the wind and current converters. In Figure 41, the WEC and the support structure are developed in this project, and the wind turbine and current turbines should be added in future projects.

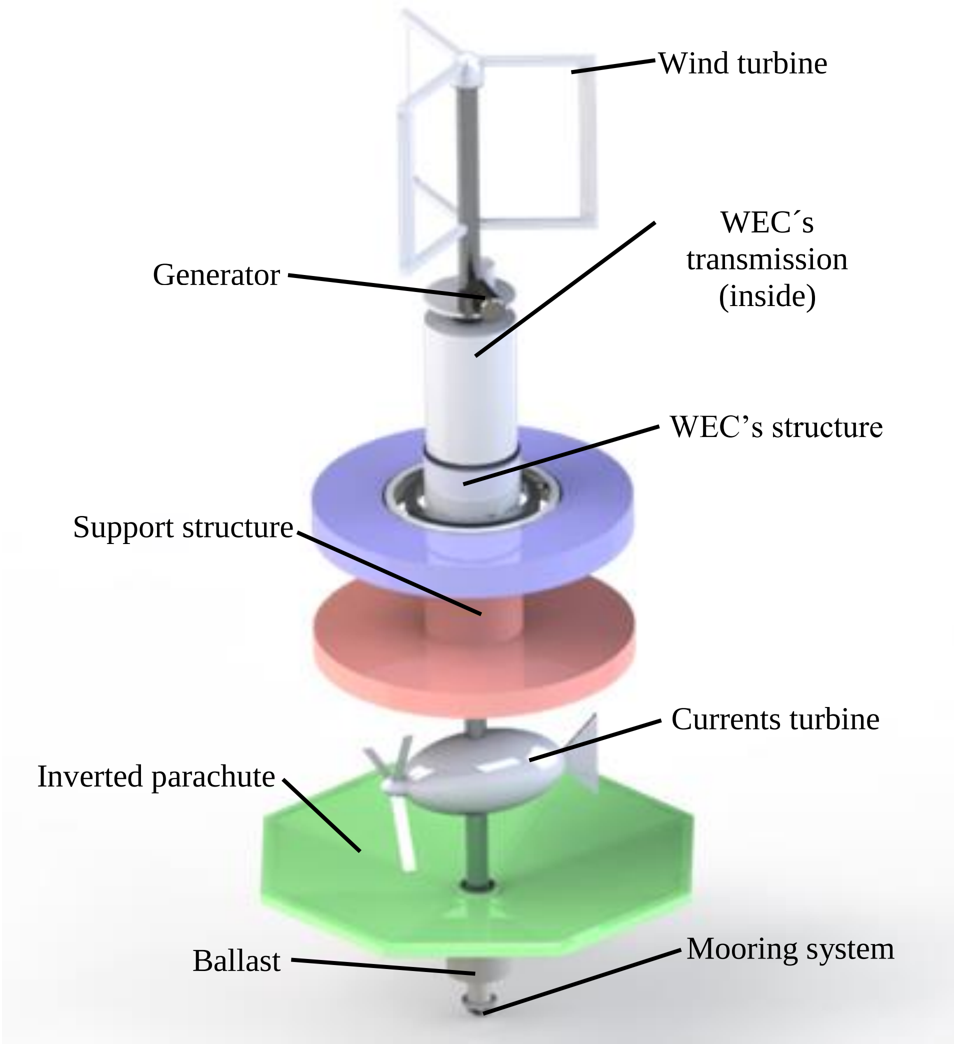

Figure 41-Overall view of our hybrid system Tripower UP

The new TRIPOWER UP is composed by a support structure and a WEC structure, as it was already seen in the previous chapter. The support structure's objective is to carry all the kinematic systems, as it can be seen in Figure 42 a), while the WEC system absorbs the wave power, as it can be confirmed in Figure 42 b).

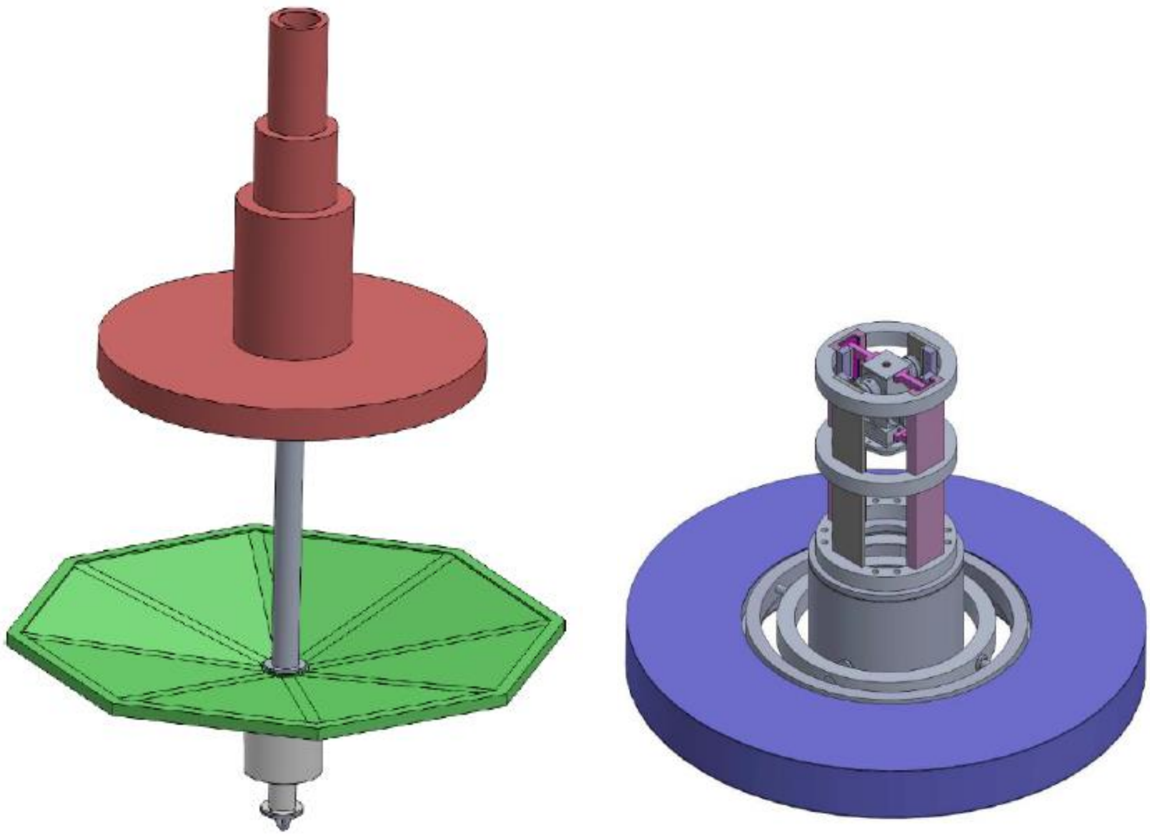

a) b)

Figure 42- New TRIPOWER UP components a) Support structure b) WEC

Instead of describing the mounting sequence it was decided to present the Exploded view in Appendix E. The overall properties are in Table 7:

Table 7- Overall characteristics

Weight	442 kg
Max height	4.00 m
Min height	3.60 m
Max width submerged	2.64 m
Max width emerge	1.50 m

Moreover, the prototype ends up being in a scale of 1:10. In the end of the mechanical design, the structure no longer fits in FEUP's tank. The maximum depth is 1.2 m and the length of the underwater structure is 2.73 m, with a total height of 4 m. Although it will have to be tested in another tank, the wave tank parameters remain constant.

Inside the WEC there are two different subgroups:

WEC´s transmission

a)

WEC’s structure

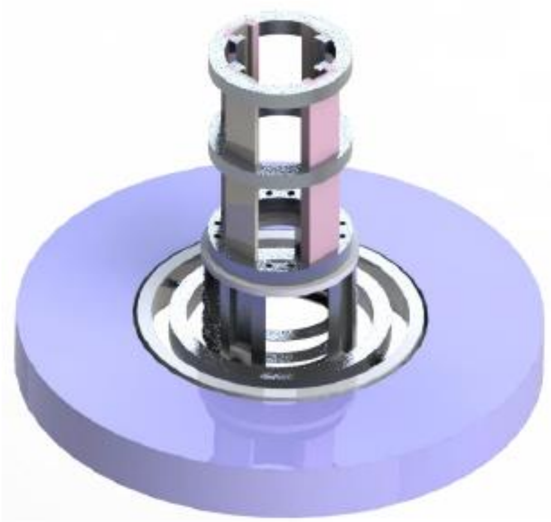

b)

Figure 43- WEC components a) WEC´s transmission b) WEC’s structure

Although they all make part of the WEC, the WEC´s transmission and exterior are analyzed separately because they were developed by two different people. They were connected by the racks and by the guidance system, as it will be explained in the next chapter.

5.2.1 How it works

Figure 44 shows the water level and the Table 7 values:

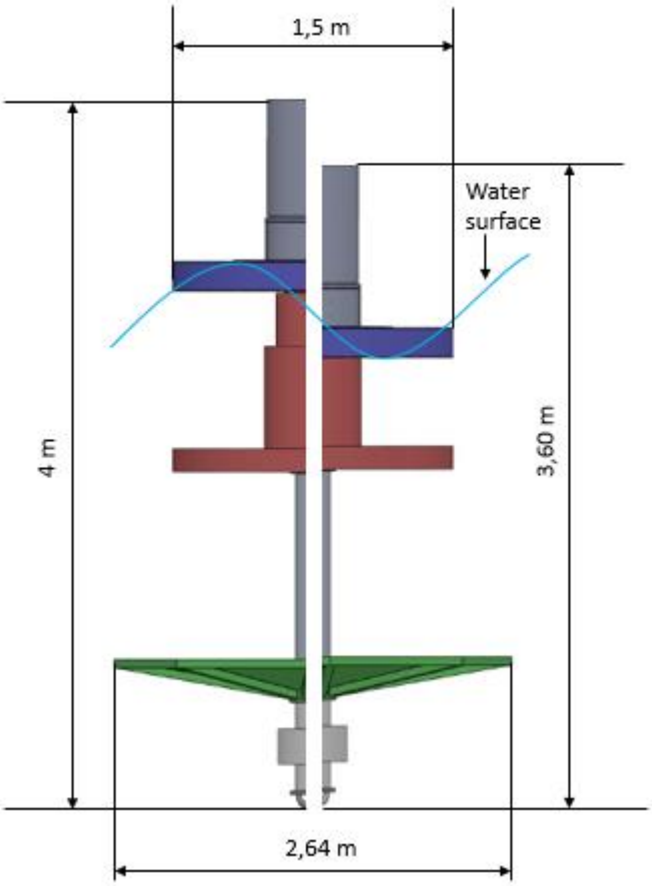

Figure 44- Tripower Up with the water level. The two extreme positions, in the crest and trough, are represented.

Figure 45 is presented to better understand how it works.

\

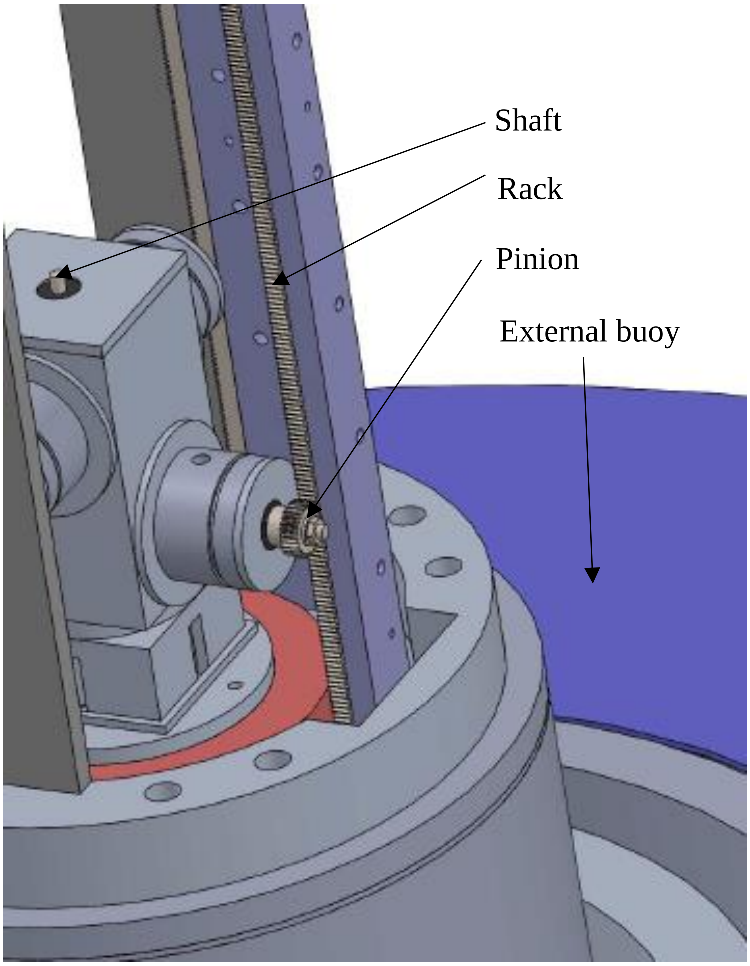

Figure 45- Power absorber scheme

When the wave comes, the buoy follows the wave oscillation movement. This oscillation is transmitted to the racks. The racks' movement creates a rotation of the pinion that induces the rotation of the shaft.

Even though the WEC's structure movement is on both directions, upwards and downwards, the shaft rotates always in the same direction due to the existence of freewheels.

In the end, the shaft is connected to the generator, producing electricity on board. While this is happening, the floating support structure has a much lower acceleration due to the difference of inertias and the increase of the drag force, which allows a displacement between the two structures.

5.3 WEC´s transmission

The creation of the WEC´s transmission was done by Miguel Godinho and the author. The generator, racks arrangement, and freewheel were developed as a team, the mechanical design of the WEC´s transmission was done by Godinho.(Godinho 2017)

The WEC´s transmission was designed based on the wave characteristics of FEUP's tank. It is responsible for absorbing the wave power through the oscillation of the WEC structure that is connected to this mechanism. While the WEC´s transmission is static, the WEC's structure oscillates due to the wave movement.

The overall design of the WEC's transmission, created by Miguel Godinho, can be seen in Figure 46:

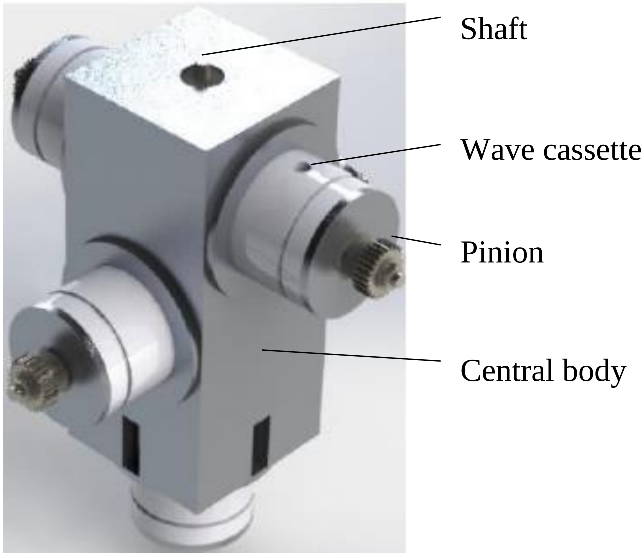

Figure 46- WEC's transmission (Godinho 2017)

5.3.1Generator

The generator was the starting point of this analysis.

Initially, the generator was selected based on a market research, adapting a brushless motor.

Consider that the energy flux of 254 W/m, as can be seen in section 5.1.2, and that the WEC's buoy has the diameter of 1.5 m, the potential power that could be extract is 381 W.

It was considered that 1/3 of the incoming power was lost throughout the kinematic chain, so 254 W were needed to fully propel the generator.

After a market research, a motor/generator was selected: a brushless, 250 W motor, as it can be seen in Figure 47.

Figure 47 - Brushless, 250 W generator selected (idle speed=8670 rpm; maximum torque=311 mNm) – (supplier: *Maxon motor*)

5.3.2 Racks’ configuration

Some problems were detected while the Tripower Up was analyzed. The system only had two racks, each of them, transmitting movement to the mechanism at a time. When the rack transmits movement to the pinion, there is a force, F, created by the rack in the structure. This load creates a moment, M, that promotes the shaft flexion, as it can be seen in Figure 48:

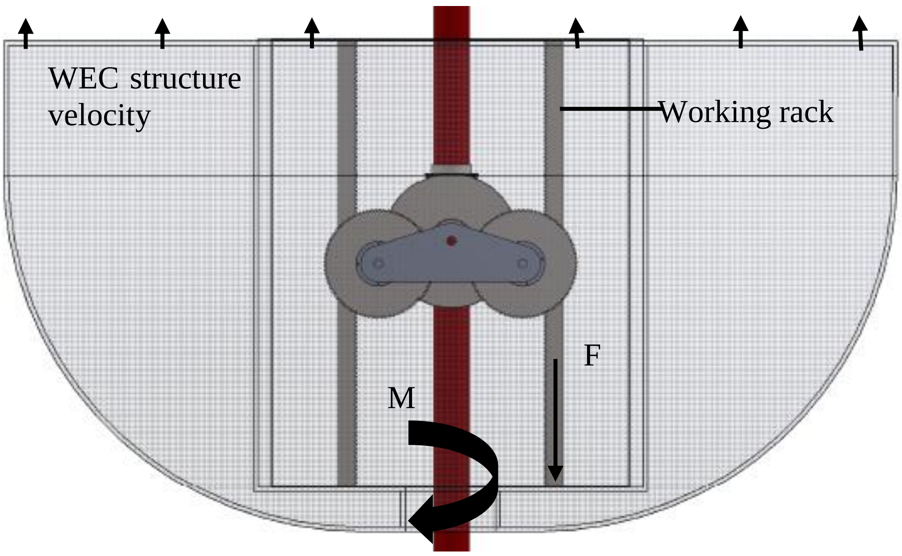

Figure 48-Force analyses due to kinematic energy (F-Force created by the rack in the structure; M- Moment created in the structure by F)

The other rack does not transmit a force because it is not transmitting mechanical energy to the system (the freewheel is decupling the movement). When the WEC structure velocity is on the opposite direction, since the working rack changes, the moment direction also changes.

This problem leads to a new configuration of the rack position, creating a completely new kinematic chain, as it can be seen in Figure 49.

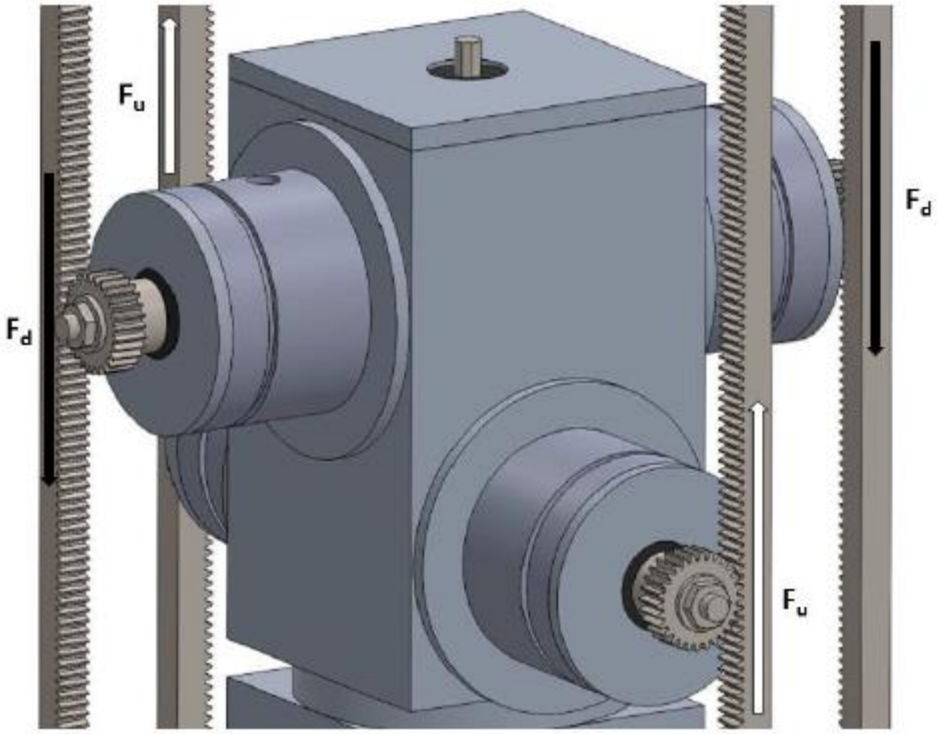

Figure 49- Forces applied to the "cross configuration" racks on the ascending movement (Fu) and on the descending movement (Fd)

This new configuration presents four racks distributed in a cross shape. With this new distribution, the racks on opposite sides work together, transmitting symmetrical forces to the structure, and as such the resultant moment is zero. The system is balanced

The four racks do not work at the same time due to the freewheel system. This system, decouples the pair of racks needed in order to create a continuous movement of the shaft. The freewheel working principle is described next.

5.3.3 Freewheel

The freewheel is the key component that allowed a couple or decouple of the movement, according to the spin direction of a shaft or gear. With this concept, it is possible to absorb the vertical wave's movement in both directions.

In the beginning, there was a custom freewheel that started to be developed, but it was not finished. The solution was not validated (neither through calculation nor simulation). And the drawing is also incomplete.

Fundraising allowed it to be changed from a custom freewheel (cheap solution) to a market solution.

5.3.3.1 Custom Freewheel

The freewheel design was based on an already existing system, as it can be seen in Figure 50 a). This mechanism is used to holster sails on sailboats. It represents only the inner part of the freewheel system. In order to reproduce the system, the metal teeth were looked for in the market. It would set the minimum dimensions for the freewheel system. Figure 50 b) shows the metal teeth.

a)

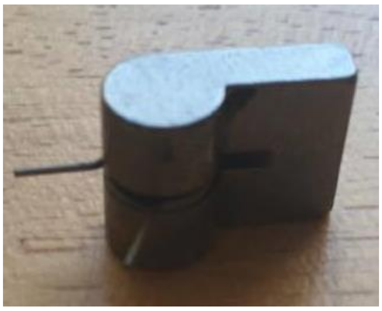

b)

Figure 50- a) Inner part of the freewheel system b) Market teeth for the freewheel system

The outer part of the freewheel consists of an internal gear where the metal teeth fits. Only the inner part was provided, so the outer part needed to be designed based on the inner part.

The three constraints that lead to the existing design are:

- Use the metal teeth that are already in the market;
- Design as much equal parts as possible since it is easier to manufacture and to assemble;
- Make a solution very close to the market dimension in order to be possible to replace it in the future;

Based on the holster sails freewheel a new one was designed, Figure 51 and Figure 52.

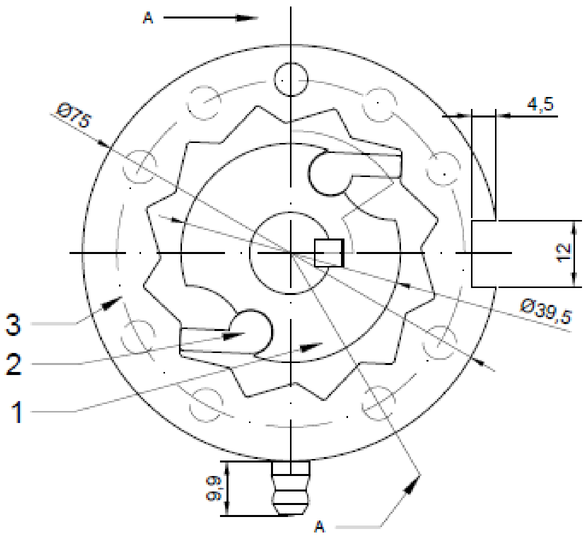

Figure 51- Front view of the freewheel system (1-Inner part; 2-metal teeth; 3-outer part)

There are two teeth (2) that circulate in an internal gear (3). When the inner body, (1), rotates clockwise the movement goes from the inner part (1) to the outer part (3). When the inner part (1) rotates anti-clockwise the teeth (2) slip and do not transmit movement.

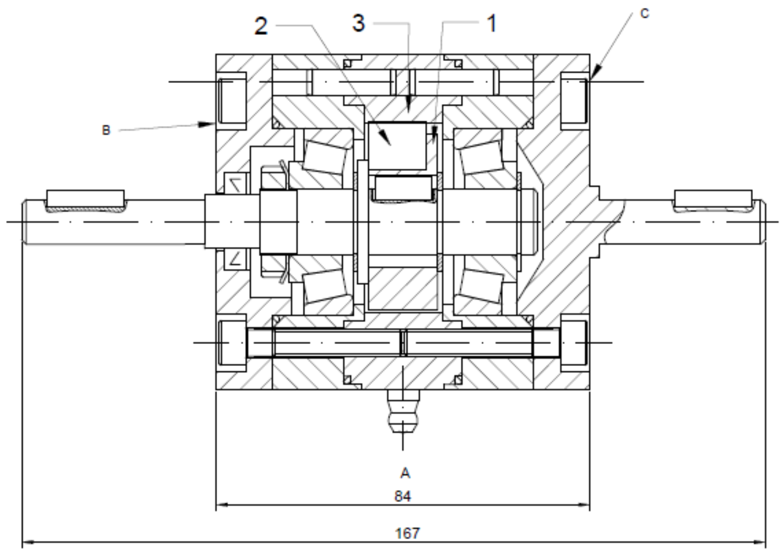

Figure 52-A-A Section cut

Based on the mounting position, it can be decided, according to a certain spinning direction, if the movement goes from left to right or from right to left. The technical draw is in

Appendix F.

5.3.3.2 Market Freewheel

Figure 53 shows the freewheel that was obtained in the market for this project.

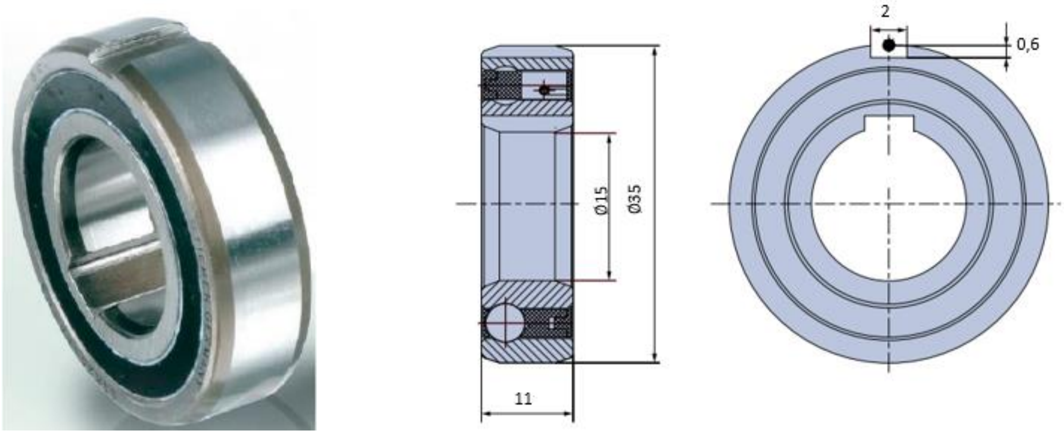

a) b)

Figure 53- a) Market Freewheel b)Dimensions

This freewheel was selected because it has an inner and outer keyway, and it has half of the dimension of the costume freewheel. Due to this, and the fact that the market freewheel is a tested solution, it was decided to discard the custom freewheel from this project, proceeding with the Stieber Clutch's freewheel.

With the market freewheel, a new concept was created, the "wave cassette". A more detailed development was held by Miguel Godinho. (Godinho 2017) This wave cassette has a freewheel within, so every time a freewheel was needed a wave cassette was installed. The "wave cassette" is presented in Figure 54.

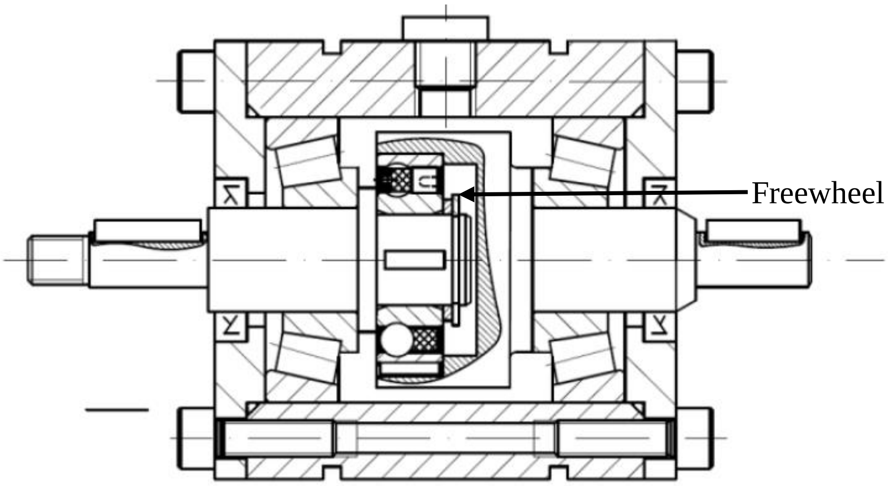

Figure 54-Wave cassette 1) Market freewheel (Godinho 2017)

Therefore, there are two shafts that can be machined in order to be adapted to the part that is connected. A more detailed explanation of the wave cassette design and the kinematics box was done in Miguel Godinho's dissertation. (Godinho 2017) The wave cassette is placed between the pinion and the central body allowing (or not) the transmission of movement across the kinematic chain, according to the mounting position.

5.4 WEC's structure

5.4.1 Previous WEC's structure

In the previous TRIPOWER UP, in the WEC's structure, the connection between the inner and the outer buoy was achieved by means of an elastomer, as it can be seen in Figure 55. This leads to considerable problems:

- Did not give the degree of freedom needed;
- It was difficult to absorb the horizontal wave forces and transmit the vertical forces;
- Regarding the mechanism, it was surrounded by water, so any leak in the inner buoy could damage the WEC´s transmission components;
- The presence of sea animals and salt would damage the elastomer.

The mechanism can be seen in Figure 55 b).

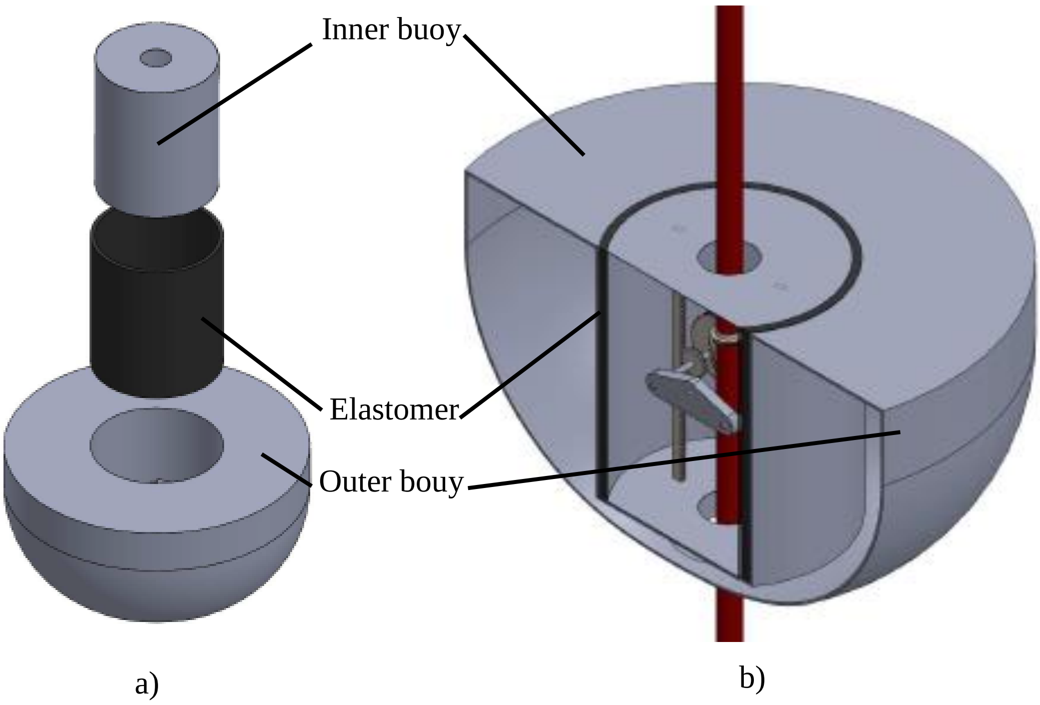

Figure 55-TRIPOWER UP component a) exploded view b) mechanism

The new type of WEC mechanical structure solved all the previous problems.

5.4.2 New WEC's structure

5.4.2.1 Framework

This framework, placed inside the WEC's Structure, provides the linkage between the guidance system to the tilting system. The framework is made by three subgroups, as it can be seen in Figure 56:

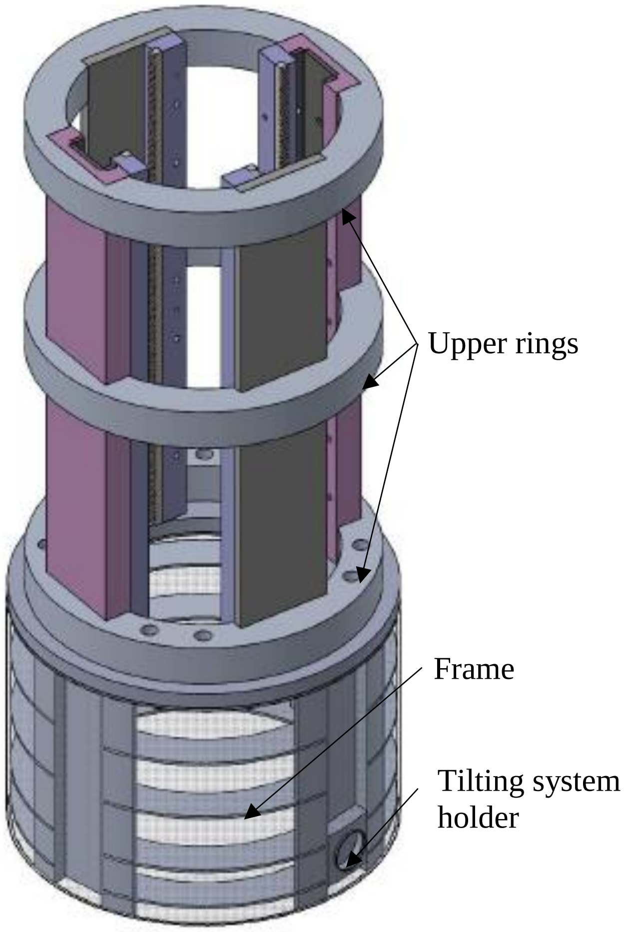

Figure 56-Framework

In the framework, each part has its own function:

- An aluminum frame was added instead of a massive structure to reduce weight while keeping the structures resistance;
- The three top rings allow to carry the guidance system;
- The tilting system arm is welded to the tilting system holder;
- The framework raised the WEC´s transmission to a level above the water level, solving the leak problem;

5.4.2.2 Tilting system

The tilting system (Figure 57 a)) was created to replace the elastomer connection. This system has two perpendicular axes that allow the rotation between the framework and the tilting system. Both axes can spin simultaneously and adapt to waves independently of their direction (360° range). This device allows the WEC’s buoy to adapt to wave angles, with a maximum angle of 30º. This rotation enables the absorption of the horizontal forces.

.

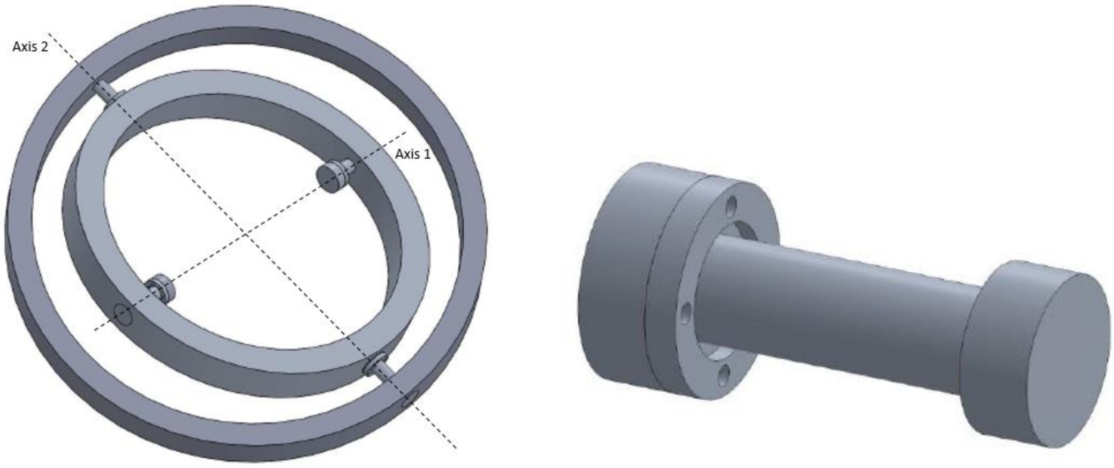

a) b)

Figure 57- a) Tilting system and b) Tilting arm

The efficiency of the tilting system increases if, in the static position, the water surface and the axis are coincident. As the tilting arm is a very dynamic part, and it is submitted to several forces, it was decided to make it of 316 inox steel.

5.4.2.3 WEC's Buoy

The WEC's buoy was made of aluminum sheets. The connection with the tilting system is made by a flange. Figure 58 shows the WEC buoy (cut view).

In section 3.1, it was proven that the floating buoy has several advantages when compared with the submerged ones allowing to validate the suppositions.

The analyses of section 3.2.6 and 3.2.7, regarding the shape and the dimensions respectively, gave some insights used for the mechanical design of the buoy.

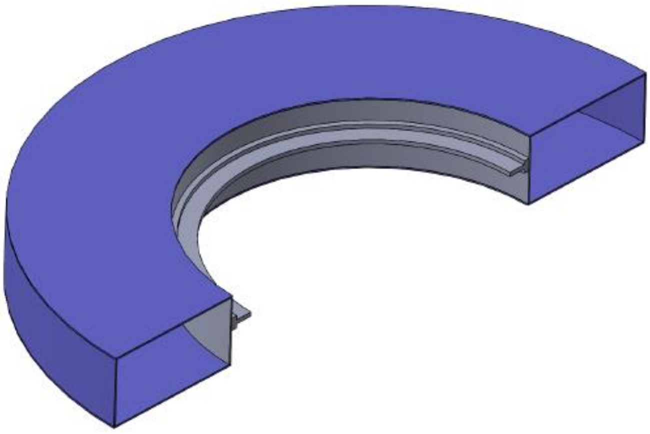

Figure 58- WEC buoy (cut view)

5.4.3 Connection between WEC's structure and WEC´s transmission

In WECs' mechanical design, the guidance system and the rack and pinion mechanism were used to make the connection between the WEC´s transmission and the WEC's structure, as it can be seen in Figure 59.

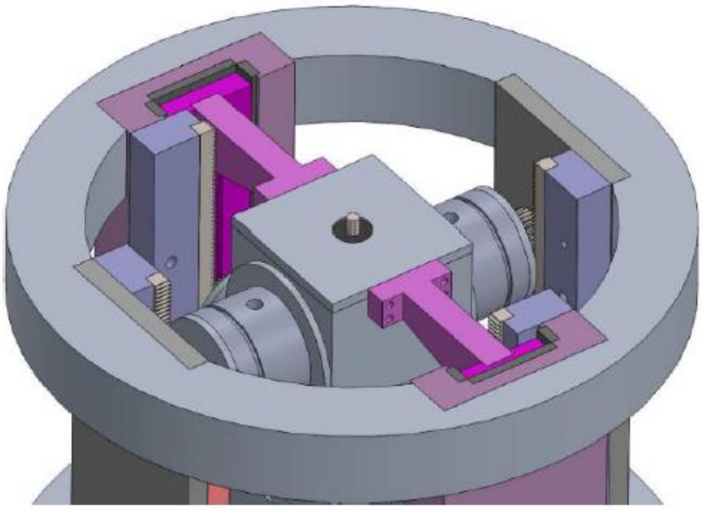

Figure 59- Connection between the WEC's transmission and WEC's structure

Appendix E (exploded view) shows the connection between the racks and the guidance system through a rack support.

5.4.3.1 Guidance system

The guidance system plays a crucial role. It is responsible for guiding the racks and the pinions connection. The WEC´s exterior has the center of gravity above the center of buoyancy, so the guidance system is responsible for absorbing the momentum that is created by this gap.

In Figure 60, the guidance system is highlighted.

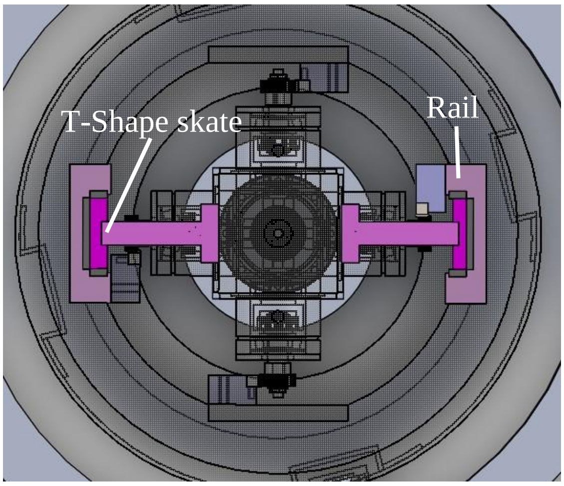

Figure 60-Guidance system

The T-Shape skate blocks all the structures degrees of freedom except the vertical movement. The rail of the guidance system is covered with Teflon because of it has a low friction coefficient.

5.5 Support structure

5.5.1 Preview Support structure

Figure 61, shows the design of the previous support structure as well as the corresponding forces.

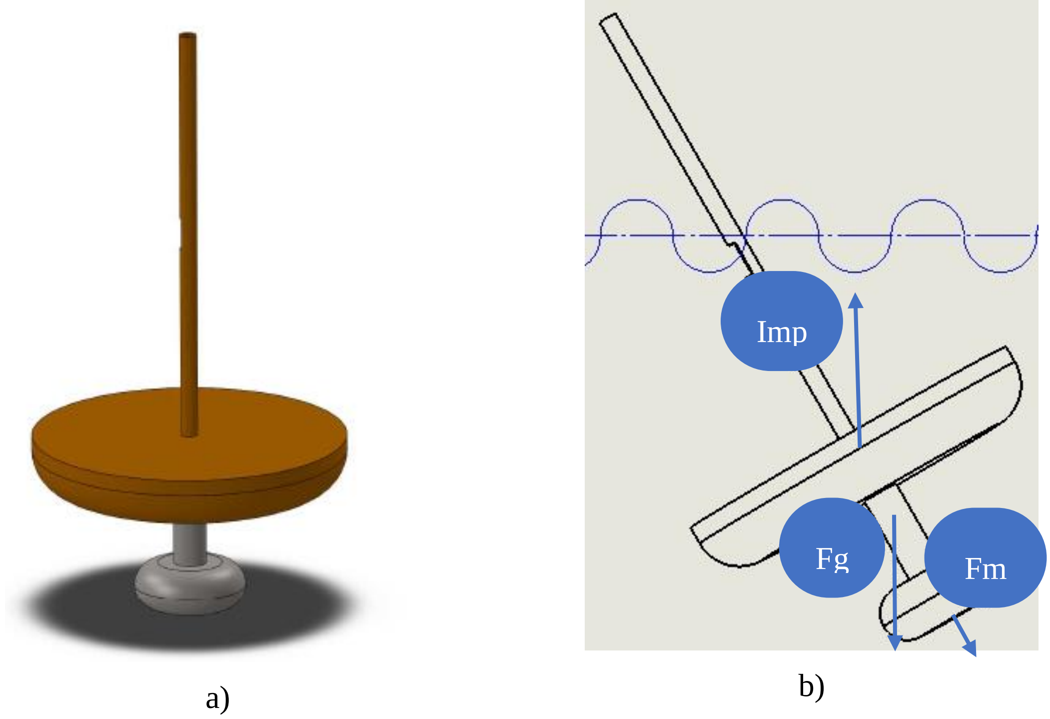

Figure 61 - 1st design of the TRIPOWER UP structure a) 3D b) placed in water with forces represented. (Macieira 2017)

Where *Imp* is buoyancy, *Fg* is the gravitational force, and *Fm* is the mooring forces.

After a closer look to the initial design of the support structure, it could be concluded that the system was difficult to stabilize. The original objective was to have the buoyancy of the structure equal to the weight plus the mooring force of the body, as can be represented in Figure 61 b). As the structural buoy as constant buoyancy (submerged volume is constant) and the weight is also constant, the system would be stabilized by the variation of the mooring forces, that are not constant, as it can be seen in section 3.2.5.2.

The design of the current structure intended to solve these problems.

5.5.2 New Support structure

It was adopted a more reliable strategy to create a stable system. It was decided to develop a floating buoy and not a submerged one. The buoyancy force will change according to the submerged volume, as it can be seen in section 3.2.3. With this strategy, a stable condition will be obtained because the variation of the buoyancy absorbs the change on the mooring forces. This concept obliged a change in the buoy design, as can be seen in Figure 61.

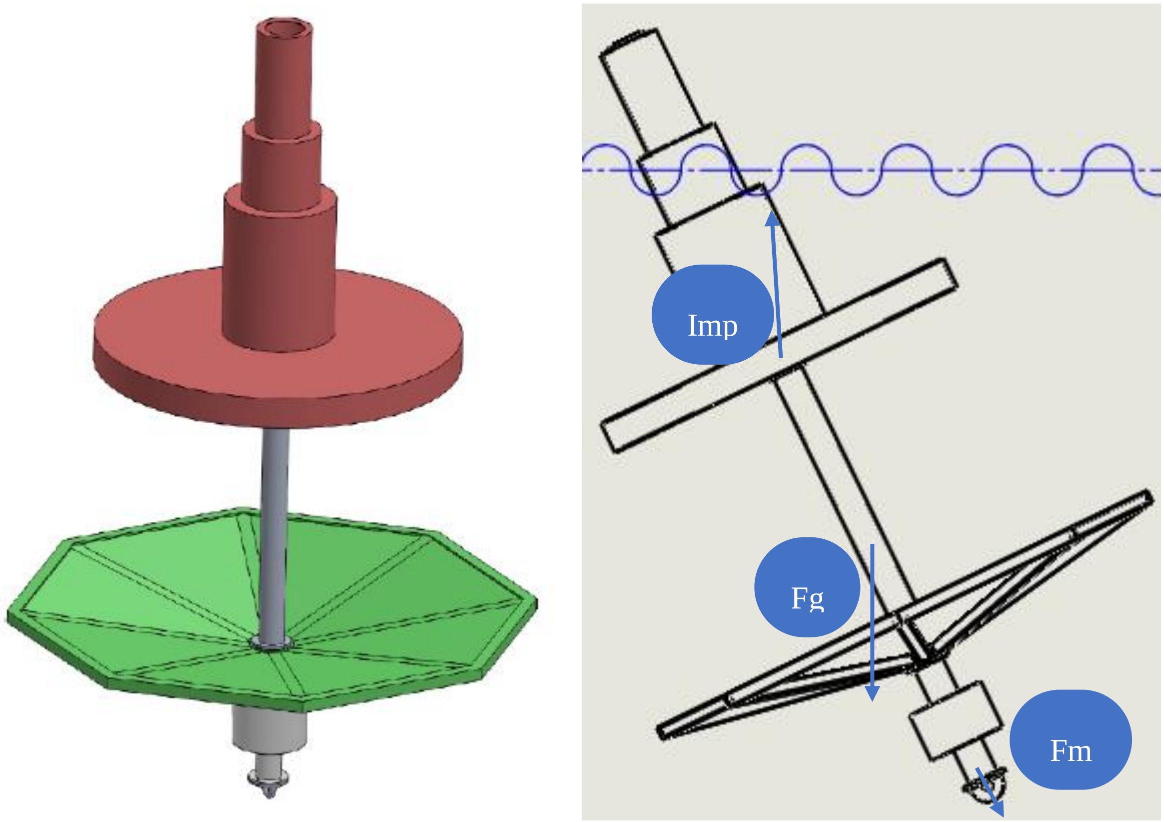

a) b)

Figure 62- Support structure that was developed a) 3D and b) placed in water with forces represented (Imp is buoyancy, Fg is the gravitational force, and Fm is the mooring force)

The support structure presents four parts: the buoy, the inverted parachute, the ballast, and the mooring system.

5.5.2.1 WEC's Buoy

The shape of the floating buoy is created by four cylindrical shapes, as it can be seen in Figure 63.

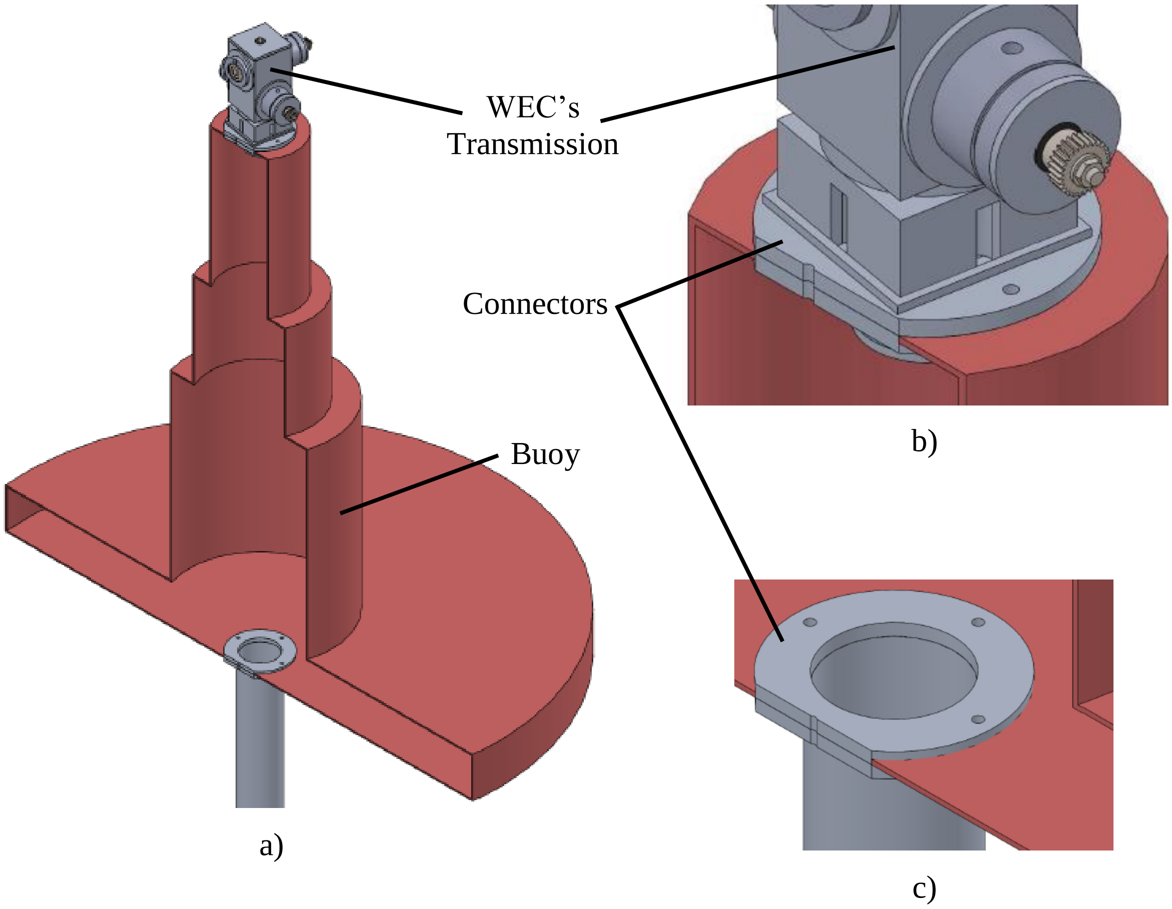

Figure 63-Structural buoy a) internal structure view b) Connection with the WEC's transmission c) Connection between tubes

The buoy has two connectors to attach the outer parts: WEC´s transmission and Structural tube. The forces between the structure and the buoy are transmitted through the connectors.

The several cylindrical shapes were created in order to increase the buoyancy force. This force depends on the submerged volume, so the increase of the diameter influences more than the same increase in height. That is why the last cylinder has a bigger diameter than the other ones. For the other diameters there was limited space, so they could not be larger than they are.

5.5.2.2 Inverted parachute

The shape of the previous support structure buoy had the aim of increasing the drag force of the support structure when a wave pushes the system upwards. Since the buoy geometry and location had changed, the buoy no longer creates opposition to the support structure movement. To create opposition to the movement, the parachute was designed.

This opposition was needed to create a difference in velocity between the WEC´s transmission and the WEC’s structure. As it is this asynchronous movement that creates mechanical energy, the inverted parachute allows to increase the drag of the support structure, and thus, to reduce the WEC´s transmission's velocity.

It was made out of 16 quadrangular beams welded to each other, connected with 3 mm sheets; all made off aluminum. The inverted parachute can be seen in Figure 64.

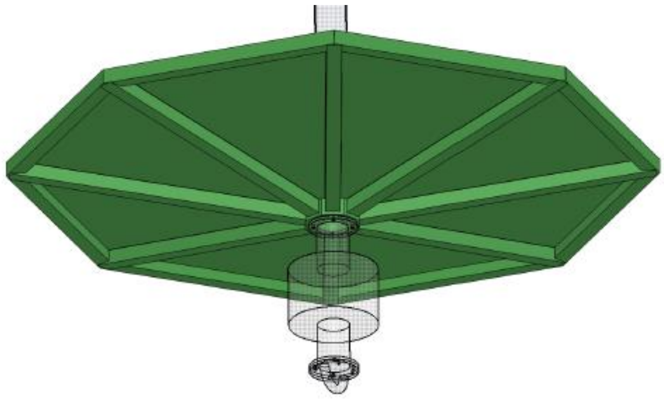

Figure 64- Inverted parachute made by aluminum tubular beams with a rectangular shape

5.5.2.3 Mooring

After the study of section 3.2.5 was made, a single mooring point was selected, more precisely a single anchor leg mooring.

There are two reasons why this system was chosen:

- A certain degree of freedom is needed to create a relative movement between structures;
- As the mooring system is one major component in the cost of WEC, it was decided to keep it simple in order to reduce the cost;

To follow the actual trend of mooring ropes, synthetic material was selected. They offer a lower weight, more elasticity, and a powerful breaking force. An original nylon mooring rope has been chosen (*ATLAS*™ from *Lankhorst/Ropes* supplier) to be used in the environment simulation, section 6.2. The cable is attached to the mooring system (Figure 66) with a shackle, both components can be seen Figure 65.

Figure 65- Atlas cable from *Landkhorst/Ropes* and shackle from *e-rigging*

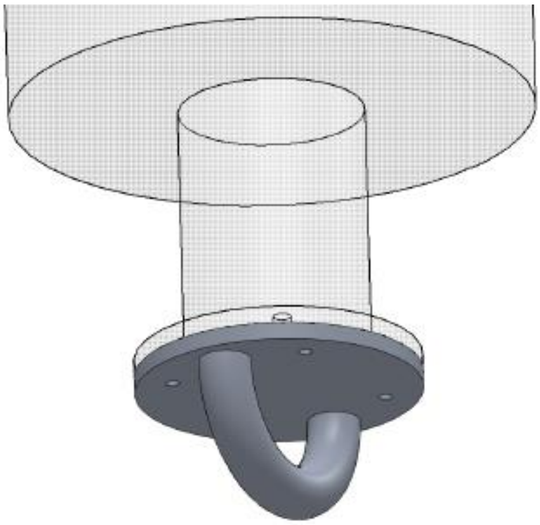

Figure 66-Mooring system

5.5.2.4 Ballast

To lower the center of gravity and confer stability to the system, a mass of high density was added to the bottom of the device, Figure 67. It was made from lead as its density is $11340\ kg/m^3$. This mass has the same weight of *195,6 kg.* This weight is *44%* of the total device weight.

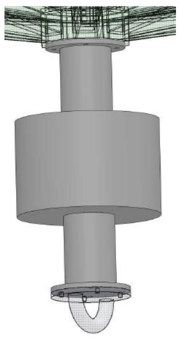

Figure 67-Balastre

6 Stability and Environment Simulation

6.1 Stability

In this section, the *TRIPOWER UP* stability is analyzed. The goal of this analysis is to balance the support structure and the WEC's structure. This is done through the calculation of the necessary buoys' dimensions to ensure the balance between the buoyancy and the gravity forces. Also, the centers of gravity and buoyancy centers of both structures are calculated. Furthermore, the stability curve and the power of the racks are also discussed.

6.1.1 Support structure and WEC´s transmission stability

6.1.1.1 Buoy dimension

A diagram is presented in Figure 68, which explains the input variables for the calculations. In this diagram, the support structure is divided into four cylindrical shapes. In Table 8, the device's defined and undefined parameters are presented.

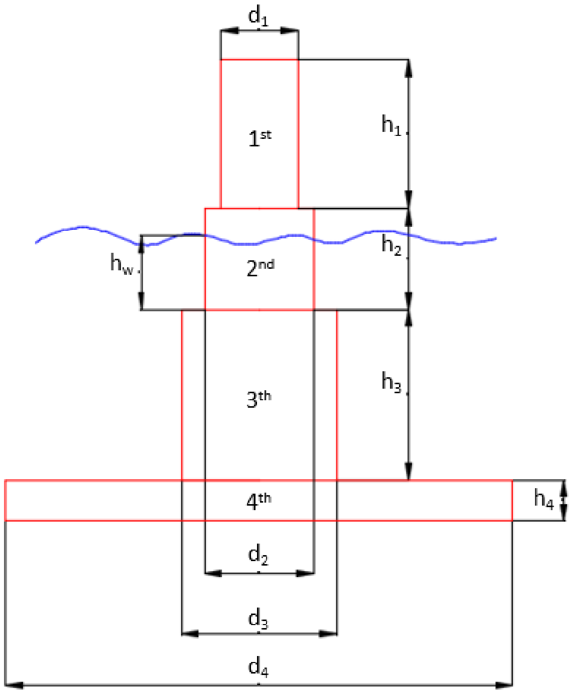

Figure 68-Diagram of the support structure

Table 8- Structural buoy's parameters

Buoy dimensions	
1st cylinder diameter (d_1)	*0.230* m
2nd cylinder diameter (d_2)	*0.325* m
3th cylinder diameter (d_3)	*0.460* m
4th cylinder diameter (d_4)	*1.50* m
1st cylinder height (h_1)	*0.440* m
2nd cylinder height (h_2)	*0.300* m
3th cylinder height (h_3)	*0.581* m
4th cylinder height (h_4)	------
Distance between water surface and the 3rd cylinder (h_w)	*0.200* m
Material density (aluminum)	*2700* kg/m^3
Thickness (e)	*0.004* m

The first cylinder, which is above water, is used when changes in the buoyancy forces are needed (the emerged part would become immersed).

A calculation considering a static equilibrium was performed to determine the height of the fourth cylinder. It was only considered the weight forces and the buoyancy forces, and not the mooring forces. The goal is to achieve a prototype static balance without requiring any mooring. Afterwards, the mooring forces were used to compute the variation in the submerged volume.

Normally, from the equilibrium analysis, it is common to extract the buoyancy height, h_w. In this project, h_w is constant, due to the kinematic chain constraints, and h_4 was calculated.

The dimension of h_w=*0.200* m is used because it is the required WEC's structure's height to reach the rack's medium height. This allows for the full absorption of the wave's amplitude.

The mass of the support structure and the weight was obtained using SolidWorks – *Ms* = 330 kg. The full data output from SolidWorks regarding the support structures can be found in Appendix B

To ensure device floatation,

$$Fgs = Imp \tag{8.1}$$

Where *Fgs* is the structural gravitation force, and *Imp* is the buoyancy force created by the different submerged cylinders. As $Imp = Imp_2 + Imp_3 + \rho_w g V\!\!\!/$, and $V\!\!\!/ = \frac{\pi\, 1.5^2}{4} * h4$, solving the first order equation,

$$h_4 = 0.123\, m \tag{8.2}$$

where Imp_2 and Imp_3 are the buoyancy forces from the second and third cylinder.

To compute this value, an iterative process was made considering the height and the mass of the structure. In the future, if the wind and current converters are added, h_4 must be recalculated considering their weights.

6.1.1.2 Center of gravity and buoyancy

In order to ensure structure stability, the metacentric height has to be positive, as it was referred to in section 3.2.3. In order for this to happen, the center of buoyancy has to be located above the center of gravity, $C_I > C_G$. To obtain the center of gravity, SolidWorks was used. The C_G coordinates relative to the origin are,

$$C_G(x, y, z) = (\,0\;, \quad -1055\;, \quad 0\,)\ \text{mm} \tag{8.3}$$

The center of gravity's position is pointed out in Figure 69.

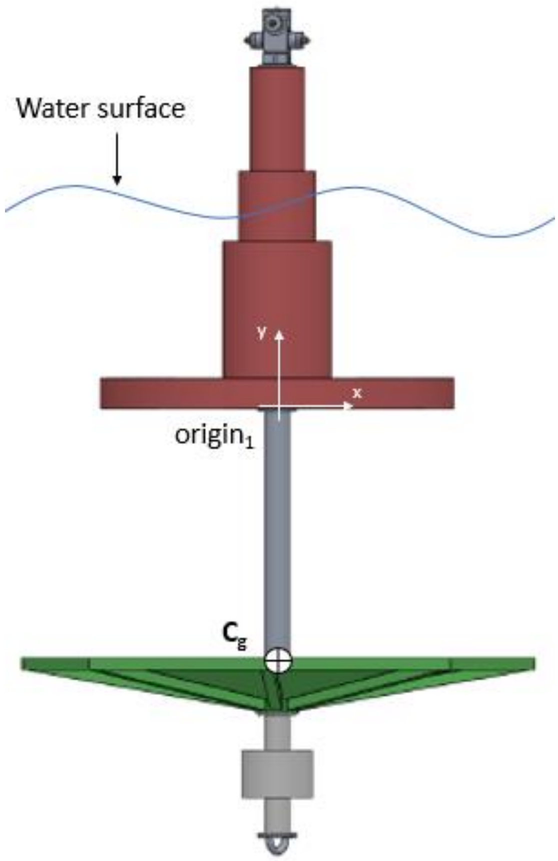

Figure 69- Center of gravity (C_g)

Afterwards, the center of buoyancy, C_I, was calculated. As it was discussed in section 3.2.3, C_I only depends of the submerged volume, $\forall$. Figure 70 represents the sketch of the submerged volume that was used to obtain the center of buoyancy. In this sketch, it was assumed that the device had the water density.

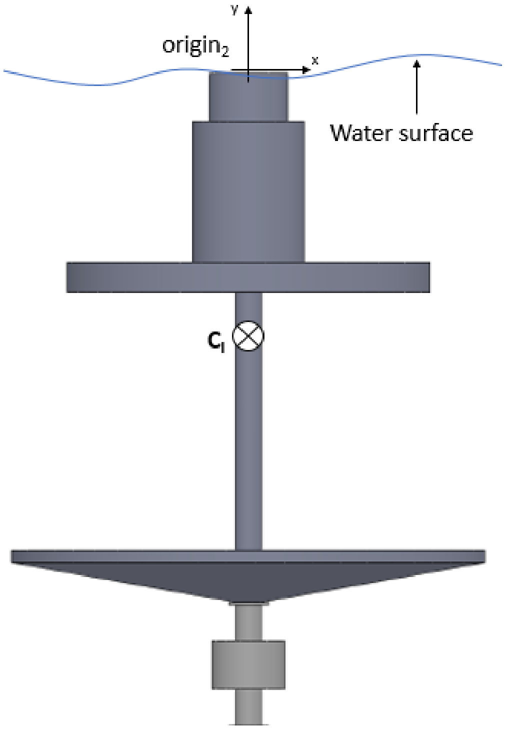

Figure 70- Sketch of submerged support structure with the density of water. Origin$_2$ is coincident with the water level)

$$C_I(x, y, z) = (\,0\,, \quad -1177, \quad 0)\ \text{mm} \tag{8.4}$$

In Equation 8.5, C_I is presented in relation to the same origin as Equation 8.3 (Origin$_1$).

$$C_I(x, y, z) = (\,0\,, \quad -273, \quad 0)\ \text{mm} \tag{8.5}$$

The distance between C_G and C_I is,

$$\overline{C_G C_I} = \ 0.904\ \text{m} \tag{8.6}$$

It can be concluded that the structure is stable because, in the y-axis, $C_I \gg C_G$. If there is an external force acting on the structure, the buoyancy will respond with a returning moment, which will restore the structure to the initial stable position.

6.1.1.3 Metacentric height

As it was described in section 4.3, the metacentric height influences the stability of the system. The formula to calculate the $\overline{MC_G}$ was deducted in this section and it is now presented:

$$\overline{MC_G} = \frac{I_o}{\forall} - \overline{C_G C_I} \tag{8.7}$$

Because C_I changes in accordance with the submerged volume, there is a metacentric height for each tilted position (please look to Figure 24 for better understanding). With the metacentric height, the righting arm can be obtained and then the righting moment can be calculated. It should be noted that the righting moment was only tested when the support structure is tilted, $\alpha = 90°$ with the vertical line, Figure 71: (The properties of the body can be seen in Appendix B

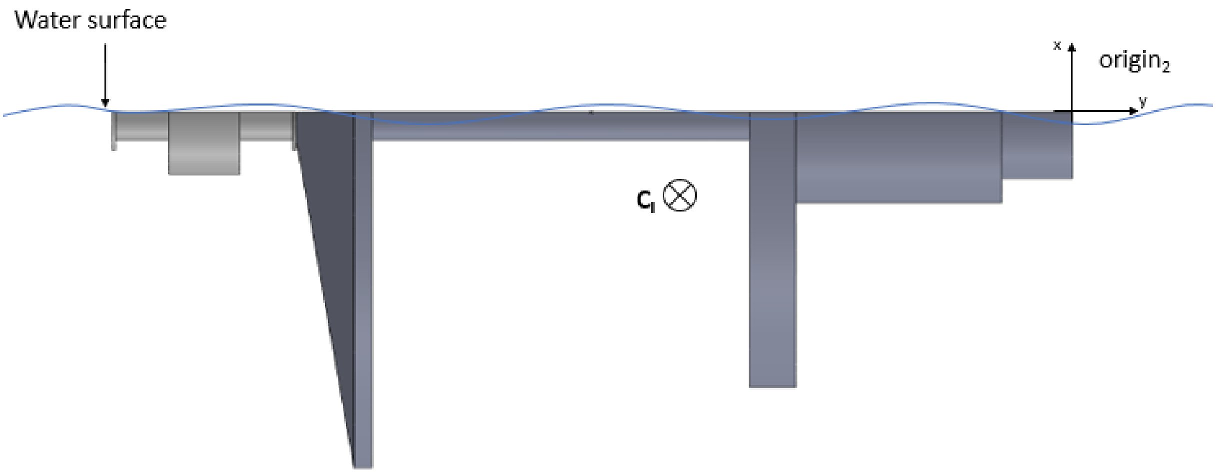

Figure 71- Support structure submerged volume when tilted 90°

In Figure 71, assuming origin$_2$, the position the C_I is,

$$C_I(x, y, z) = (-259.78\,, \quad -1171.50\,, \quad 0\,)\; mm \tag{8.8}$$

So as C_G is constant and assuming the same reference, in the y direction,

$$\overline{C_G C_I} = 0.7875\; m \tag{8.9}$$

To calculate Io (moment of area located in the water's level) Figure 72 was assumed. This was done considering C_F in the Coordinate System2 and I_o=L_{zz}.

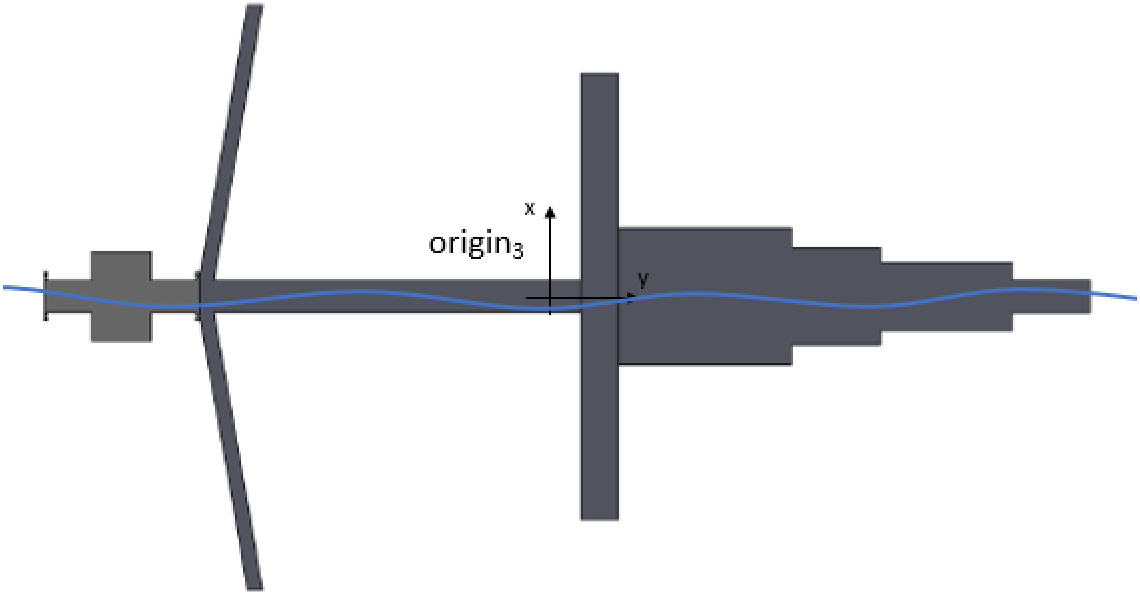

Figure 72-Cross section area of the support structure to calculate moment of inertia

$\overline{MC_G}$ was calculated assuming the value from Table 9: (The properties of the body can be seen in Appendix B

Table 9- Submerged volume parameters used to compute the metacentric height

Inertia moment of area ($\boldsymbol{I_o}$)	0.900 $\boldsymbol{m^4}$
Submerged volume ($\boldsymbol{V}$)	0.297 m^3
Distance between $\overline{\boldsymbol{C_G C_I}}$	0.7875 m

The metacentric height is,

$$\overline{MC_G} \sim 2.24\ m. \tag{8.10}$$

The righting moment is,

$$\overline{GZ} = \overline{C_G M} * sen(\alpha) = 0.0614\ m \tag{8.11}$$

$$P * \overline{C_G M} * sen(\alpha) = P * \overline{GZ} = 198\ Nm \tag{8.12}$$

Assuming the stability curve, it can be stated that, for $\alpha = 90°$, the system is still stable.

It should be remarked that $\overline{C_G C_I}$ is not constant. A variation of α leads to a change in C_I as it depends on the submerged volume.

Equation 8.13 should be computed, with the assistance of simulation software, to allow a better understanding of the $C_I's$ variation. This would allow the calculation of the stability curve.

$$C_I = \frac{1}{V\!\!\!-} \iiint_{V\!\!\!-} r \, dV\!\!\!- \tag{8.13}$$

6.1.2WEC's structure stability

6.1.2.1 WEC's Buoy dimension

The best buoy's sizes and shapes were analyzed in Section 4. Regarding the size, it was stated that the bigger the radius the bigger the absorbed power is. Hence, it was decided to have a big diameter, able to create the necessary buoyancy force. This buoy, however, is not a perfect cylinder because there were some dimensional constraints that lead to the existence of a hole in the middle, Figure 73:

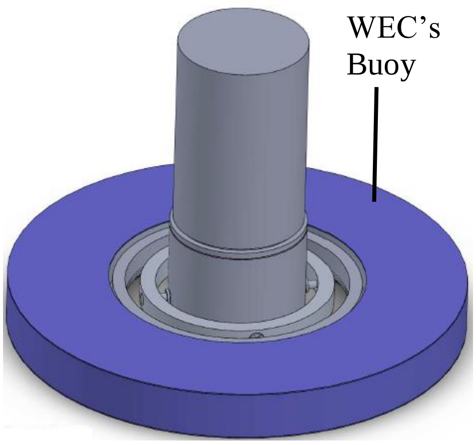

Figure 73-WEC structure. Buoy in blue

A diagram is presented in Figure 74 for calculation purposes. Firstly, for dimension purposes, only the weight and the buoyancy were taken into consideration (in the calculation of h_5).

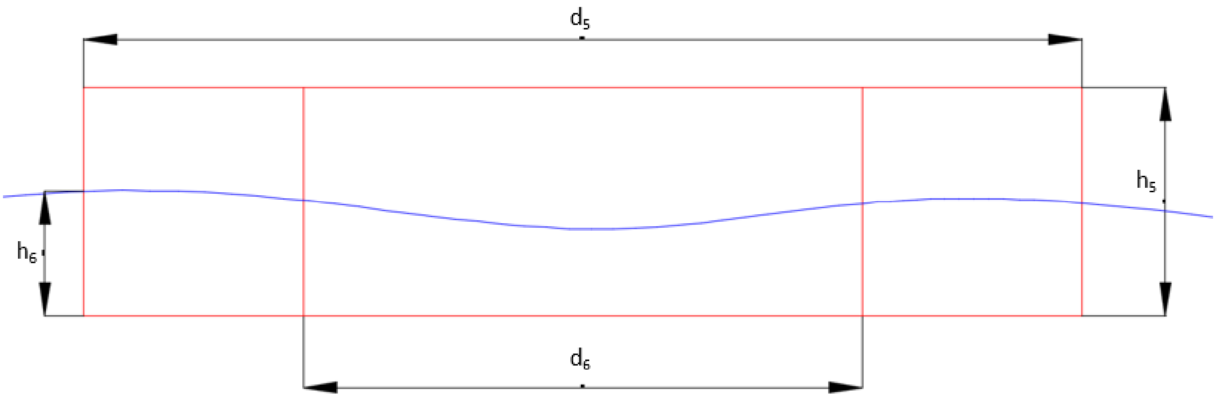

Figure 74- WEC's buoy diagram

In Table 10, the device's defined and undefined parameters are presented.

Table 10- WEC's buoy parameters

WEC's structure diameter (d_5)	*1.50* m
Interior diameter (d_6)	0.846 m
External buoy height (h_5)	----
Distance between water surface and the buoy's lower end (h_6)	h_6=h_5/2 m
Material density (aluminum)	2700 kg/m^3
Thickness (e)	0.004 m

The distance between the water's surface and the buoy's lower end has to be half of the buoy's height. That will allow, in a static consideration, for the water surface to be coincident with the tilting system's axis, increasing its efficiency.

The mass of the external structure was calculated, with the assistance of SolidWorks: *Mext = 97.36* kg. This can be retrieved in Appendix B

In order for the device to float,

$$F_{gWEC} = Imp2$$

Where, F_{gWEC} is the WEC gravitational force and Imp is the buoy buoyancy.

As $Imp2 = \rho_w g V\!\!\!/$, as stated in section 4.3, the submerged volume can be obtained: $V\!\!\!/ = 0.097 \text{ m}^3$. So, to have that volume submerged,

$$h_6 = 0.080 \ m$$

Because $h_6 = h_5/2$,

$$h_5 = 0.160 \, m$$

In order to compute this value, an iterative process was held considering the height and the mass of the structure.

.

6.1.2.2 Center of gravity and buoyancy

To analyze stability, the center of mass was obtained with SolidWorks, Figure 75.

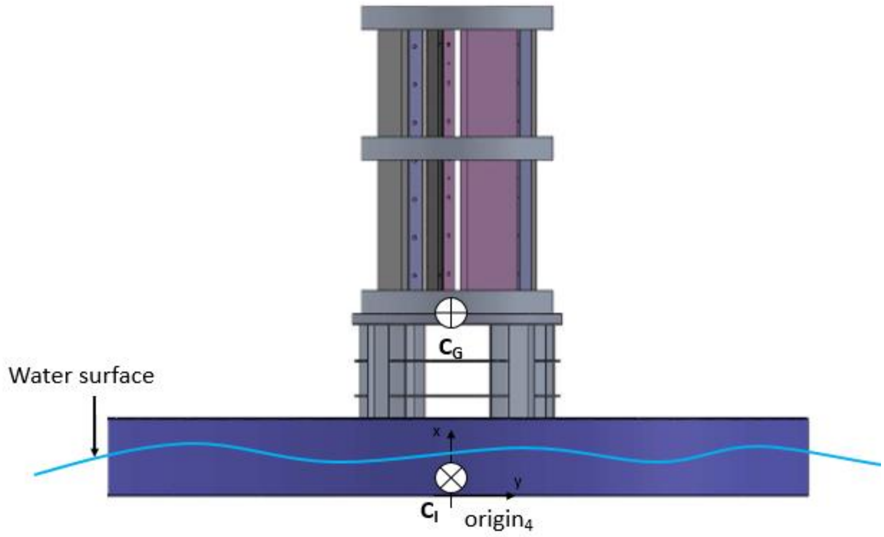

Figure 75- Internal part of the WEC structure

Please note that the origin (orange dot) is not in the same place that it was in the support structure. So C_G according to this origin,

$$C_G(x, y, z) = (0.11\,, \quad 348.98, \quad -0.08)$$

This can be consulted in Appendix B.

The relevant coordinate is y. The variation in x and z directions exists because, during the mechanical design, the axis of the tilting system was not aligned with the origin axis. If that had been done, they would be both zero.

The calculation of the center of buoyancy follows. As it has a symmetric shape, the point will be in the middle of the submerged height,

$$C_I(x, y, z) = (0\;, \quad 0.04\;, \quad 0)$$

From this equation, it can be concluded that the structure is unstable, as $C_G \gg C_I$. That will create a tilting moment that will try to capsize the structure. That moment will be applied in the guidance system that will keep the structure vertical.

6.1.2.3 Submerged height variation

The rack movement creates a force that has to be balanced by the buoyancy force. This causes a rise of the submerged height as the submerged volume increases.

After obtaining the buoy's size, it's possible to calculate how much of the submerged area will increase due to the rack's movement. As it was mentioned in section 7.2, the wave tank can generate a power of *260.33* W/m. Knowing that the external diameter of the WEC buoy is *d5=1.5* m, the maximum power that can be absorbed is

$$P = J\, d_5 = 390.5\, W$$

In the best-case scenario, all the wave power will be transmitted to the racks throughout the structure.

It is known that the rack velocity v=0.490 m/s, assuming a regular approach and $v = A\,\omega$. Knowing that $P = F\, v$, the force created by the four racks in the structure is $F = 796.93$ N. This assumes that the reaction force will be generated by the buoyancy force, $F = Imp_5$, where Imp_5 is the buoyancy of the external buoy. This Imp_5 creates a submerged volume, $\Delta vsub = 0.079$ m^3.

The variation in height will then be $\Delta h = 0.065$ m, which is less than the emerged height of the buoy, 0.080 m.

6.2 Environment Simulation

In this section, the 3D design prototype was submitted to real environment conditions in terms of winds and water currents, and to tank conditions when analyzing waves. This happened because the tank characteristics for wind and current were unknown.

In Section 3.2.2, four different forces were described in the wave-structure interaction, but not all of them were simulated:

- The wave forces, described by the Morrison's Equation, were decomposed in drag from the currents, drag from waves and inertia forces. It was only able to simulate the wave and current drag forces;
- The dynamic pressure forces obtained in the wind and current analyses were almost zero;
- The wind drag force was simulated;
- The radiation force was not simulated because it is complicated in the SolidWorks environment;

6.2.1 Water forces

In section 3.2.2 Morison's equation is used to calculate the interaction between a wave and structure. SolidWorks does not allow to simulate the Morison's inertia forces, so only the Morison's drag forces from waves and currents were analyzed.

The calculation of the Morison's equation can only be performed after knowing the device's motion in oscillation flow and hydrodynamic coefficients. Both are related to the device movement The Morrison Equation could be applied to our system since $d5 < 0.2\,\lambda$ (Faizal, Ahmed, and Lee 2014).

The currents and waves acting on the device were simulated separately because one was done in SolidWorks Flow simulation tool and other was done in SolidWorks simulation tool.

6.2.1.1 Wave drag force

The wave drag force is created when the fluid pushes the support structure upwards. This force is mainly felt in the inverted parachute.

The forces that act in the inverted parachute were analyzed by SolidWorks simulation tool. To create the impute parameters come assumptions were made.

This assumption where made to calculate the drag force:

- c_d=1.75 ; typical drag force coefficient for a parachute shape; (Benson)
- v =0.49 m/s; considering the linear wave theory, the wave behaves like a sinusoidal wave. Assuming wave movement is described by $x(t) = A\sin(\omega t)$, the velocity can be written as $v(t) = A\omega\cos(\omega t)$, so its maximum value is $v = A\omega$. Table 5 parameters were used in this calculation.
- S= 3.37 m^2 was obtained with SolidWorks.

Having in consideration that,

$$F_D = 0.5 c_d\, S\, \rho_w\, g\, v^2$$

Where cd is the drag force coefficient, v, is the fluid velocity, ρ_w is the water density and A is the cross-area section to the velocity direction. This leads to,

$$F_D = 6938.4\text{ N}$$

The vertical mooring forces were also considered, $F_V = 42.4\,N$. The mooring forces are calculated in section 6.2.3.

The results of the simulation in are presented Table 11 and Table 12.

Table 11- SolidWorks report results- von Mises Stress

Name	Type	Min	Max
Stress	VON: von Mises Stress	16199.3 N/m^2 Node: 7625	7.69218e+006 N/m^2 Node: 47101

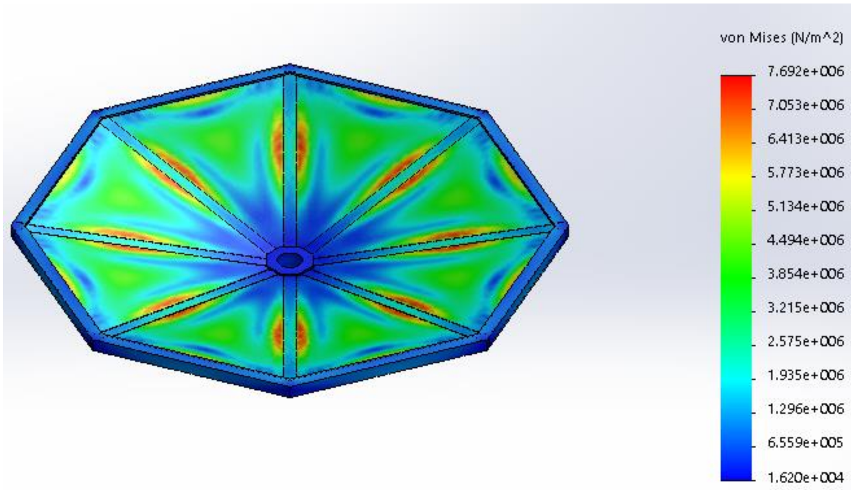

Table 12- SolidWorks report results- Resultant Displacement

Name	Type	Min	Max
Displacement	URES: Resultant Displacement	0 mm Node: 390	0.641597 mm Node: 51160

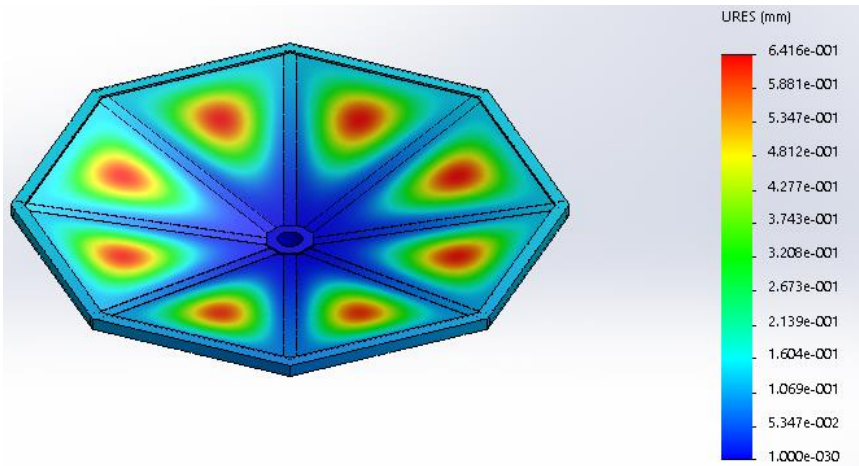

It was concluded that the maximum stress is 7.6 MPa which is lower than the yield strength. For 7000 aluminum series the yield strength is between 300 to 700 MPa, and for 5000, it can go from 200-400 MPa. For 5000, there are some aluminums that present yield strength between 200-400 MPa. With that in mind, it is possible to be said that the structure is in elastic regime.

(CES Edu Pack 2017-Appendix C) Furthermore, 5000 aluminum have excellent resistance to corrosion.

The maximum displacement id presented between the sheet metals, its value is 0.64 mm. For now, that does not seems a concern. If it needs to be reduced, increasing the sheet metal thickens higher than 3 mm is one of the solutions. The maximum safety factor is 65 so the fatigue check is not needed.

6.2.1.2 Current drag force

In order to simulate the current drag force acting on the device, it was assumed that only the main structure is influenced by the water flow. Even though it is not true, because half of the external buoy is also submerged, it is very close to reality. The support structure was model instead of the overall model because it will take a massive computation power.

It was assumed that the water current is v=1.6 m/s as it is an extreme value according to the Portuguese sea shore. (IPMA 2017)

Figure 76 shows the simulation results (From SolidWorks flow simulation). The arrows represent the trajectory of the sea current, and their colors represent their velocity value. The structure colors represent the total pressure due to the current flow. The color scale for the pressure and the velocity is represented on the left and right sides, respectively.

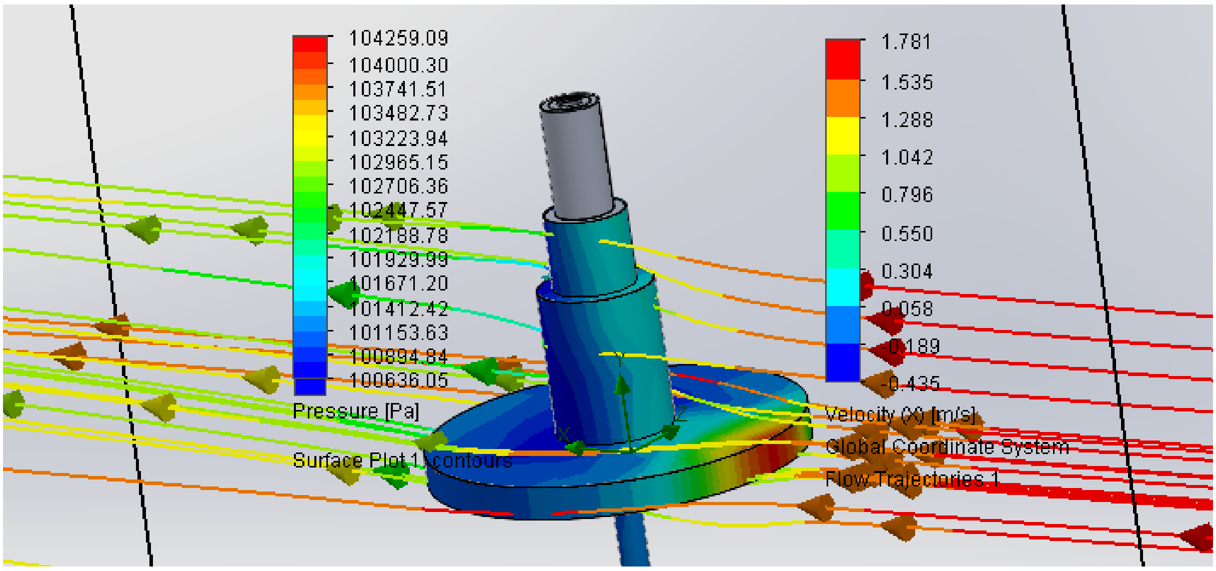

Figure 76- Current flow simulation on the support structure

There are some conclusions that can be drawn from current flow simulation:

- When the current passes through the solid, the flow reduces its velocity.
- The maximum pressure is obtained when the flow first hits the structure.

The simulation results are presented in Table 13:

Table 13- Results from the current flow simulation

Flow simulation	
Max Static Pressure	*0.1 MPa*
Max Total Pressure	*0.1 MPa*
Max Velocity (X)	*1.78 m/s*
Normal Force (X)	*1.3 kN*
Friction Force (X)	*20 N*
Torque (Z)	*157 Nm*

The current drag force creates a torque in the z-axis. This torque is not steep enough to tilt the structure because it is smaller then the righting moment for 90º, 197.8 Nm, calculated in section 6.1.1.3.

In a scenario like this, it should be better to towed to the seashore because the values are very close to each.

6.2.2Wind force

The wind flow simulation was applied to the WEC's structure because it is the one that is in contact with the air flow. The velocity, *v=15.43 m/s*, assumed that the air flow was obtained through the analyses of the environment maximum conditions.

Figure 77 shows the simulation results (From SolidWorks flow simulation). The arrows represent the winds' trajectory, and their colors represent their velocity value. The structure colors represent the total pressure created by the wind flow. The color scale for the pressure and the velocity is represented on the left and right, respectively.

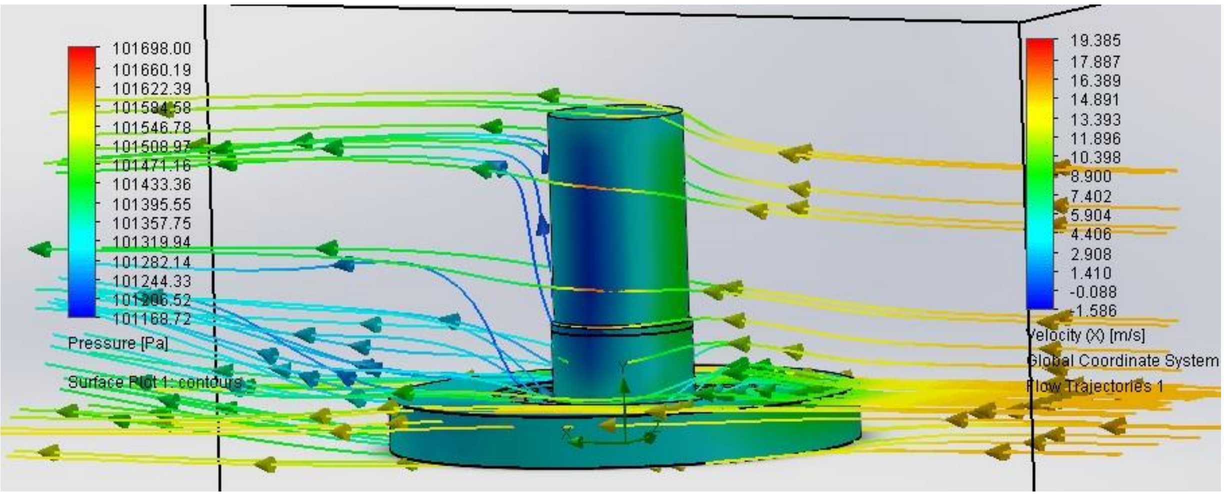

Figure 77- Wind flow simulation

There are some conclusions that can be drawn from current flow simulation:

- When the current passes through the solid, the flow reduces its velocity.
- The maximum pressure is obtained when the flow first hits the structure.

The simulation results are presented in Table 14.

Table 14- Results from the wind flow simulation

Flow simulation	
Max Static Pressure	*0.1* MPa
Max Total Pressure	*0.1* MPa
Max Velocity (X)	*19.67* m/s
Normal Force (X)	*52* N
Friction Force (X)	*0.8* N
Torque (Z)	*5* Nm

The tilt torque acting on the Z-axis is not enough to capsize the system. This moment will create reactive forces in the buoy and in the guidance system. These forces were not calculated because they seem irrelevant. The dynamic pressure is negligible.

These flow results will no longer be valid when the wind system is added. In that case, the wind will also be seen as a source of energy.

6.2.3 Mooring forces

The parameters of the synthetic rope selected in the design section 5.5.2.3 are:

Table 15- *ATLAS*™ rope parameters from *Lankhorst/Ropes* supplier

Diameter (mm)	Weight (kg/100 m)	MBF-Breaking strength (kN)
18	22	69

Section 5.5.2.3 shows the constraints that influenced the catenary system selection.

To compute the mooring forces, equation form section 3.2.5.33.2.5.2 were used. The tank depth was assumed to be $h_t = 6\ m$. It is reasonable to consider that the mooring rope length is four times longer than the water depth, $l = 24\ m.$ (Sailboat-crusing.com 2017)

The results from the mooring system parameters, assuming a catenary mooring, can be seen in Table 16.

Table 16- Mooring system parameters

w	$\boldsymbol{F_H}$	$\boldsymbol{F_V}$	s	x	$\Delta\boldsymbol{h}$
5.28 kg	*258* N	*125.97* N	*24* m	*23* m	*0.1+0.124* m

When there is a strong current, all the rope is being used, so the Δh is *0.1+0.124* m. Which means that, the second cylinder is totally submerged and the first cylinder is submerged 0.124 m (see Figure 68 for better understanding). If this happens, the kinematic system will absorb less wave power.

When the mooring system resistance is tested, according the parameters that were set previously, the simulation results from Table 17 can be obtain. It was assumed that the four screws are fixed, and the force of *390* N is applied at each point.

Table 17- Stress analyses of the mooring system

Name	Type	Min	Max
Stress1	VON: von Mises Stress	1270.28 N/m^2 Node: 10684	966552 N/m^2 Node: 9494

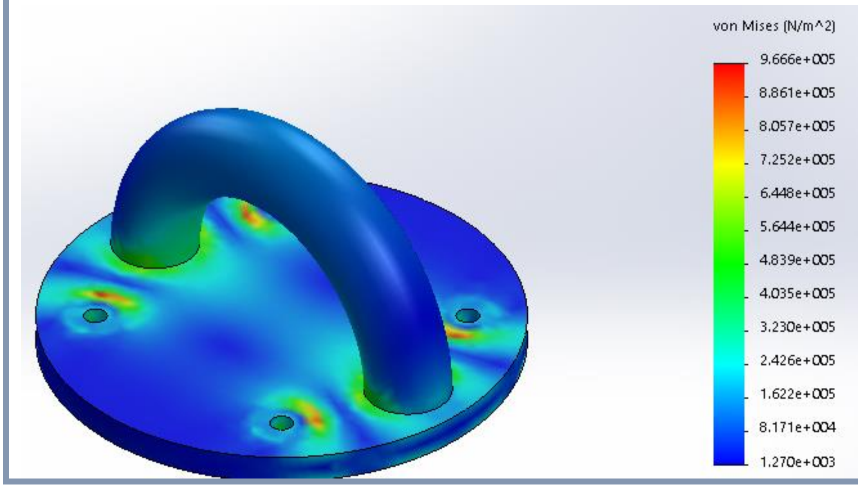

Table 18- Displacement analyses of the mooring system

Name	Type	Min	Max
Displacement1	URES: Resultant Displacement	0 mm Node: 240	0.00080286 mm Node: 12989

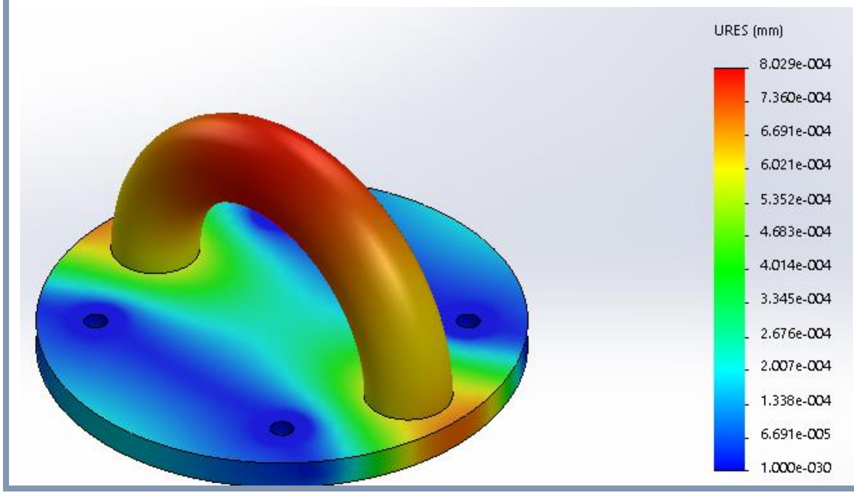

Table 18 shows that the displacement is almost zero and the maximum stress is 0.29 MPa. As it is was seen previously, it is an irrelevant stress for 7000 or 5000 aluminum series.

6.2.4 Simulations Summary

The simulations results made it possible to draw some conclusions:

- The wave's drag forces were easily supported by the inverted parachute because the materials remained in the elastic domain;
- The current's drag forces could almost capsize the device, so it would have to be towed;
- The wind forces could not tilt the system.

7 SPIDER UP Patent

During this project, another WEC was idealized and patented, SPIDER UP (Figure 78). Miguel Godinho and the author developed the presented concept. It is a WEC that uses a kinematic chain to produce mechanical energy and which is going to be converted into electrical by a single shaft. An overall picture can be seen in,

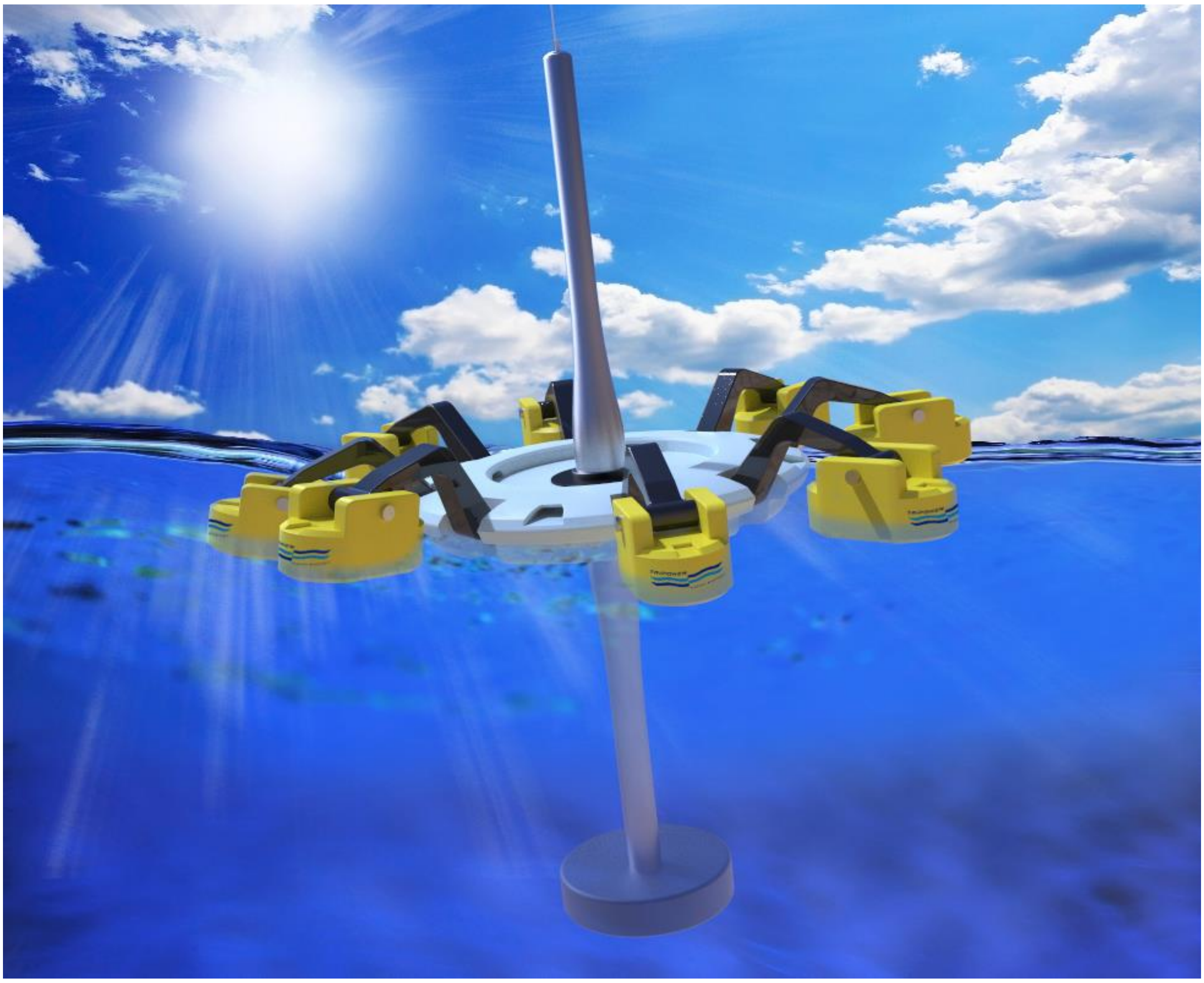

Figure 78- SPIDER UP (*Cortesy of Vasco Canavarro*)

The device presents multiple arms that oscillate according to the wave movement. When a wave comes in a radial direction, this circular displacement allows the absorption of "twice" its wave power. This means that after the wave is in contact with the first buoy, if the mechanism does not absorb all the wave power, the second buoy will oscillate and absorb the rest of the wave power.

This floating device can be placed at any sea level (deep sea or shallow waters) as long as it has waves. Being afloat also allows, if needed, to ease in transportation to the shore for maintenance or to avoid storms. The patent is in Appendix G.

7.1 Kinematic connection

All the buoys are connected with the kinematic chain that can be seen in Figure 79.

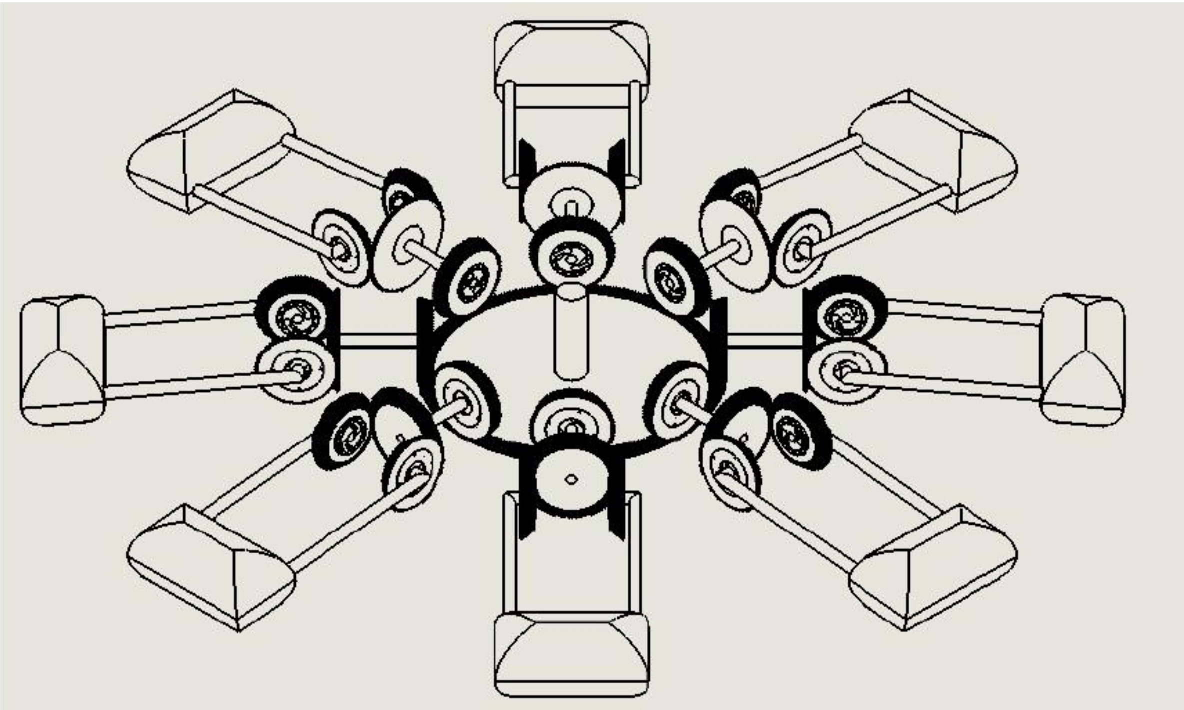

Figure 79- SPIDER UP overall mechanism

The mechanisms have several gears all attached to a central one in order to create a continuous movement. The aim of this configuration is that whatever the buoys which are oscillating with the waves, the gear transmits movement to the internal one, creating a persistent movement. It converts the vertical movement into a rotational movement.

The rotation of the internal gear can turn a central shaft that will be connected to a generator and produce electricity. The generator can also be connected directly to the central gear.

The WEC can have as many arms as it is desired, but, like in the hydraulic motors, it is recommended to have an odd number for a more fluid movement.

7.2 Spider arm

One of the arms of the SPIDER UP is presented in Figure 80.

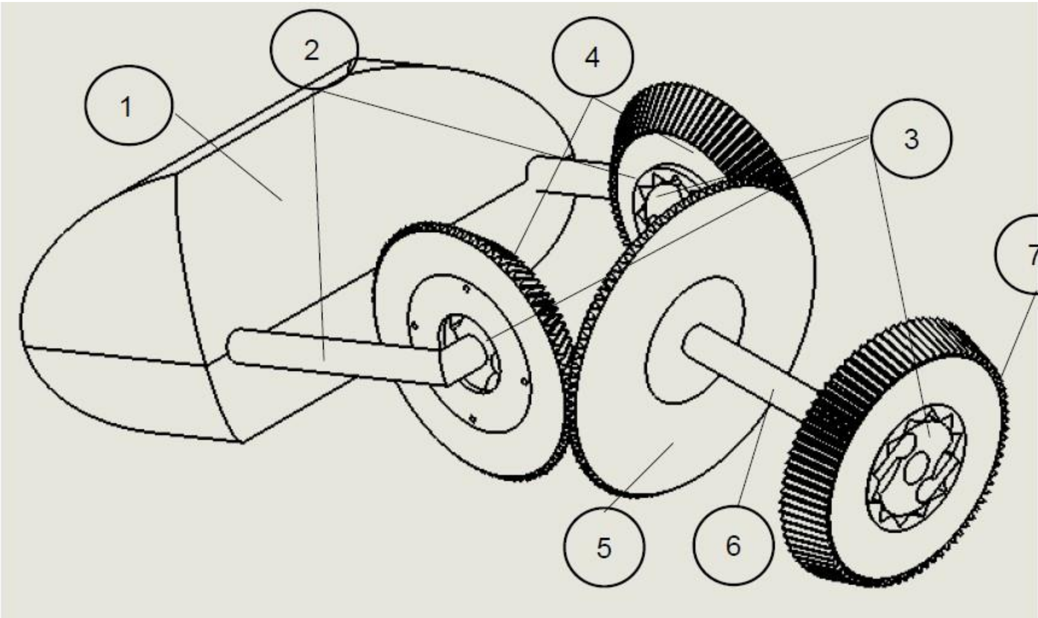

Figure 80- Spider arm

The freewheel is a key component, nº 3. It has two roles:

- The two placed in the back allow absorption of the upper and downward wave movements;
- The one in the front allows decoupling the movement between the inner big wheel and each arm. It is necessary because if the big internal wheel is rotating faster than the gear nº 7, the movement will not go to the shaft nº 6 (inverting the process);

The oscillation of the buoy, nº1, rotates the two rear freewheel. According to its positioning, the rotation of one of the nº4 gears makes nº5 spin. That rotation will be transmitted to the shaft nº6 and then to the last freewheel.

If the last freewheel starts to rotate faster than the gear nº 7, the power movement is transmitted to the gear. The gear nº 7 spins the main central gear creating electricity.

The two rear freewheel are mounted in opposition because if the buoy nº1 moves upwards, one of them transmits movement, if the buoy goes downwards it is the other one that is working.

The kinematic chain is stored in an inner buoy, and it is connected with the external ones with the “L” connectors, nº 2. In this way, there is a relative movement between the external and internal buoys that it is necessary to create mechanical energy.

The main concepts of this new WEC are created. For the future, the design and dimensions will be needed. It is an idea with a lot of potential, unfortunately, the time was short so this idea was not deeply developed.

8 Conclusions and future works

8.1 Conclusion

The research about the main energy source of the TRIPOWER UP device, waves, gave some insights during the design process. From the ocean waves' studies, it was concluded that:

- Even though that, in reality, waves assume an irregular behavior, for the purposes of wave energy converter's design, the waves' linear theory was applied;
- In deep water, waves are less influenced by the seabed, so they have higher energy density;
- The wave's velocity (or phase velocity) depends on the seabed depth;
- The density variation, due to temperature and salinity changes, influence the buoyancy forces in a structure.

Amongst the several types of WECs, the TRIPOWER UP can be considered as a PA, which led to a comparison between floating and submerged PA.

In a regular or irregular approach, the floating PA can extract a higher amount of wave power (for bigger wave periods), and it has a larger bandwidth. These conclusions indicated that the hypotheses that were assumed for the design concept of TRIPOWER UP were correct.

After this comparison, the key concepts for designing a floating PA were studied and some conclusions were drawn:

- The PTO system from TRIPOWER UP is considered a direct system;
- To have a stable system, it is crucial that the center of gravity is below the center of buoyance;
- The resonance between the device and waves, within a defined frequency, can maximize the harnessed power, so the equation of motion of the device should be defined;
- The mooring forces vary according to the material and configuration of the mooring line;
- For a submerged analysis, a cylindrical shaped PA can absorb more power than a sphere shaped PA;
- For a single buoy, the radius and the absorbed power are direct proportional;
- A single buoy extracts less power than several small buoys, assuming the same volume;
- To maximize the power extraction, the type of array depends on the direction of the wave front;
- When a scaled model is being designed, the Reynold's number, Froud's number and the Keulegan-Carpenter's number has to be taken into consideration.

The state-of-the-art analysis allowed for a better understanding of the concept's weaknesses and to find the solutions that would transition from the concept idea to a finished design.

The mechanical design was based on the wave's characteristics that would be possible to create in FEUP's wave tank. In the end, due to several constraints (such as buoyancy forces, stability, etc.) the device would not fit in the tank.

The mechanical design solutions to solve the concept problems are now presented:

- The rack asymmetry posed a stability issue, which was solved using a cross rack configuration.
- The development of the freewheel allowed to decouple or couple the racks' movement;
- The balance of the support structure uses the change of buoyancy forces instead of the mooring forces, creating a more stable device;
- The connection between the inner and the outer buoy was done by a developed tilting system rather than an elastomer;

As it was described in the state-of-the-art, stability plays the main role in a floating structure. Calculations were made to ensure that the structure does not capsize when placed in water:

- The buoys' dimensions were calculated to ensure that there is a balance between the gravitational force and the buoyancy force;
- The center of gravity was computed to make sure it was above the center of buoyance, conferring a positive righting moment, ensuring stability;
- The change in the submerged volume, due to the force created between the racks and the pinions, was also determined to guarantee wave power absorption;

Finally, the TRIPOWER UP was tested considering environment conditions. Although extreme real conditions were used for the current and wind tests, for the wave's test, wave tank characteristics were assumed. The simulations results made it possible to draw some conclusions:

- The wave's drag forces were easily supported by the inverted parachute because the materials remained in the elastic domain;
- The current's drag forces could almost capsize the device, so it would have to be towed;
- The wind forces could not tilt the system.

For the mooring forces' analyses, it could be concluded that even though the mooring system could support the forces, the variation of submerged height would lead to a reduction of the wave amplitude that could be absorbed.

During this project, the SPIDER UP concept came up and it was submitted for patent approval. This opened up a new possibility of a WEC that can be developed in future works.

8.2 Future Works

Besides the development of the SPIDER UP, a lot of work is yet to be done regarding the TRIPOWER UP project:

- Make all the technical drawings for all the parts that require specific manufacturing, and buy the market components that were selected;
- Find a tank where the TRIPOWER UP can be tested, or study the possibility of reducing weight and dimensions using composite materials for the buoys;
- Describe the equation of motion and maximize the wave power extraction;
- Understand the best array according to the Portuguese wave front direction;
- Calculate the forces acting on the guidance system due to internal and external loads;
- Develop the concept idea of SPIDER UP and create a mechanical design;
- Compare the Reynold’s number, Froud’s number and Keulegan-Carpenter’s number between the prototype and the real-scale model;
- Calculate the prototype’s energetic efficiency, through the prototype’s testing.

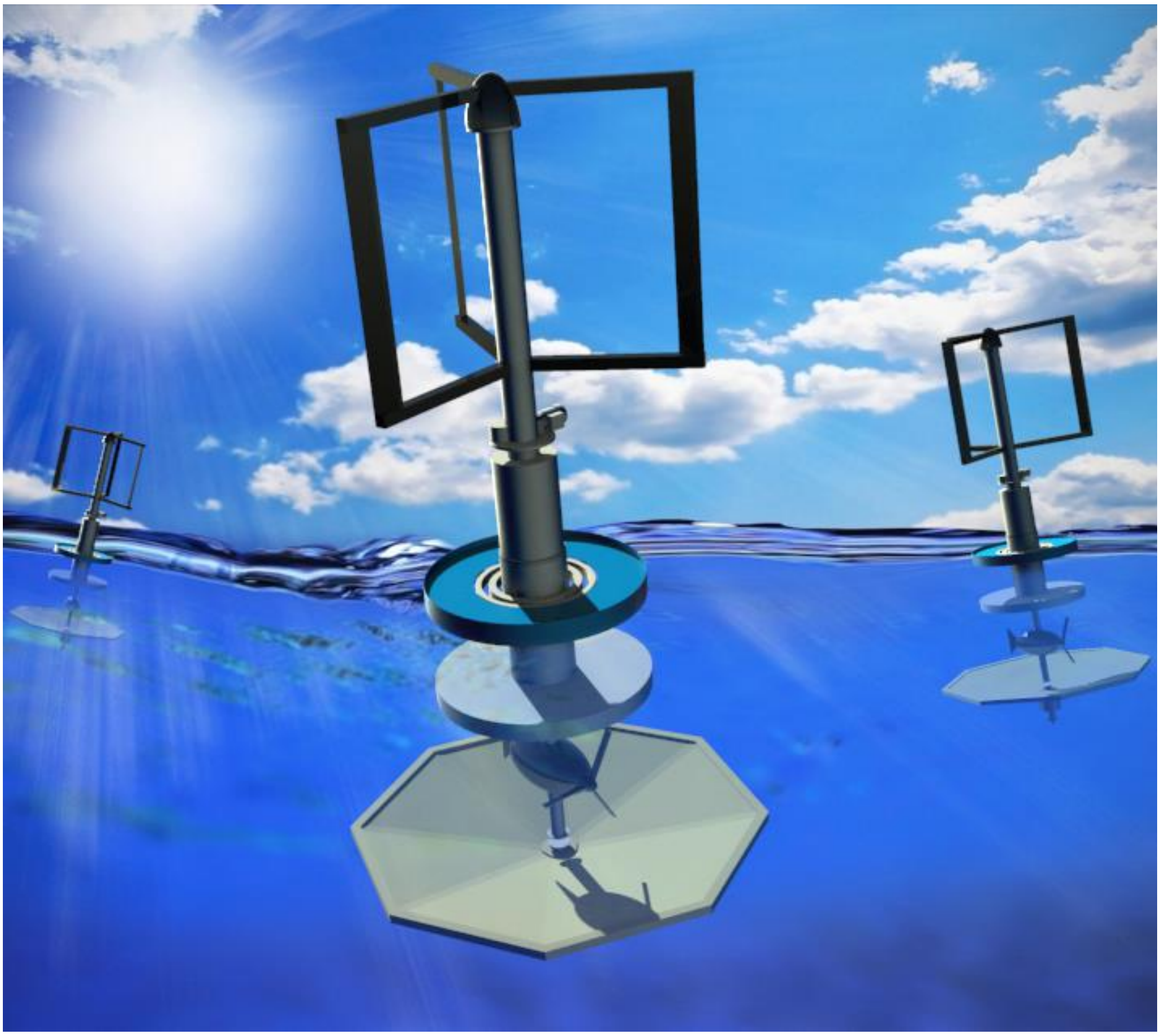

Figure 81- Tripower Up in the sea (courtesy of Vasco Canavarro)

List of References

Anthoni, Dr J Floor. 2000. "Theory and principles of waves, how they work and what causes them." accessed 26 of May. http://www.seafriends.org.nz/oceano/waves.htm.

Ashank Sinha, D. Karmakar, C. Guedes Soares. 2016. "Performance of optimally tuned arrays of heaving point absorbers." *Elsevier*.

Benson, Tom. "Velocity During Recovery." https://www.grc.nasa.gov/WWW/k-12/VirtualAero/BottleRocket/airplane/rktvrecv.html.

Boyle, Godfrey. 2004. *Renewable energy*. Vol. 2nd ed. Oxford: Oxford University Press.

C. Guedes Soares, Eugen Rusu. 2008. "Numerical modelling to estimate the spatial distribution of the wave energy in the Portuguese nearshore." *El Sevier*.

Dias, Helena Raquel Fereira. 2013. "Uma contribuição para conheciment do comportamento de âncoras em leitos marinhos arenosos para estrututras flutuantes." Master in Civil Engineering, FEUP.

Faizal, Mohammed, M. Rafiuddin Ahmed, and Young-Ho Lee. 2014. "A Design Outline for Floating Point Absorber Wave Energy Converters." *Advances in Mechanical Engineering* 6:846097. doi: 10.1155/2014/846097.

Godinho, Miguel Eduardo dos Santos. 2017. "TRIPOWER UP: Mechanical Design Kinematic structure of the wave energy converter." Master of Science in Mechanical Engineering, FEUP.

Haym Benaroya, Mark L. Nagurka. 2009. *Mechanical Vibration: Analysis, Uncertainties, and Control, Third Edition*.

IPMA. 2017. "Previsão da corrente à superficie ". https://www.ipma.pt/pt/maritima/currents/.

Macieira, José Miguel Soares. 2017. "Energia Renovável Oceânica - Conceção de um dispositivo para aproveitamento da Energia Eólica, das Ondas e das Correntes: TRI POWER UP." FEUP.

Magagna, Davide, and Andreas Uihlein. 2015. "Ocean energy development in Europe: Current status and future perspectives." *International Journal of Marine Energy* 11:84-104. doi: 10.1016/j.ijome.2015.05.001.

Marinha, Hidrográfico. 2017. "Bóias Ondógrafo." accessed 26 May, 2017. http://www.hidrografico.pt/boias-ondografo.php.

Morais, Tiago António Nunes da Silva. 2009. "Estudo da Operação de Parques de Sistemas de Conversão de Energia das Ondas em Energia Eléctrica." Mestre em Engenharia Electrotécnica e de Computadores, FEUP.

N.Y. Sergiienko, B.S. Cazzolato, B. Ding, P. Hardy, M. Arjomandi. 2017. *Performance comparison of the floating and fully submerged quasipoint absorber wave energy converters*,

OpenCourseWare, MIT. 2009. *2.017J Design of Electromechanical Robotic Systems*

Paredes, Guilherme Moura. 2008. "Estudo exprimental de um sistema Offshore para produção de energia das ondas." Mestrado Integrado em Engenharia Civil - 2007/2008, FEUP.

Rodrigues, Ricardo J. 2014. "Que ondas são estas?". http://www.dn.pt/revistas/nm/interior/amp/que-ondas-sao-estas-3640693.html.

Sailboat-crusing.com. 2017. "The Minimum Anchor Chain Length Needed To Properly Secure Your Boat." accessed 15/06/2017. http://www.sailboat-cruising.com/anchor-chain-length.html.

Sato, Iku. 2009. Wave Response Experiment on SPAR-type Floating Bodies for Offshore Wind Turbine. Department of Civil and Earth Resources Engineering, Kyoto University.

Strömgren, William Healy. 2005. "Automatic Adjustment of the Floatation Level for Tight-moored Buoy." Division of Electricity and Lightning Research, Uppsala University.

Thomas, G. 2008. *The theory behind the conversion of ocean wave energy: a review*, *Ocean Wave Energy: Current Status and Future Perspectives*. Berlin, Germany.

Thorpe, T. W. 1999. A Brief Review of Wave Energy.

V. Piscopo, G. Benassai, R. Della Morte, A. Scamardella. 2017. "Towards a cost-based design of heaving point absorbers." *Elsevier*.

Vefnámskeid, Plato. "Stability of fishing vessels." http://plato.is/stability_of_fishing_vessels/righting_lever/.

Waters, Rafael. 2008. "Energy from Ocean Waves." UPPSALA Universitet -Faculty of Science and Technology

White, Frank M. 1999. *Fluid Mechanics*. Mc Graw Hill.

Appendix

Appendix A

Table of wave properties

Wave property	SHALLOW WATER $(d/\lambda < 1/20)$	INTERMEDIATE WATER $(1/20 < d/\lambda < 1/2)$	DEEP WATER $(d/\lambda > 1/2)$
Velocity potential ($u = \nabla\phi$)	$\phi = \frac{ag}{\omega}\frac{\cosh k(z+d)}{\cosh kd}\cos(\omega t - kx)$	$\phi = \frac{ag}{\omega}\frac{\cosh k(z+d)}{\cosh kd}\cos(\omega t - kx)$	$\phi = \frac{ag}{\omega}e^{kz}\cos(\omega t - kx)$
Dispersion relation	$\omega^2 = g k^2 d$	$\omega^2 = gk \tanh kd$	$\omega^2 = gk$
Wave length - wave period relation	$\lambda = T\sqrt{gd}$	$\lambda = \frac{g}{2\pi}T^2 \tanh\frac{2\pi d}{\lambda}$	$\lambda = \frac{g}{2\pi}T^2 \ (\approx 1.56\ T^2)$
Wave profile	$\eta = a\sin(\omega t - kx)$	$\eta = a\sin(\omega t - kx)$	$\eta = a\sin(\omega t - kx)$
Dynamic pressure	$p_d = \rho g a \sin(\omega t - kx)$	$p_d = \rho g a \frac{\cosh k(z+d)}{\cosh kd}\sin(\omega t - kx)$	$p_d = \rho g a\, e^{kz}\sin(\omega t - kx)$
Horizontal particle velocity	$u = \frac{\omega a}{kd}\sin(\omega t - kx)$	$u = \omega a \frac{\cosh k(z+d)}{\sinh kd}\sin(\omega t - kx)$	$u = \omega a e^{kz}\sin(\omega t - kx)$
Vertical particle velocity	$w = \omega a \frac{z+d}{d}\cos(\omega t - kx)$	$w = \omega a \frac{\sinh k(z+d)}{\sinh kd}\cos(\omega t - kx)$	$w = \omega a e^{kz}\cos(\omega t - kx)$

Figure 82- Basic equations of linear wave theory. Part of booklet Linear Wave Theory. Note that symbols might differ from the rest of this text.(Paredes 2008)

Wave property	SHALLOW WATER	INTERMEDIATE WATER	DEEP WATER
Horizontal particle acceleration	$\dot{u} = \frac{\omega^2 a}{kd} \cos(\omega t - kx)$	$\dot{u} = \omega^2 a \frac{\cosh k(z+d)}{\sinh kd} \cos(\omega t - kx)$	$\dot{u} = \omega^2 a\, e^{kz} \cos(\omega t - kx)$
Vertical particle acceleration	$\dot{w} = -\omega^2 a \frac{z+d}{d} \sin(\omega t - kx)$	$\dot{w} = -\omega^2 a \frac{\sinh k(z+d)}{\sinh kd} \sin(\omega t - kx)$	$\dot{w} = -\omega^2 a\, e^{kz} \sin(\omega t - kx)$
Group velocity	$c_g = c$	$c_g = \frac{1}{2} c \left(1 + \frac{2kd}{\sinh 2kd}\right)$	$c_g = \frac{1}{2} c$

$\omega = 2\pi / T$, $k = 2\pi / \lambda$
T = wave period
λ = wave length
a = wave amplitude
g = acceleration of gravity
$c = \lambda / T$ = phase speed

t = time
x = direction of propagation
z = vertical co-ordinate positive upward, origin at still water level
d = water depth

p_d = dynamic pressure
$p_d - \rho g z + p_o$ = total pressure in the water ($-\rho g z$ = hydrostatic pressure, p_o = atmospheric pressure).
$E = \frac{1}{2} \rho g a^2$ = wave energy (per unit surface area)
$P = E c_g$ = wave energy flux (per unit width along the wave crest)

Figure 83- Figure 83Figure 82 continuation

Appendix B

SolidWorks Design Properties

```
Mass properties of Support Structure_com Lastro
    Configuration: Default
    Coordinate system: -- default --

Mass = 330141.32 grams

Volume = 67054913.90 cubic millimeters

Surface area = 23344165.24  square millimeters

Center of mass: ( millimeters )
     X = 0.00
     Y = -1055.24
     Z = 0.00

Principal axes of inertia and principal moments of inertia: ( grams *  square millimeters )
Taken at the center of mass.
      Ix = ( 0.00,  1.00,  0.00)      Px = 51081663859.62
      Iy = (-0.78,  0.00,  0.62)      Py = 247763538356.50
      Iz = ( 0.62,  0.00,  0.78)      Pz = 247764191005.92

Moments of inertia: ( grams *  square millimeters )
Taken at the center of mass and aligned with the output coordinate system.
     Lxx = 247763789296.69       Lxy = -86575.80             Lxz = -317495.14
     Lyx = -86575.80             Lyy = 51081663860.90        Lyz = -494630.13
     Lzx = -317495.14            Lzy = -494630.13            Lzz = 247763940064.45

Moments of inertia: ( grams *  square millimeters )
Taken at the output coordinate system.
     Ixx = 615386927483.27       Ixy = -53246.85             Ixz = -317495.12
     Iyx = -53246.85             Iyy = 51081663861.04        Iyz = -275862.30
     Izx = -317495.12            Izy = -275862.30            Izz = 615387078250.91
```

Figure 84- Support structure mass properties

Mass properties of CI_Assemb
Configuration: Default
Coordinate system: Coordinate System1

Mass = 512976.65 grams

Volume = 512976647.19 cubic millimeters

Surface area = 12829964.97 square millimeters

Center of mass: (millimeters)
X = 0.00
Y = -1177.33
Z = 0.00

Principal axes of inertia and principal moments of inertia: (grams * square millimeters)
Taken at the center of mass.

Ix = (0.00, 1.00, 0.00)	Px = 137291420733.18
Iy = (0.00, 0.00, 1.00)	Py = 308151203342.39
Iz = (1.00, 0.00, 0.00)	Pz = 308151203342.39

Moments of inertia: (grams * square millimeters)
Taken at the center of mass and aligned with the output coordinate system.

Lxx = 308151203342.39	Lxy = 0.00	Lxz = 0.00
Lyx = 0.00	Lyy = 137291420733.18	Lyz = 0.00
Lzx = 0.00	Lzy = 0.00	Lzz = 308151203342.39

Moments of inertia: (grams * square millimeters)
Taken at the output coordinate system.

Ixx = 1019194591831.76	Ixy = 0.00	Ixz = 0.00
Iyx = 0.00	Iyy = 137291420733.18	Iyz = 0.00
Izx = 0.00	Izy = 0.00	Izz = 1019194591831.76

Figure 85- Properties of the submerged support structure with water density

Mass properties of CI_Assemb_90
Configuration: Default
Coordinate system: Coordinate System1

Mass = 277502.73 grams

Volume = 277502728.30 cubic millimeters

Surface area = 7595028.61 square millimeters

Center of mass: (millimeters)
X = -259.78
Y = -1171.50
Z = 0.00

Principal axes of inertia and principal moments of inertia: (grams * square millimeters)
Taken at the center of mass.

Ix = (0.11, 0.99, 0.00)	Px = 50402001169.97
Iy = (0.00, 0.00, 1.00)	Py = 147732780121.46
Iz = (0.99, -0.11, 0.00)	Pz = 169604914793.24

Moments of inertia: (grams * square millimeters)
Taken at the center of mass and aligned with the output coordinate system.

Lxx = 168270147510.50	Lxy = 12542987898.13	Lxz = 0.02
Lyx = 12542987898.13	Lyy = 51736768452.71	Lyz = -0.13
Lzx = 0.02	Lzy = -0.13	Lzz = 147732780121.46

Moments of inertia: (grams * square millimeters)
Taken at the output coordinate system.

Ixx = 549115207200.41	Ixy = 96995680651.55	Ixz = -0.01
Iyx = 96995680651.55	Iyy = 70464219766.14	Iyz = -0.22
Izx = -0.01	Izy = -0.22	Izz = 547305291124.81

Figure 86- Properties of the submerged support structure when tilted 90°

Section properties of the selected faces of CI_Assemb_90

Area = 952358.69 millimeters^2

Centroid relative to assembly origin: (millimeters)
X = 0.00
Y = 446.24
Z = 0.00

Moments of inertia of the area, at the centroid: (millimeters ^ 4)

Lxx = 758234300351.02	Lxy = 0.00	Lxz = 0.00
Lyx = 0.00	Lyy = 72778443234.00	Lyz = 0.06
Lzx = 0.00	Lzy = 0.06	Lzz = 685455857117.02

Polar moment of inertia of the area, at the centroid = 758234300351.02 millimeters ^ 4

Angle between principal axes and assembly coordinate axes = -0.00 degrees

Principal moments of inertia of the area, at the centroid: (millimeters ^ 4)
Ix = 72778443234.00
Iy = 685455857117.01

Moments of inertia of the area, at the output coordinate system: (millimeters ^ 4)

LXX = 947881302024.83	LXY = 0.00	LXZ = 0.00
LYX = 0.00	LYY = 72778443234.00	LYZ = -0.06
LZX = 0.00	LZY = -0.06	LZZ = 875102858790.83

Figure 87- Properties of the cross-section area of the support structure when tilted 90°

Mass properties of tubo2.2
Configuration: Default
Coordinate system: -- default --

The center of mass and the moments of inertia are output in the coordinate system o
Density = 0.00 grams per cubic millimeter

Mass = 4932.25 grams

Volume = 1826760.73 cubic millimeters

Surface area = 848487.63 square millimeters

Center of mass: (millimeters)
X = 0.00
Y = -611.50
Z = 0.00

Principal axes of inertia and principal moments of inertia: (grams * square millimeter
Taken at the center of mass.
Ix = (0.00, 1.00, 0.00) Px = 14534116.18
Iy = (0.00, 0.00, 1.00) Py = 782128294.54
Iz = (1.00, 0.00, 0.00) Pz = 782128294.54

Moments of inertia: (grams * square millimeters)
Taken at the center of mass and aligned with the output coordinate system.

Lxx = 782128294.54	Lxy = 0.00	Lxz = 0.00
Lyx = 0.00	Lyy = 14534116.18	Lyz = 0.00
Lzx = 0.00	Lzy = 0.00	Lzz = 782128294.54

Moments of inertia: (grams * square millimeters)
Taken at the output coordinate system.

Ixx = 2626457119.32	Ixy = 0.00	Ixz = 0.00

Figure 88- Tube submerged volume

Mass properties of contramovimento
Configuration: Default
Coordinate system: -- default --

The center of mass and the moments of inertia are output in the coordinate system o
Mass = 59958.64 grams

Volume = 22206904.77 cubic millimeters

Surface area = 10449812.45 square millimeters

Center of mass: (millimeters)
X = 0.00
Y = -1137.26
Z = 0.00

Principal axes of inertia and principal moments of inertia: (grams * square millimeter
Taken at the center of mass.

Ix = (0.00, 0.00, 1.00)	Px = 17417175827.12
Iy = (1.00, 0.00, 0.00)	Py = 17417175827.12
Iz = (0.00, 1.00, 0.00)	Pz = 34399027099.54

Moments of inertia: (grams * square millimeters)
Taken at the center of mass and aligned with the output coordinate system.

Lxx = 17417175827.12	Lxy = 0.00	Lxz = 0.00
Lyx = 0.00	Lyy = 34399027099.54	Lyz = 0.00
Lzx = 0.00	Lzy = 0.00	Lzz = 17417175827.12

Moments of inertia: (grams * square millimeters)
Taken at the output coordinate system.

Ixx = 94965093725.61	Ixy = 0.00	Ixz = 0.00
Iyx = 0.00	Iyy = 34399027099.54	Iyz = 0.00
Izx = 0.00	Izy = 0.00	Izz = 94965093725.61

Figure 89-Inverted parachute volume

Mass properties of WEC structure(Sem capacidade de rodar para medir o centro de gravi
Configuration: Default
Coordinate system: -- default --

Mass = 102361.49 grams

Volume = 55162446.91 cubic millimeters

Surface area = 15116083.43 square millimeters

Center of mass: (millimeters)
X = 0.10
Y = 388.08
Z = -0.08

Principal axes of inertia and principal moments of inertia: (grams * square millimeters)
Taken at the center of mass.

Ix = (0.00, 1.00, 0.00)	Px = 13679759018.05
Iy = (0.62, 0.00, 0.78)	Py = 17442748539.36
Iz = (0.78, 0.00, -0.62)	Pz = 17597753150.75

Moments of inertia: (grams * square millimeters)
Taken at the center of mass and aligned with the output coordinate system.

Lxx = 17538201806.43	Lxy = -1242845.45	Lxz = 75394357.66
Lyx = -1242845.45	Lyy = 13679759659.27	Lyz = 983689.47
Lzx = 75394357.66	Lzy = 983689.47	Lzz = 17502299242.46

Moments of inertia: (grams * square millimeters)
Taken at the output coordinate system.

Ixx = 32954429314.90	Ixy = 2827831.71	Ixz = 75393561.33
Iyx = 2827831.71	Iyy = 13679761324.12	Iyz = -2032133.14
Izx = 75393561.33	Izy = -2032133.14	Izz = 32918527235.83

Figure 90-WEC's structure properties

Section properties of the selected faces of CI_Assemb_90

Area = 822030.70 millimeters^2

Centroid relative to assembly origin: (millimeters)
X = 25.11
Y = -1091.51
Z = 0.00

Moments of inertia of the area, at the centroid: (millimeters ^ 4)

Lxx = 550979468470.99	Lxy = 0.00	Lxz = 0.00
Lyx = 0.00	Lyy = 72090212151.06	Lyz = 0.06
Lzx = 0.00	Lzy = 0.06	Lzz = 478889256319.93

Polar moment of inertia of the area, at the centroid = 550979468471.00 millimeters ^ 4

Angle between principal axes and assembly coordinate axes = -0.00 degrees

Principal moments of inertia of the area, at the centroid: (millimeters ^ 4)
Ix = 72090212151.06
Iy = 478889256319.93

Moments of inertia of the area, at the output coordinate system: (millimeters ^ 4)

LXX = 1530341566154.93	LXY = -22525727133.88	LXZ = 0.00
LYX = -22525727133.88	LYY = 72608313049.71	LYZ = -0.06
LZX = 0.00	LZY = -0.06	LZZ = 1458769454902.51

Figure 91-Cross-section properties of the support structure

Appendix C

Aluminum material properties

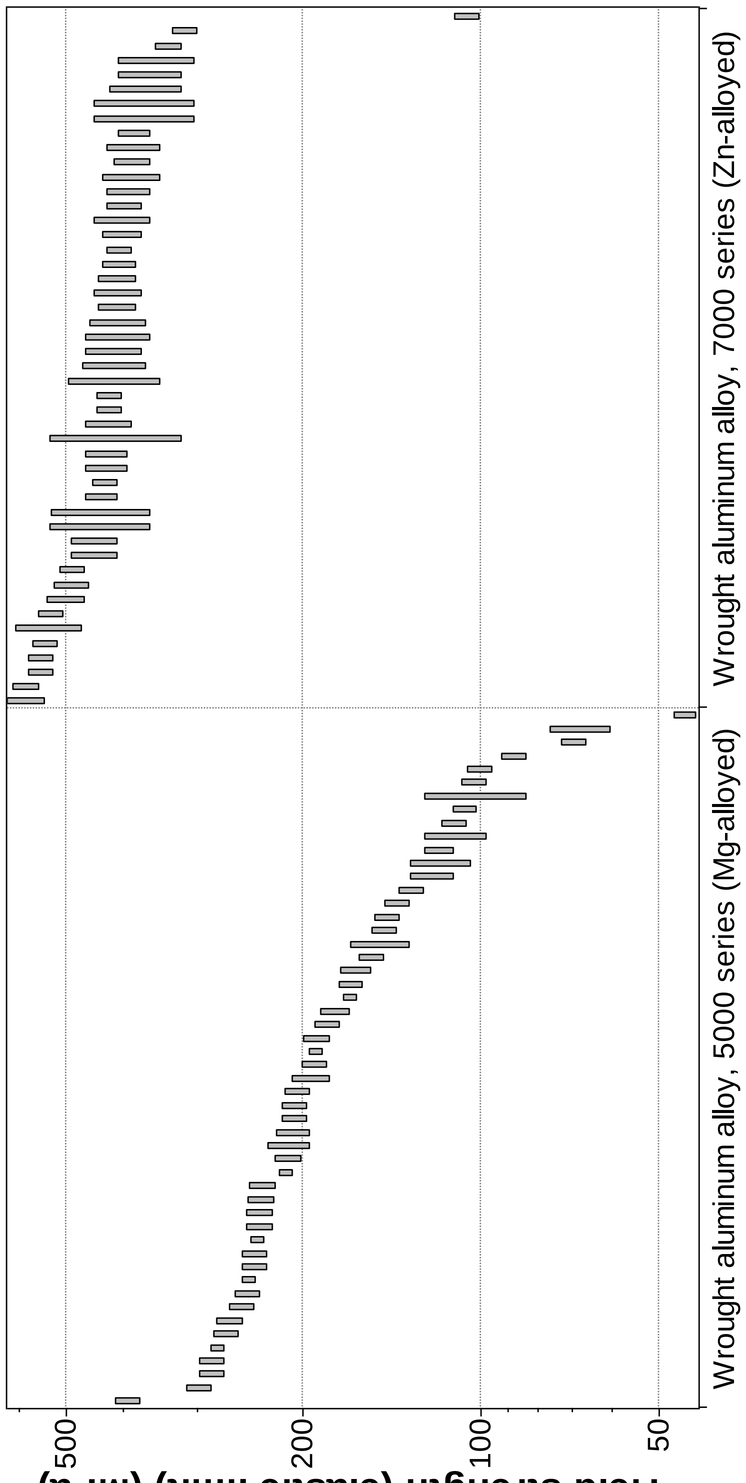

Figure 92- Yield strength (elastic limit) for 7000 and 5000 series- CES Edu Pack 2017

Appendix D

Power limit for regular waves: Explanation of upper and lower boundaries

- Upper-boundary: a high-frequency limit PA defined by the body's ability to radiate waves (from Equation 3.1 assuming deep water conditions $\omega^2 = kg$): (N.Y. Sergiienko, 2017)
-

$$\boldsymbol{P_A = c_\infty T^3 H^2} \quad \text{(B.1)}$$

where$c_\infty = \rho(g/\pi)^3/128$, $H = 2A$ is the wave height, $T = 2\pi/\omega$ is the wave period. It has the same expression for submerged and floating bodies.

The lower-boundary depends on the PA's type. If the buoy is submerged, the shape also affects the lower boundary.

- Floating buoy, lower-boundary: a low-frequency limit $P_{B,f}$ defined by the maximum swept volume of the body, which applies when the velocity of the converter is smaller than the optimal value due to physical constraints:

$$\boldsymbol{P_{B,f} = \frac{c_0 VH}{T}} \quad \text{(B.2)}$$

Where $c_0 = \rho g\pi/4$, V is the body volume, and the subscript f corresponds to the floating case.

- Submerged buoy, lower-boundary: $P_{B,s}$ curve strongly depends on shape and should be derived for the next two case, when the buoy his spherical,

$$\boldsymbol{P_{B,s} = 4\pi^3 \rho e^{-kd_s} s_{3,max} \frac{VH}{T^3}} \quad \text{(B.4)}$$

Where s corresponds to the floating case, $s_{3,max}$ is the maximum displacement of the sphere under the water and d_s is the displacement under the water. When the buoy is cylindrical the lower-boundary is,

$$\boldsymbol{P_{B,s} = \frac{\pi^2 a\rho g H}{T} s_{3,\max} \left(\frac{2J_1(ka)}{kJ_0(ka)\cosh(kd1)} - ae^{-kd_2}\right)} \quad \text{(B.5)}$$

where $d_2 = d_1 + h_c$, J_0 and J_1 are Bessel functions of the first kind of order 0 and 1 respectively, k is the real solution of the dispersion equation $\omega^2 = kgd_1$ using shallow water conditions for the water domain above the cylinder.

Please note that in here only the final formulas are presented. The way the formulas are obtained can be seen in the article of N.Y. Sergiienko 2017.

Appendix E

Tripower Up Exploded view

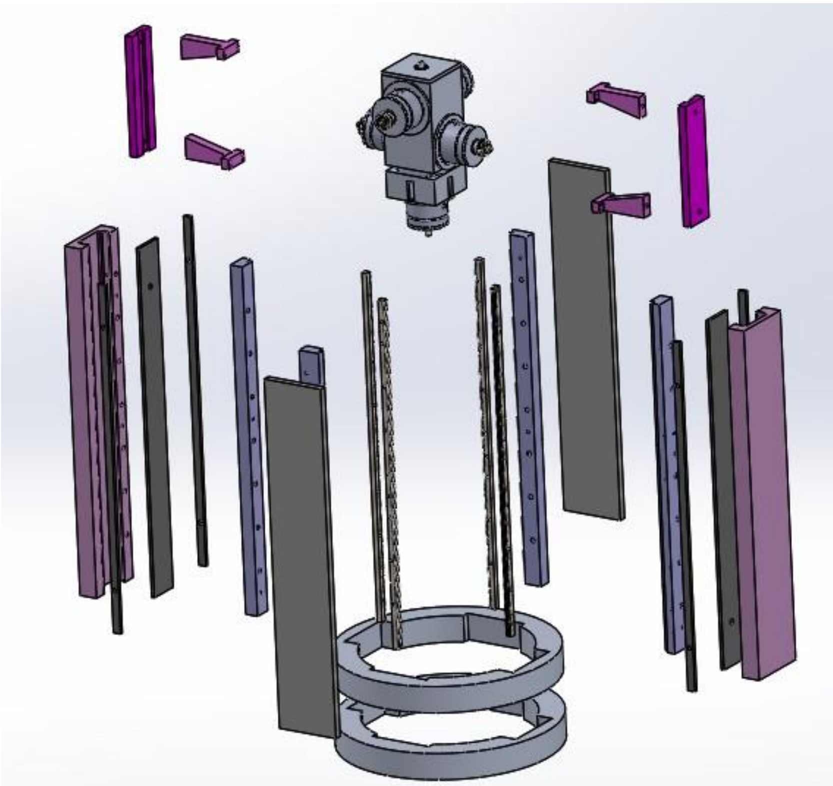

Figure 93-Upper part of the WEC’s structure

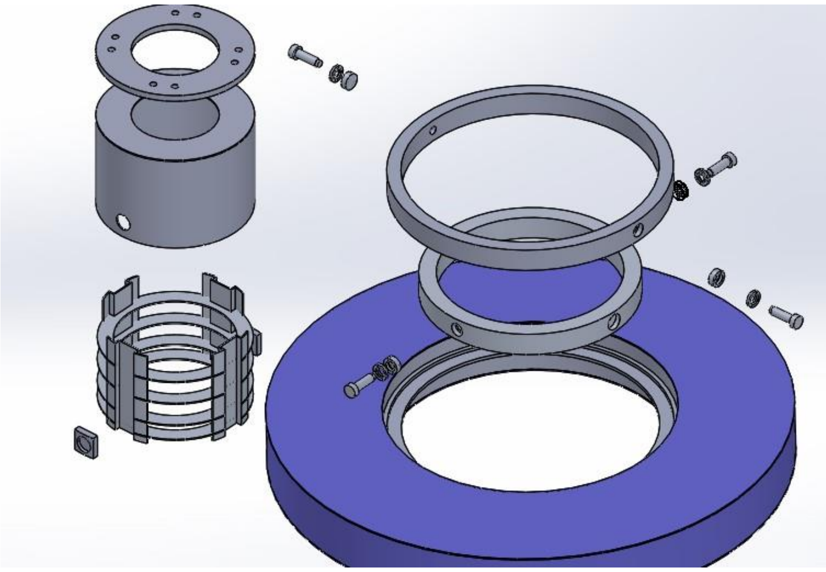

Figure 94- Lower Part of the WEC´s transmission

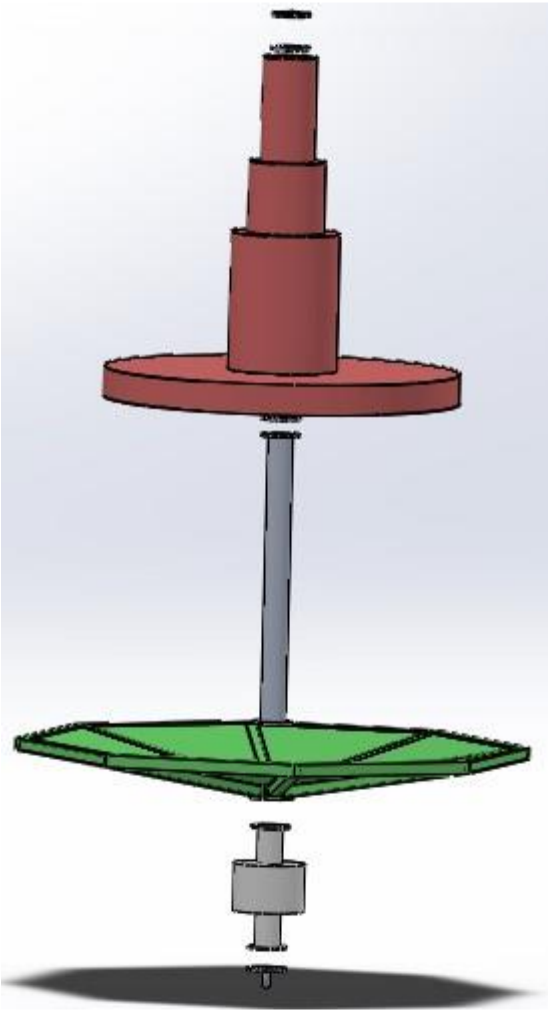

Figure 95- Support structure

Appendix F

Costume Freewheel technical drawing

Appendix G

SPIDER UP Patent

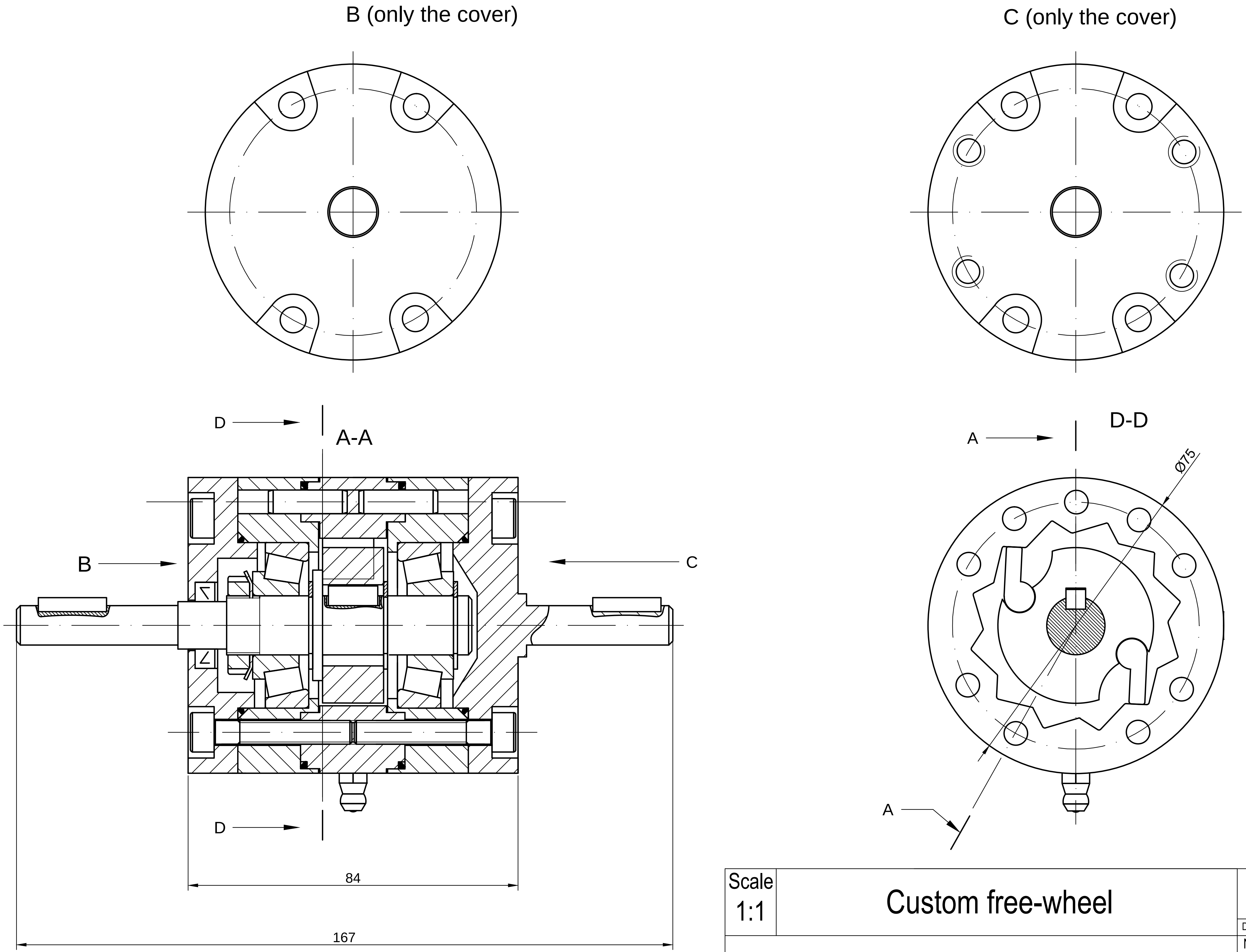

Scale 1:1	Custom free-wheel	Faculdade de Engenharia da Universidade do Porto
		Departamento de Engenharia Mecânica - DEMec
Designed by: Miguel Godinho and Diogo Telo Rodrigues		Number: MG_DT 1_2017
		Revision: — Date: 23/06/2017

DISPOSITIVO MÚLTIPLO DE CONVERSÃO DE ENERGIA DAS ONDAS

Patent No.:
Int. Cl.
F03B

Requerente: Augusto Barata da Rocha

Inventores: Augusto Barata da Rocha; Diogo Telo de Castro Rodrigues; Miguel Eduardo dos Santos Godinho; Miguel Macieira

RESUMO

A presente invenção consiste num dispositivo de aproveitamento da energia oceânica, que converte o movimento vertical oscilante das ondas em energia elétrica.

Este dispositivo pode ser instalado em qualquer plano de água oceânico, longe da costa (offshore), perto da costa ou na costa, independentemente da profundidade, por ser flutuante. Nas duas primeiras situações, o sistema é mantido na sua posição com recurso a um sistema de amarração constituído por uma âncora e uma corrente de amarração. Caso seja instalado na costa, pode ser fixo a uma estrutura montada num pontão ou outra estrutura semelhante.

A energia associada ao movimento das ondas é captada por um dispositivo de boias que, através de pelo menos um sistema pinhão-cremalheira, converte este movimento vertical oscilante em movimento de rotação, que, por sua vez, aciona um gerador elétrico.

O mecanismo é constituído por um ou vários braços articulados, responsáveis pela transformação da energia potencial das ondas em energia cinética e posteriormente elétrica.

Cada braço atua de modo independente, transmitindo a energia cinética para uma roda dentada comum que, por sua vez, aciona um gerador elétrico.

O dispositivo pode ser facilmente desacoplado do sistema de amarração, para que possa ser rebocado para operações de manutenção ou para proteção do dispositivo em situações de tempestade.

Num estágio de exploração comercial, o dispositivo de conversão da energia das ondas pode ser combinado em rede, com outros dispositivos semelhantes, para formar um parque de energia oceânica.

Figura para Publicação

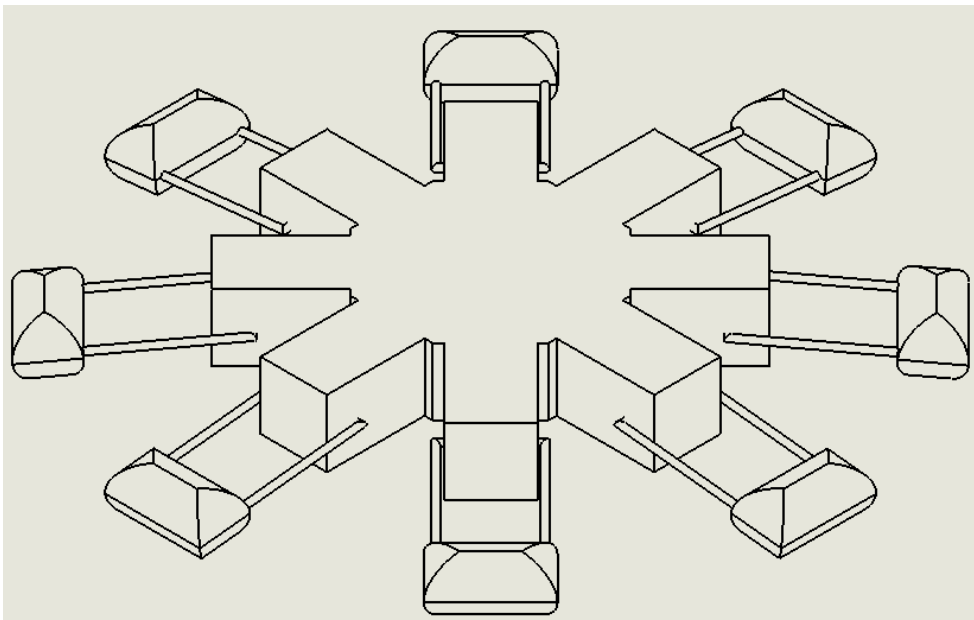

DESCRIÇÃO

Área técnica da invenção

No mundo atual, altamente competitivo e submetido à globalização dos mercados, a energia é um vetor importante e estratégico de desenvolvimento.

O consumo de energia primária atual é já de cerca de 12 GTep/ano (Tep – Tonelada equivalente de petróleo) sendo que os combustíveis fósseis representam 70% deste total; o carvão e o petróleo representam 26% cada, o gás natural 18% e as fontes de energia não fósseis 30%. As fontes de energia não fósseis dividem-se quase em partes iguais, entre as energias renováveis e a energia nuclear.

A disponibilidade e independência energética são fatores considerados fundamentais no desenvolvimento económico de um País.

As alterações climáticas e a escassez destes recursos impõem novos modelos energéticos assentes em energias limpas e renováveis.

Se por um lado é essencial mudar o padrão de consumo energético, também a mudança da matriz de consumo de energia primária está entre os maiores desafios que o mundo terá de enfrentar, se quiser reduzir as emissões de gases que causam o efeito estufa (e contribuem para o aquecimento global) e minimizar outros problemas resultantes da utilização dos combustíveis fosseis.

O aumento quase exponencial da população mundial, e dos seus padrões de consumo, implicará uma crescente procura de energias renováveis, que poderá ser extraída dos oceanos.

Estima-se que, até 2030, as energias renováveis offshore deverão registar um aumento de 22%.

Entre as energias renováveis offshore destaca-se a energia das ondas que advém do movimento contínuo das águas do mar, devido à ação do campo gravítico terrestre e do vento na superfície dos oceanos.

A energia contida nas ondas oceânicas apresentam uma grande densidade energética, não só devido à sua amplitude, mas também devido ao valor de densidade da água.

A natureza oscilante de uma onda torna este recurso intermitente, pelo que é importante encontrar formas de converter energia de uma forma mais contínua.

Atualmente existem poucos dispositivos de conversão de energia das ondas num estágio de exploração comercial. A maioria dos sistemas desenvolvidos estão num estado avançado de I&D (Investigação e Desenvolvimento), protótipo ou num estágio pré-comercial.

Considerando que ainda não existem soluções comerciais, economicamente viáveis, para o aproveitamento da energia das ondas (facto que se pode constatar pela diversidade de soluções em estado embrionário de maturidade tecnológica que se tentaram implementar), esta invenção apresenta uma solução viável para uma conversão mais constante de energia das ondas.

Estado da Técnica

Revisão bibliográfica

Existem diversos sistemas desenvolvidos e patenteados ao longo dos anos que convertem a energia das ondas em energia elétrica.

Atualmente existem poucos dispositivos num estágio de exploração comercial. A maioria dos sistemas desenvolvidos estão num estado avançado de I&D (Investigação e Desenvolvimento), protótipo ou num estágio de maturidade pré-comercial.

Alguns dos sistemas mais avançados e representativos são descritos em seguida.

O sistema PowerBuoy, instalado na costa do Oceano Pacífico dos Estados Unidos, é baseado numa boia, ancorada ao fundo do mar, que, através de um sistema hidráulico, aciona um gerador elétrico.

O sistema Pelamis Wave Energy Converter, testado na Aguçadoura, Portugal, consiste em vários cilindros articulados que, através da passagem das ondas, acionam um conjunto de cilindros hidráulicos. A conceção das articulações, sujeitas a grandes esforços, revelou-se problemática, tendo conduzido a falhas constantes e persistentes.

O sistema Wave Dragon, utilizado na Dinamarca, utiliza turbinas hidroelétricas para a produção de energia elétrica. Este sistema faz convergir a onda numa rampa que seguidamente atua uma turbina. O rendimento do sistema é baixo e a dimensão do sistema pode interferir com a navegação. Tem também vários elementos móveis facilmente danificáveis em caso de tempestade.

O Sistema Oyster Wave Energy Converter, instalado nas costas escocesas, é um conversor de energia das ondas oscilante, que aciona bombas hidráulicas que fazem mover uma turbina. A solução hidráulica introduz perdas importantes no sistema e gera problemas de desgaste nos vedantes.

O Sistema WaveRoller, instalado em Peniche, Portugal, aproveita as correntes submarinas de vaivém junto à costa e à rebentação, acionando elementos planos que, por sua vez, transmitem movimento a cilindros hidráulicos. A proximidade da costa e do fundo do mar potencia problemas nas articulações e vedações hidráulicas, devido às areias e detritos.

Patentes

A patente US2016333858 (A1), System And Method for Generating Electricity Using Grid of Wind and Water Energy Capture Devices, descreve um sistema de grelha ou estrutura de posicionamento relativo de várias unidades de conversão de energia, de modo a evitar colisões. A combinação da energia gerada é feita eletricamente.

A patente US2015266549 (A1), Oscillating Piston-Type Wave Power Generation Method and System, descreve uma invenção que capta a energia das ondas. Neste dispositivo, a boia move-se de acordo com a passagem das ondas para fazer movimentar um pistão que pressuriza um fluído hidráulico que induz rotação a um motor hidráulico, que, por sua vez, está acoplado a um gerador elétrico.

Na patente US9115688 (B1), Wind Resistance Wave Generator, é descrito um sistema que contem apenas uma turbina, que é movimentada pela ação conjunta da passagem das correntes, vento e ondas. A flutuabilidade do sistema é conseguida através de pneus cheios com espuma flutuante.

A patente WO2015086033 (A1), Hybrid Electricity Generators Using Wind Energy and Wave Energy, regista um dispositivo de captação de energia eólica, das correntes e das ondas. A energia das ondas é aproveitada de uma das 3 formas concebidas:

a. Por um sistema de molas de torção e com um mecanismo de roda livre que, com o movimento de oscilação de uma boia, colocam a mola sobre tensão, o que provoca a rotação de um veio. Com a instalação de um mecanismo de roda livre, o movimento alternado de tração e compressão das molas gera um movimento de rotação de um veio sempre no mesmo sentido;

b. Pela pressurização de um fluido hidráulico.

c. Por um mecanismo de roldanas. Com esta solução, é aproveitado o facto de o sistema ter de ser ancorado, para fazer passar o cabo de ancoragem por uma roldana colocada numa boia. Assim, o movimento de oscilação provocado pela passagem das ondas obriga a boia a movimentar-se da mesma forma, o que faz movimentar a roldana. Com um mecanismo de roda livre, o movimento de rotação alternado da roldana pode ser convertido num movimento de rotação com um só sentido.

A patente GB2515577 (A), Hybrid Electricity Generators Using Wind Energy and Wave Energy, descreve um sistema que apenas capta a energia das correntes e do vento.

A patente WO2014196921 (A1), A Water Based Modular Power Plant, descreve um sistema em que a energia é captada para produzir hidrogénio sendo que apenas indiretamente produz energia elétrica.

A patente US2014246792 (A1), Power Transfer and Generation Using Pressurize Fluids, descreve uma turbina (eólica ou de correntes) utilizada para bombear um fluido sob pressão, armazenado num reservatório, utilizado para movimentar um gerador elétrico.

A patente WO2014056049 (A1), Device Using Multiple Renewable Energy Sources, descreve um sistema ancorado no fundo do mar que utiliza a energia cinética das ondas para bombear água para um depósito, que posteriormente aciona uma turbina.

Na patente US2014091576 (A1), Offshore Combined Power Generation System, a energia eólica e das correntes é combinada eletricamente, numa estrutura não flutuante, ancorada no fundo do mar.

Na patente US2013028729, Power Generation Systems and Methods, o princípio de funcionamento é baseado em hidráulica. Além disso, é um sistema desenhado para apenas captar energia das correntes e do vento através de um fluído pressurizado.

Na patente WO2012076851 (A1), Wave Energy Converter, a energia das ondas é captada através de um ou vários geradores elétricos lineares.

Na patente US2011215650 (A1), Offshore Energy Harvesting, Storage and Power Generation System, a energia das ondas é captada através de um sistema que inclui uma câmara interna com uma turbina hidroelétrica.

A patente WO2010080043 (A2), Energy System, descreve formas de otimização na combinação de diferentes tipos de energia. No caso da energia das ondas, o sistema descreve dispositivos com canais de receção das ondas.

Na patente WO2009005383 (A1), Joint System for Conversion of Eolic, Solar, Sea Waves And maritime Currents Energies, 15.é descrito um dispositivo, que, apesar de captar energia das ondas, do vento e das correntes, não utiliza uma solução de um gerador único, optando por dedicar um gerador para aproveitar individualmente cada uma destas fontes de energia.

Na patente US2008101865 (A1), Hydrodynamic Drive Train For Energy Converters That Use Ocean Currents, é descrito um sistema em que apenas a energia das correntes é convertida em energia elétrica, através de uma solução hidráulica.

A patente WO2006010783 (A1), Wind, Wave And Current Power Stations With Different Foundations Solutions And Methods How To Manufacture, Transport, Install And Operate These Power Stations, descreve sistemas não flutuantes e refere-se essencialmente às fundações dos dispositivos de captação de energia do vento, correntes e ondas;

Na patente US20030145587 (A1), Wind And Wave Energy Plant, é descrito um sistema que capta a energia das ondas e do vento. O movimento de oscilação de uma boia é utilizado para fazer movimentar um pistão, fazendo a bombagem de água do mar até um reservatório. A partir desse reservatório, a água faz movimentar uma turbina. Este princípio de funcionamento é o mesmo que faz movimentar as turbinas instaladas em barragens hidroelétricas.

Na patente US20130118176 (A1), Regenerative Offshore Energy Plant, é descrito um sistema que capta a energia do vento e das ondas. Para aproveitar a energia das ondas é aproveitado o movimento orbital das partículas de água de uma onda para fazer movimentar um rotor.

Sumário da invenção

A presente invenção permite converter a energia das ondas em energia elétrica.

Este processo é feito através de uma cadeia cinemática, com rodas cónicas e rodas livres, que permitirá que a oscilação vertical das boias provoque a rotação de uma roda central. Esta roda central pode ser acoplada a um gerador elétrico diretamente ou através de um veio intermédio.

Na Fig.1 está representada a cadeia cinemática do sistema mecânico. A estrutura exterior poderá apresentar várias configurações que suportem a cadeia cinemática. Este sistema mecânico pode ser instalado em zonas "offshore", junta da costa ou em pontões.

O dispositivo apresenta "n" boias, sendo "n" maior ou igual a um.

Uma descrição mais detalhada da cinemática estará presente na secção "Descrição da concretização preferida".

O gerador poderá estar acoplado na parte superior ou inferior do veio central ou até mesmo diretamente na roda central, não estando, por isso, representado.

Este mecanismo poderá ser implementado individualmente ou ser replicado, em rede, de forma a constituir um parque de conversão de energia das ondas.

Breve descrição dos desenhos

Na Fig.1, apresenta-se o mecanismo do sistema que poderá ter "n" boias, sendo "n" maior ou igual a um. A oscilação das "n" boias, provoca, de forma mecanicamente aditiva, a rotação de um veio central, através da cadeia cinemática.

Na Fig. 2, podemos ver, em perspetiva, apenas um dos braços e a sua cadeia cinemática. Estes braços são constituídos por uma boia, nº 1, e é a partir daí que se desenvolve toda a cadeia cinemática até à roda cónica final, nº7. A boia nº 1 está articulada através de dois tirantes, nº 2, que acionam duas rodas cónicas, nº4, com uma conexão de roda livre, nº 3. As rodas cónicas nº 4 induzem uma rotação da roda cónica nº 5, que transmite rotação á roda cónica nº 7, através do veio nº 6 e da roda livre nº 3.

Nas Figs. 3 e 4, podemos ver a vista lateral de apenas um dos braços e do seu engrenamento na roda cónica nº 8. É na roda cónica central nº 8 que todos os braços são acoplados.

Descrição da concretização preferida

Este sistema mecânico tem como vantagens uma rotação estável da roda central nº 8 e do veio central nº 9, que vão estar acoplados ao gerador elétrico, gerando energia elétrica de forma menos oscilante.

Esta estabilidade do sistema é garantida pelas ondas que passam pelo dispositivo, acionando as boias em momentos distintos e desfasados.

O dispositivo apresenta também a vantagem de só necessitar de movimento relativo entre a boia grande interior (Estrutura nº 2), que contém o mecanismo central, e as boias exteriores (Estruturas nº 1, para provocar rotação na roda interna nº 8 e posteriormente gerar energia elétrica, através de um gerador.

Outra das vantagens deste dispositivo é o facto das potências mecânicas, geradas pelo movimento das diferentes boias serem aditivas mecanicamente. Estes sistemas cinemáticos mecânicos apresentam rendimentos superiores aos dos sistemas hidráulicos.

Por último, este dispositivo permite o aproveitamento do potencial energético da onda não só na subida como também na descida da onda, através das rodas livres.

Relativamente ao dispositivo em si, há a realçar que os elementos do nº 3 até ao nº 9 estarão suportados por uma boia grande interior (Estrutura nº 2), flutuante ou numa estrutura fixa ao solo. As inércias das estruturas nº 1 e nº 2 são diferentes para permitir o movimento relativo entre elas.

O funcionamento do dispositivo será explicado através da descrição de um dos braços do sistema, sendo que este se repete para os "n" braços.

A boia, nº 1, está conectada por dois tirantes, nº 2, a dois sistemas de roda livre, que por sua vez estão conectados a uma roda cónica cada, nº 4.

Nas rodas cónicas nº 4 estão acopladas rodas livres nº 3, montadas em oposição, montagem que permite o aproveitamento da energia resultante da subida e descida da onda.

No movimento ascendente da boia, devido à passagem da onda, o sistema da roda livre engrena e permite a transmissão de movimento entre uma das rodas cónicas nº 4 e a roda cónica nº 5. Durante esta transmissão de movimento, a roda livre montada na outra roda cónica nº 4 peliça, não havendo rotação da mesma. Quando a boia nº 1 desce, devido ao movimento da cava da onda, acontece o contrário.

A roda cónica, nº 5, transmitirá a sua rotação para o veio nº 6 que está acoplado a outra roda livre nº 3, que criará o engrenamento com a roda cónica nº 7.

A rotação da roda cónica nº 7 levará à rotação da roda central nº 8, que, por sua vez, induz a rotação do veio nº 9. Neste veio, ou mesmo diretamente na roda nº 8, será conectado um gerador que produzirá energia elétrica.

Reivindicações

1. Um dispositivo múltiplo de aproveitamento da energia oceânica, que converte o movimento vertical oscilante das ondas em energia elétrica, através de um movimento relativo entre duas estruturas, uma constituída por um conjunto central e outra por pelo menos uma boia periférica. O sistema é constituído por uma cadeia cinemática aditiva, puramente mecânica, constituído por pelo menos uma boia oscilante, conectada(s) por rodas livres e rodas dentadas, que induzem a rotação de um elemento único, permitindo a produção de energia elétrica.

2. O dispositivo múltiplo de aproveitamento da energia oceânica, de acordo com a reivindicação 1, contem uma estrutura central, composta por rodas livres, rodas dentadas e veios e uma estrutura composta por pelo menos uma boia periférica, conectada por tirantes a sistemas de roda livre, conectados a rodas cónicas.

3. O dispositivo múltiplo de aproveitamento da energia oceânica, de acordo com a reivindicação 1, pode ser flutuante ou ser uma estrutura fixa ao solo. As inércias das estruturas são diferentes para permitir o movimento relativo entre elas.

4. O dispositivo múltiplo de aproveitamento da energia oceânica, de acordo com a reivindicação 1, permite o aproveitamento da energia resultante da subida e descida da onda.

5. O dispositivo múltiplo de aproveitamento da energia oceânica, de acordo com a reivindicação 1, permite o aproveitamento da energia das ondas através de um gerador, que produzirá energia elétrica, acoplado ao veio ou roda central rotativos.

6. O dispositivo múltiplo de aproveitamento da energia oceânica, de acordo com a reivindicação 1, inclui duas estruturas, que poderão ter três configurações: ambas flutuantes, obtendo-se o movimento relativo através da diferença de inércia; uma estrutura móvel e outra fixa, sendo que a fixa poderá ser a interior ou a exterior e a outra será a móvel.

7. O dispositivo múltiplo de aproveitamento da energia oceânica, de acordo com a reivindicação 1, pode trabalhar em qualquer maré e para qualquer tamanho de onda, desde que seja assim dimensionado.

8. O dispositivo múltiplo de aproveitamento da energia oceânica, de acordo com a reivindicação 1, pode ser rebocado para terra, separando-o do sistema de amarração.

9. O dispositivo múltiplo de aproveitamento da energia oceânica, de acordo com a reivindicação 1, pode ter variantes com combinações de acoplamentos mecânicos, hidráulicos e/ou elétricos;

10. O dispositivo múltiplo de aproveitamento da energia oceânica, de acordo com a reivindicação 1, pode ser combinado em rede, com outros dispositivos semelhantes, para formar um parque de energia oceânica.

Porto, 25 de janeiro de 2017

Desenhos

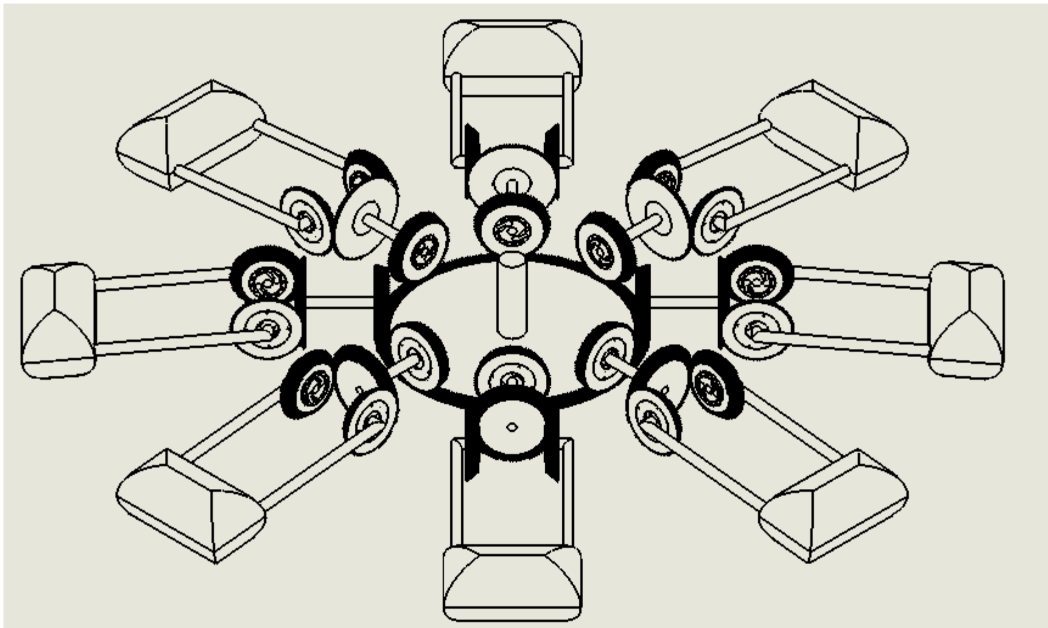

Fig.1- Desenho geral do sistema

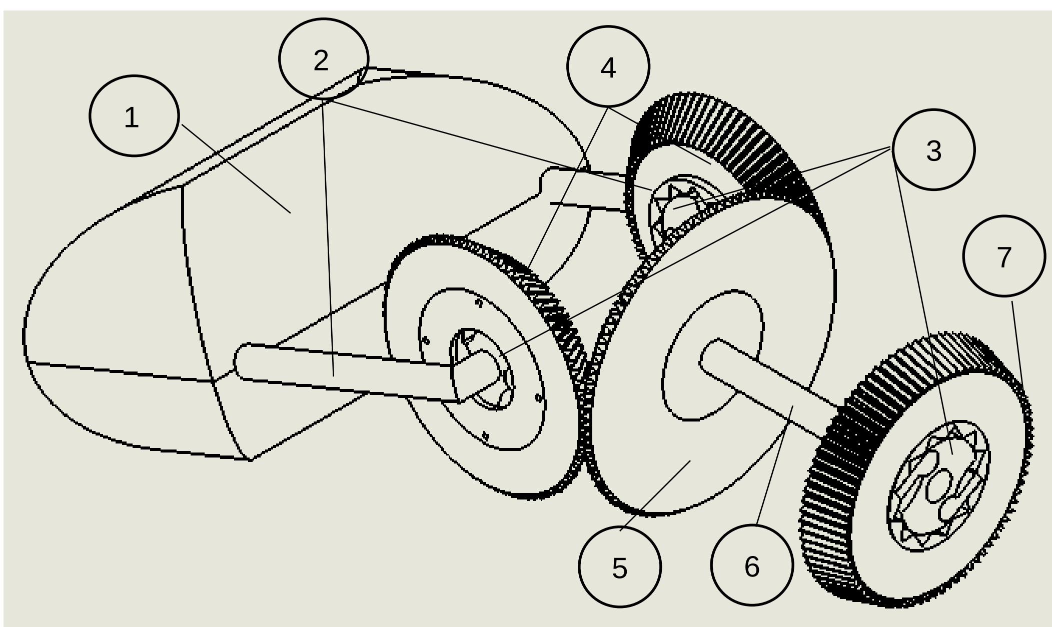

Fig.2- Conjunto braço

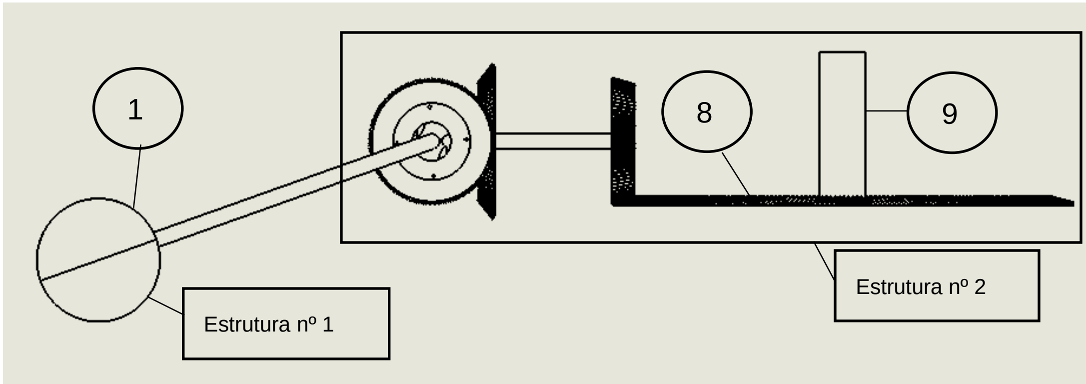

Fig.3 – Ligação do subsistema braço-boia à estrutura central (vista lateral)

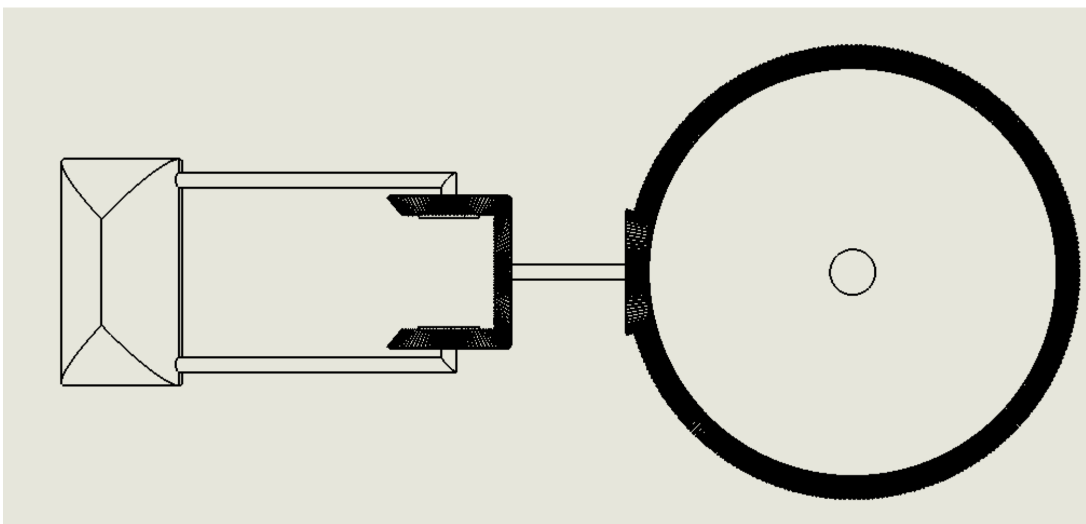

Fig.4 – Ligação do subsistema braço-boia à estrutura central (vista de cima)